

AD 731216

BRL MR 2108

BRL

AD

MEMORANDUM REPORT NO. 2108

AIR BLAST MEASUREMENTS FROM THE DETONATION OF AN EXPLOSIVE GAS CONTAINED IN A HEMISPHERICAL BALLOON (OPERATION DISTANT PLAIN, EVENT 2a)

Details of illustrations in
this document may be better
studied on microfiche
by

Ralph E. Reisler
Noel H. Ethridge
Daniel P. LeFevre
Louis Giglio-Tos

DDC
RECEIVED
OCT 20 1971
RECEIVED
D

July 1971

This document has been approved for public release and sale;
its distribution is unlimited.

Reproduced by
NATIONAL TECHNICAL
INFORMATION SERVICE
Springfield, Va. 22151

U.S. ARMY ABERDEEN RESEARCH AND DEVELOPMENT CENTER
BALLISTIC RESEARCH LABORATORIES
ABERDEEN PROVING GROUND, MARYLAND

Security Classification

DOCUMENT CONTROL DATA - R & D		
<i>(Security classification of title, body of abstract and indexing annotation must be entered when the overall report is classified)</i>		
1. ORIGINATING ACTIVITY (Corporate author) U. S. Army Aberdeen Research & Development Center Ballistic Research Laboratories Aberdeen Proving Ground, Maryland 21005		2a. REPORT SECURITY CLASSIFICATION Unclassified
		2b. GROUP
3. REPORT TITLE Air Blast Measurements from the Detonation of an Explosive Gas Contained in a Hemispherical Balloon (Operation Distant Plain, Event 2a)		
4. DESCRIPTIVE NOTES (Type of report and inclusive dates)		
5. AUTHOR(S) (First name, middle initial, last name) Reisler, R. E. Ethridge, N. H. Giglio-Tos, L. LeFevre, D. P.		
6. REPORT DATE July 1971	7a. TOTAL NO. OF PAGES 115	7b. NO. OF REFS 10
8a. CONTRACT OR GRANT NO.	9a. ORIGINATOR'S REPORT NUMBER(S) Memorandum Report No. 2108	
b. PROJECT NO. 1.01 Operation Distant Plain		
c.	9b. OTHER REPORT NO(S) (Any other numbers that may be assigned this report)	
d.		
10. DISTRIBUTION STATEMENT This document has been approved for public release and sale; its distribution is unlimited.		
11. SUPPLEMENTARY NOTES		12. SPONSORING MILITARY ACTIVITY Defense Atomic Support Agency Washington, D. C.
13. ABSTRACT Air blast was measured from the detonation of a mixture of oxygen and propane equivalent to 20 tons of TNT in a hemispherical balloon anchored to the ground surface. Measured values of shock arrival time, overpressure, duration of positive and negative phase, overpressure impulse, dynamic pressure, and dynamic pressure impulse are plotted as functions of ground range. Pressure-distance comparisons with TNT show the overpressure to be less than TNT at pressures greater than 30 psi. Comparisons made of overpressure waveshape and impulse as a function of shock overpressure show an equivalent yield of 20 tons or larger and a dynamic pressure impulse about 60 percent larger than for a corresponding 20 Ton TNT charge.		

DD FORM 1473
1 NOV 66

REPLACES DD FORM 1473, 1 JAN 64, WHICH IS OBSOLETE FOR ARMY USE.

Security Classification

Destroy this report when it is no longer needed.
Do not return it to the originator.

Secondary distribution of this report by originating or
sponsoring activity is prohibited.

Additional copies of this report may be purchased from
the U.S. Department of Commerce, National Technical
Information Service, Springfield, Virginia 22151

ACCESSION OF	
CFSTI	WFO SECTION <input checked="" type="checkbox"/>
DDC	DDP SECTION <input type="checkbox"/>
UNAN. DES.	<input type="checkbox"/>
JUSTIFICATION	
BY	
DISTRIBUTION/AVAILABILITY CODES	
DIST.	AVAIL. and/or SPECIAL
A	

The findings in this report are not to be construed as
an official Department of the Army position, unless
so designated by other authorized documents.

*The use of trade names or manufacturers' names in this report
does not constitute indorsement of any commercial product.*

BALLISTIC RESEARCH LABORATORIES

MEMORANDUM REPORT NO. 2108

JULY 1971

AIR BLAST MEASUREMENTS FROM THE DETONATION OF
AN EXPLOSIVE GAS CONTAINED IN A HEMISPHERICAL
BALLOON (OPERATION DISTANT PLAIN, EVENT 2a)

Ralph E. Reisler
Noel H. Ethridge
Daniel P. LeFevre
Louis Giglio-Tos

Terminal Ballistic Laboratory

This document has been approved for public release and sale;
its distribution is unlimited.

Program was supported by the Defense Atomic Support Agency and
represents a portion of the activities of Project 1.01, Operation
Distant Plain.

ABERDEEN PROVING GROUND, MARYLAND

BALLISTIC RESEARCH LABORATORIES

MEMORANDUM REPORT NO. 2108

REReisler/NHEthridge/DPLLeFevre
LGiglio-Tos/lse
Aberdeen Proving Ground, Md.
July 1971

AIR BLAST MEASUREMENTS FROM THE DETONATION OF
AN EXPLOSIVE GAS CONTAINED IN A HEMISPHERICAL
BALLOON (OPERATION DISTANT PLAIN, EVENT 2a)

ABSTRACT

Air blast was measured from the detonation of a mixture of oxygen and propane equivalent to 20 tons of TNT in a hemispherical balloon anchored to the ground surface. Measured values of shock arrival time, overpressure, duration of positive and negative phase, overpressure impulse, dynamic pressure, and dynamic pressure impulse are plotted as functions of ground range. Pressure-distance comparisons with TNT show the overpressure to be less than TNT at pressures greater than 30 psi. Comparisons made of overpressure waveshape and impulse as a function of shock overpressure show an equivalent yield of 20 tons or larger and a dynamic pressure impulse about 60 percent larger than for a corresponding 20 Ton TNT charge.

TABLE OF CONTENTS

	Page
ABSTRACT	3
LIST OF ILLUSTRATIONS	7
LIST OF TABLES	11
1. INTRODUCTION	13
1.1 Objectives	13
1.2 Background	14
2. EXPERIMENT DESIGN AND INSTRUMENTATION	15
2.1 Experimental Plan	15
2.2 Instrumentation	16
2.3 Calibration	22
3. RESULTS	22
3.1 Environmental Conditions	22
3.2 Instrumentation Performance	26
3.3 Method of Data Reduction	26
3.4 Presentation of Data	29
4. DISCUSSION	45
4.1 Gage Records	45
4.2 Comparison of Elevated and Surface or Near Surface Gage Records	45
4.3 Scaling	62
4.4 Comparison of Data	63
5. CONCLUSIONS AND RECOMMENDATIONS	76
ACKNOWLEDGEMENTS	79
REFERENCES	80
APPENDIX A. Pressure Records	82
APPENDIX B. Data from the Premature Detonation of Distant Plain Event 2B	104
DISTRIBUTION LIST	109

LIST OF ILLUSTRATIONS

Figure No.		Page
2.1	Field Layout	17
2.2	Blast Line Showing the Filled Balloon	18
2.3	Typical Instrument Station	19
2.4	Tower-Mounted Instrument Station	20
2.5	Schematic of Bi-Axial Drag Gage	21
3.1	Detonation of Event 2A	24
3.2	Post Shot View of Blast Line	25
3.3	Final Smoothing Technique Applied to Drag Gage Record Obtained at 2 Foot Elevation, Station 6	28
3.4	Arrival Time versus Ground Range for Event 2A	35
3.5	Maximum Overpressure versus Ground Range for Event 2A	36
3.6	Positive Duration, Primary Shock Only, versus Ground Range for Event 2A	37
3.7	Positive Duration, Primary and Secondary Shock, versus Ground Range for Event 2A	38
3.8	Positive and Negative Duration versus Ground Range for Event 2A	39
3.9	Positive Overpressure Impulse versus Ground Range for Event 2A	40
3.10	Maximum Negative Pressure versus Ground Range for Event 2A	41
3.11	Negative Overpressure Impulse versus Ground Range for Event 2A	42
3.12	Dynamic Pressure versus Ground Range for Event 2A	43
3.13	Dynamic Pressure Impulse versus Ground Range for Event 2A	44
4.1	Overpressure versus Time Measured at Different Elevations at Station 6, 156 Feet	47

LIST OF ILLUSTRATIONS (CONTINUED)

Figure No.		Page
4.2	Stagnation Pressure versus Time Measured at Different Elevations at Station 6, 156 Feet	48
4.3	Dynamic Pressure versus Time for Different Elevations at Station 6, 156 Feet	49
4.4	Drag Pressure versus Time Measured at Different Elevations at Station 6, 156 Feet	50
4.5	Overpressure versus Time Measured at Different Elevations at Station 7, 201 Feet	52
4.6	Stagnation Pressure versus Time Measured at Different Elevations at Station 7, 201 Feet	53
4.7	Dynamic Pressure versus Time at Different Elevations at Station 7, 201 Feet	55
4.8	Drag Pressure versus Time Measured at Different Elevations at Station 7, 201 Feet	56
4.9	Direction of Flow as Derived from Drag Gage at 22 Foot Elevation, Station 7, 201 Feet	58
4.10	Direction of Flow as Derived from Drag Gage at 52 Foot Elevation, Station 7, 201 Feet	59
4.11	Drag Coefficients versus Time at Stations 6 and 7 using Dynamic Pressure Measured at the Gage Locations .	60
4.12	Drag Coefficients versus Time at Stations 6 and 7 using Dynamic Pressure Records Obtained at the 2 Foot Elevation	61
4.13	Measured Arrival Time for Event 2A, Scaled	66
4.14	Measured Overpressure for Event 2A, Scaled	68
4.15	Measured Positive Phase Duration for Event 2A, Scaled .	69
4.16	Measured Overpressure Impulse for Event 2A, Scaled . . .	70
4.17	Dynamic Pressure for Event 2A, Scaled	71

LIST OF ILLUSTRATIONS (CONTINUED)

Figure No.		Page
4.18	Dynamic Pressure Impulse Compared with Australian Data, Scaled	72
4.19	Exponential Decay Constant C versus Shock Front Overpressure for Event 2A and 1 pound Hemispherical TNT Charge at Sea Level	74
4.20	Overpressure Impulse Versus Maximum Overpressure for Event 2A and a 1 Pound Hemispherical TNT Charge at Sea Level	75
4.21	Dynamic Pressure Impulse versus Shock Front Overpressure for Event 2A and a 1 Pound Hemispherical TNT Charge at Sea Level	77
A.1	Pressure-Time Records, Stations 4-6	84
A.2	Pressure-Time Records, Stations 7 and 8	85
A.3	Pressure-Time Records, Stations 9 - 12	86
A.4	Pressure-Time Records, Stations 13 - 15	87
A.5	Pressure-Time Records, Elevated Positions, Station 6	88
A.6	Pressure-Time Records, Elevated Positions, Station 7	89
A.7	Pressure-Time Records Showing Negative Phase, Stations 4 and 5	90
A.8	Pressure-Time Records Showing Negative Phase, Station 6	91
A.9	Pressure-Time Records Showing Negative Phase, Station 7	92
A.10	Pressure-Time Records Showing Negative Phase, Stations 8 - 10	93
A.11	Pressure-Time Records Showing Negative Phase, Stations 12 - 15	94
A.12	Dynamic Pressure-Time Data, 2 ft. Elevation Station 6	95

LIST OF ILLUSTRATIONS (CONTINUED)

<u>Figure No.</u>		<u>Page</u>
A.13	Dynamic Pressure-Time Data, 10 ft. Elevation, Station 6	96
A.14	Dynamic Pressure-Time Data, 30 ft. Elevation, Station 6	97
A.15	Dynamic Pressure-Time Data, 2 ft. Elevation, Station 7	98
A.16	Dynamic Pressure-Time Data, 22 ft. Elevation, Station 7	99
A.17	Dynamic Pressure-Time Data, 52 ft. Elevation, Station 7	100
A.18	Dynamic Pressure-Time Data, 2 ft. Elevation, Station 8	101
A.19	Drag Pressure-Time Records, Station 6	102
A.20	Drag Pressure-Time Records, Station 7	103
B.1	Maximum Overpressure versus Ground Range for Event 2B	107

LIST OF TABLES

<u>Table No.</u>		<u>Page</u>
3.1	Environmental Conditions, Event 2A	23
3.2	Instrumentation Results, Event 2A	30
3.3	Instrumentation Results, Secondary Shock and Negative Pressure, Event 2A	32
3.4	Dynamic Pressure Results	33
3.5	Drag Gage Results	34
4.1	Measured Overpressure Data Scaled to 1 pound Sea Level Conditions	64
4.2	Measured Dynamic Pressure Data Scaled to 1 pound Sea Level Conditions	65
B.1	Peak Overpressure Data, Event 2B	108

1. INTRODUCTION

A series of shock and blast experiments known as Operation Distant Plain were sponsored by The Technical Cooperation Program (TTCP) during the calendar years 1966 and 1967. The operation was conducted at the Defence Research Establishment, Suffield (DRES), Ralston, Alberta, Canada, and at a site near Hinton, Alberta, Canada. Material presented in this report describes the measurements made on Event 2A, which was fired on 22 July 1966 at the DRES.

The charge for the experiment identified as Event 2A, consisted of a 125 foot diameter hemispherical balloon filled with an oxygen-propane mixture having a mole mixture of $O_2/C_3H_8 = 3.50$. Mylar was the basic material used in the construction of the balloon. A horizontally oriented ballonet was incorporated in the construction to permit rapid inflation with air to sustain the balloon against wind conditions during the long filling time. Relief valves were attached on the envelope in order not to exceed the desired internal pressure. Sections of $2\frac{1}{2}$ inch diameter pipe were placed in Nylon sleeves bonded around the equator of the balloon. The pipes were fitted together and tied into 42 anchor positions for securing the balloon to the ground. Reference 1 describes in greater detail the Project 1.10 balloon efforts.

The trial was conducted at the Drowning Ford Range of DRES where the composition of the soil is a silty clay alluvium.

1.1 Objectives

The objectives of the Ballistic Research Laboratories (ERL) in Event 2A were to measure the airblast parameters on the earth's surface and at

selected heights above the surface. Comparisons with data obtained on related past experiments were to be performed.

1.2 Background

An economical substitute for TNT as a blast source has been under investigation for several years. Basic research work with detonable gas balloons led to the establishment of a detonable gas explosion development program. The Operation Distant Plain Event 2A was a logical continuation of experimental work conducted under this program in 1965 with 17 and 32 foot diameter balloons with yields up to 5 tons. Advantages of a detonable gas balloon were considered to be: (1) The cost of the detonable gas mixture is low, less than 4 cents per pound for oxygen, propane and methane in large quantities. (2) The technique provides safe working conditions for the experimenters, i.e., the test site can be prepared, gages installed and calibrated without the work being done in the presence of a large charge of TNT. The gas mixture can be injected into the balloon the day of the test. (3) The detonable gas mixture adapts itself to air blast phenomena studies more readily than the TNT. A buoyant gas mixture can be used and the balloon positioned at the desired height of burst. No heavy support mechanism is required like that for TNT. (4) A well defined blast wave is generated with little or no perturbations. (5) Little, if any ejecta is produced. A disadvantage is the lack of duplication of the very high pressure phenomena associated with a high explosive due to the low detonation pressures of the gas (approx. 500 psi).

In a discussion of the blast effects produced by the two types of explosions, Project 1.10, General American Transportation Corporation

(GATX), states in reference 1, "During the early stages of the Detonable Gas Explosion program, it was theorized that the blast effects produced by a detonable gas explosion and a TNT explosion should be comparable according to the energies released by the respective explosions. Subsequent experiments with both methane-oxygen and propane-oxygen detonable gas mixture and additional analyses have shown that this is not the best parameter for judging the air blast equivalence of a detonable gas explosion. It has been found that the peak overpressure versus distance curve from a detonable gas explosion cannot be made to match the comparable curve from a TNT explosion over a wide range of distance from the center of the explosion. If one adjusts the weights of TNT and detonable gas so that the peak overpressure decay curves are matched in the range from approximately 10 to 50 psi, it has been found that the weight of gas mixture must equal the weight of the TNT charge. In this case, however, the detonable gas explosion releases approximately twice as much energy as the TNT explosion."

Predictions of the air blast parameters for TNT were prepared by Mr. John Keefer of BRL in Reference 2 utilizing empirical data. GATX developed a computer code to predict the air blast parameters from the detonable gas as described in Reference 1. The predicted values of blast parameters used for comparisons in this report were derived from the above references.

2. EXPERIMENTAL DESIGN AND INSTRUMENTATION

2.1 Experimental Plan

The experimental program was established so the same blast line would be used for three successive events, namely Events 1, 2 and 2A.

Following Event 1, a 20 ton shot on a 81.3 foot steel tower, the blast line was refurbished and necessary instruments replaced and calibrated in preparation for Event 2. Event 2 was to be a gas bag shot with an 85 foot height of burst, however, the balloon ruptured during inflation and the event was postponed. Consequently, with Event 2 instrumentation in a readied condition, the decision was made to proceed with Event 2A as soon as the balloon could be deployed. Ground zero was displaced from the two previous Event zero positions by precisely 10 feet on a bearing of $79^{\circ} 28' 11''$, (see Reference 3). The 30 foot and 55 foot instrument towers programmed for Event 2 were included with the surface instrumentation. The blast line started at 71 feet as seen in the layout presented in Figure 2.1. Shown in Figure 2.2 is a photograph of the blast line and balloon looking down the line from Station 8. A typical surface station is shown in Figure 2.3. A typical tower station is shown in Figure 2.4. The total head gage is located on the right, the drag gage in the center, and the side-on sensor on the left. The photograph shows the drag gage with the stainless steel drag cup used in calibration; a roughened cup replaces it for the event.

2.2 Instrumentation

The sensors and mounting systems used for all measurements of over-pressure, dynamic pressure, and drag will be only briefly mentioned in the text. A detailed discussion will be found in Reference 4.

All electronic pressure transducers were the general strain-type which were commercially available. The drag sensor was designed and developed at BRL around a commercially available bi-axial strain sensing

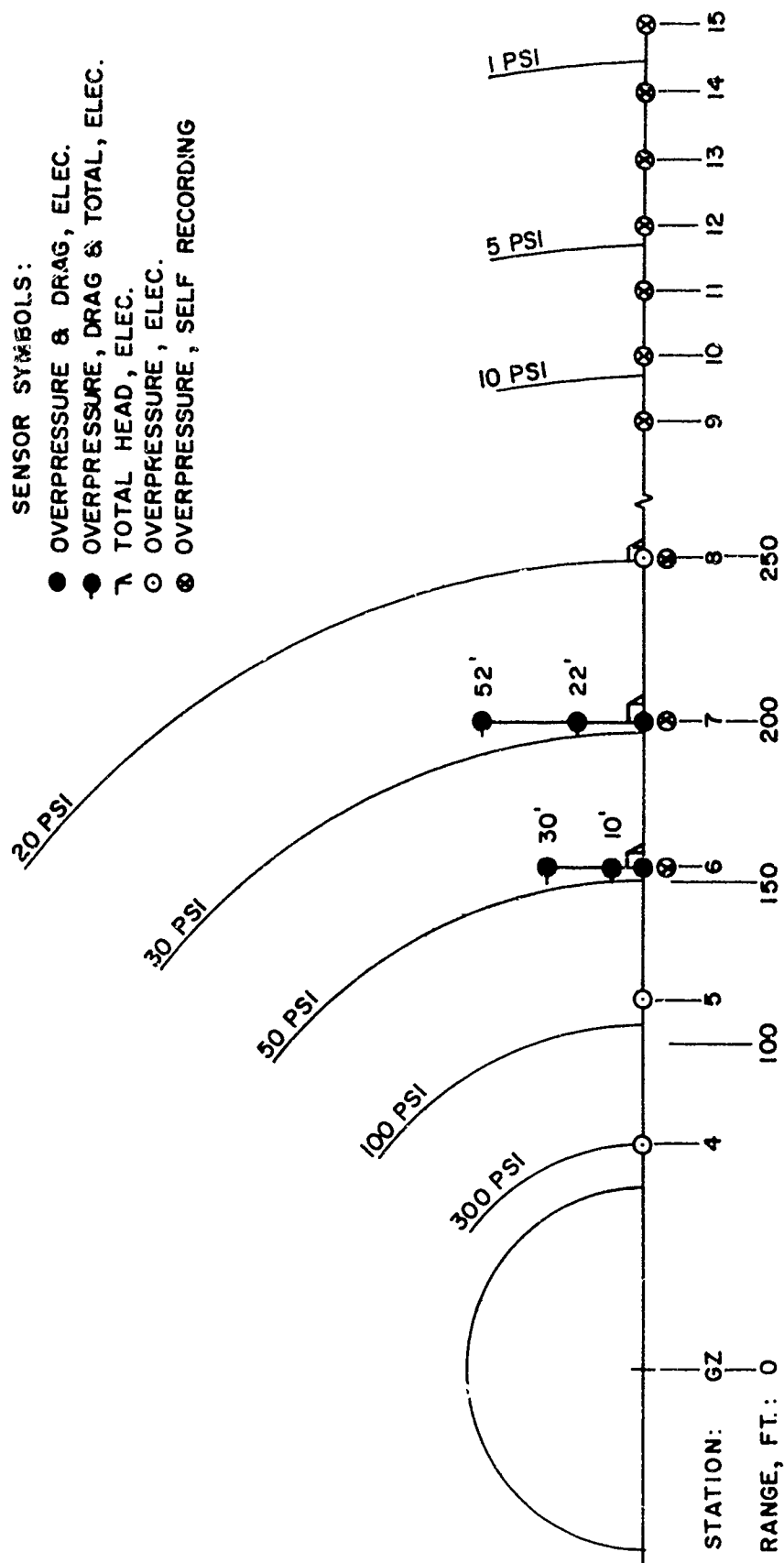


Figure 2.1 Field Layout

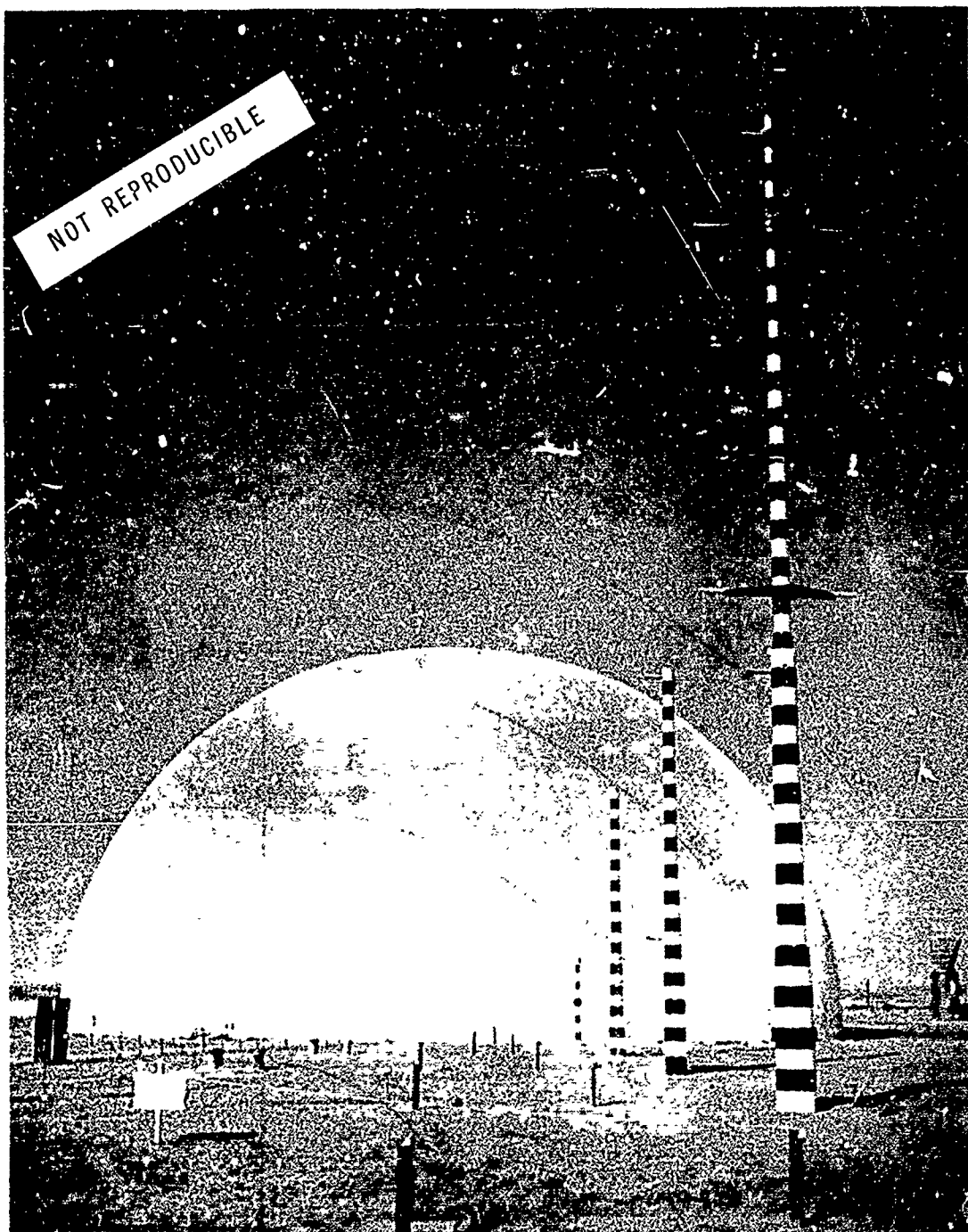


Figure 2.2 Blast Line Showing the Filled Balloon



Figure 2.3 Typical Instrument Station

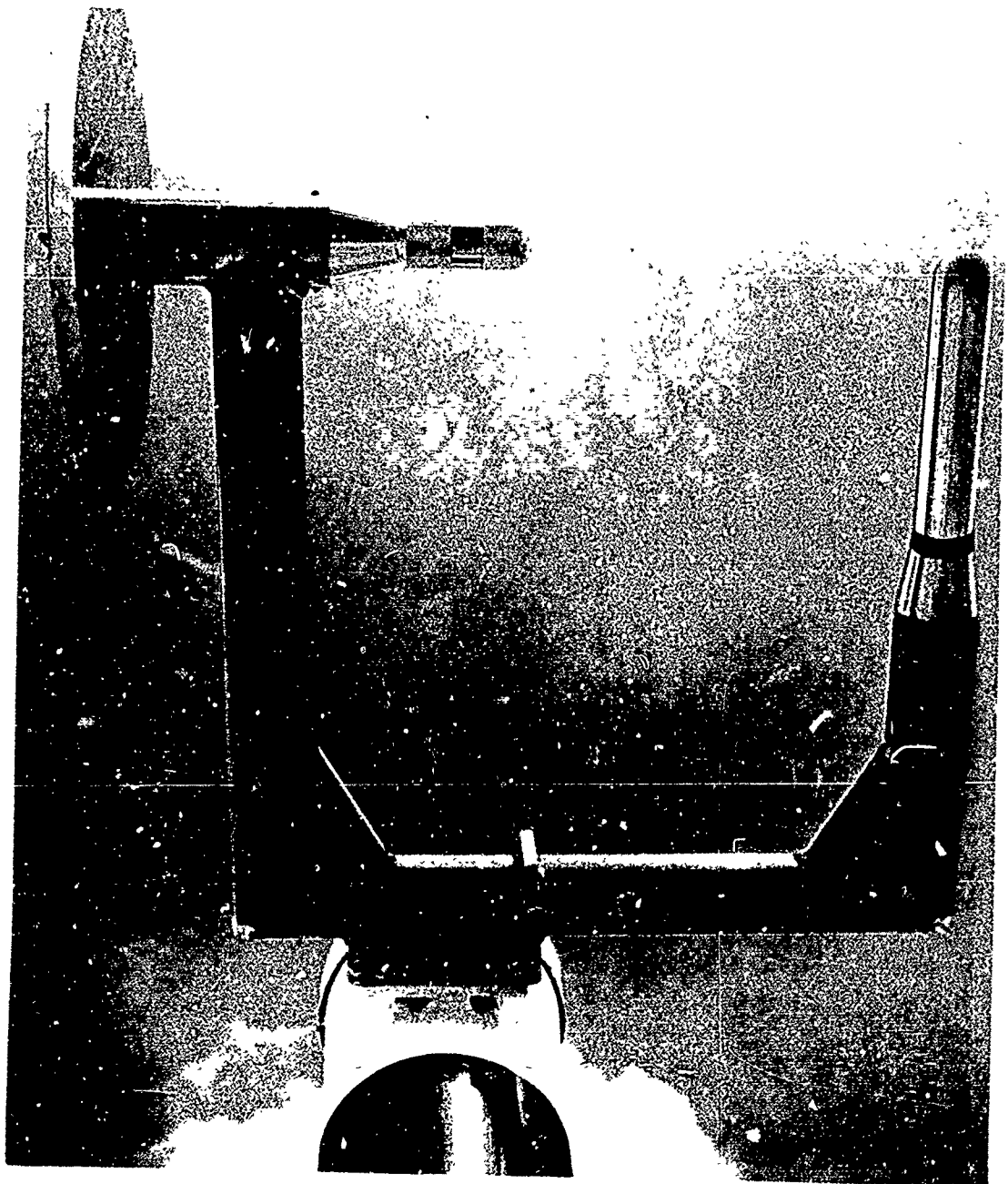


Figure 2.4 Tower Mounted Instrument Station

BRL BI-AXIAL DRAG GAGE

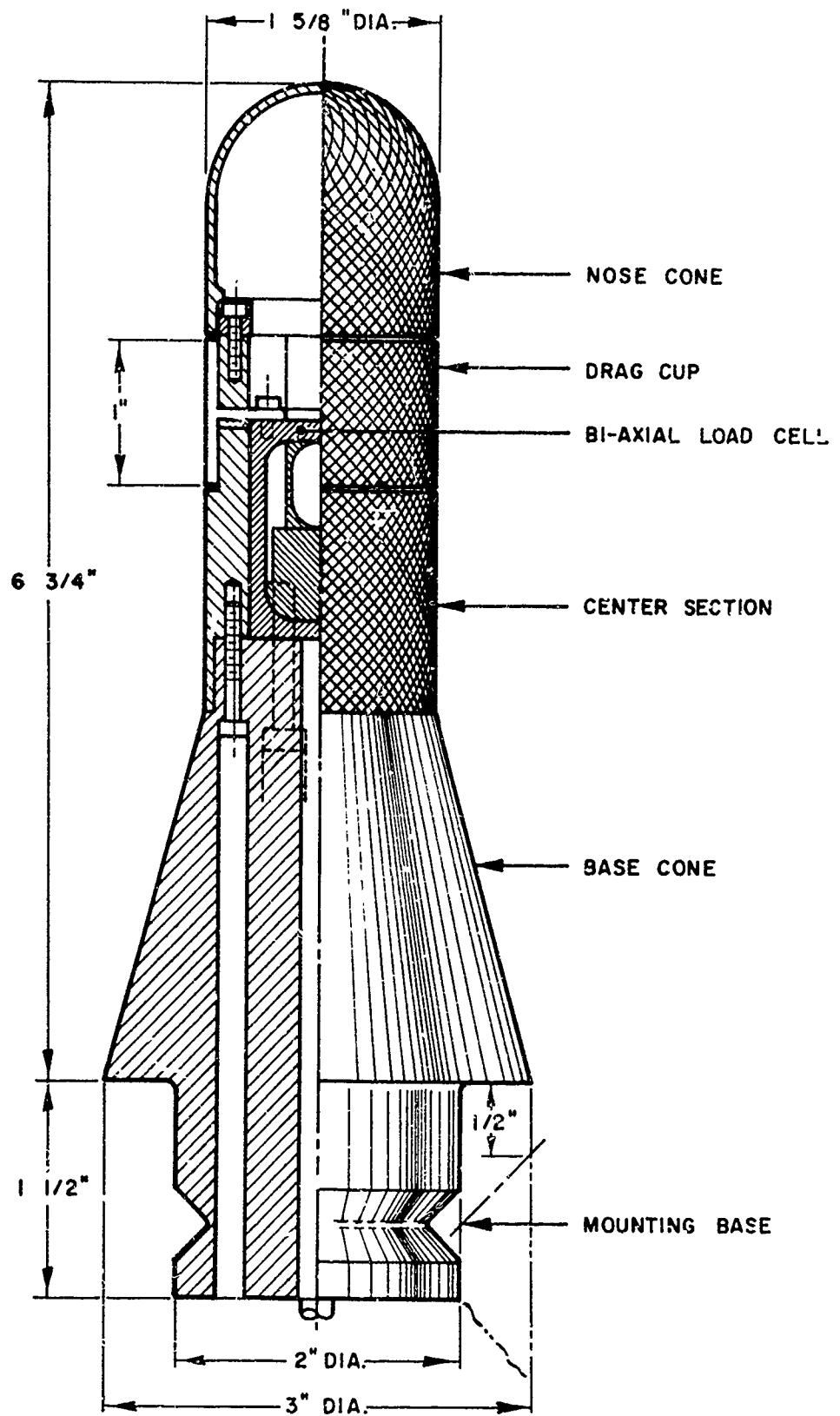


Figure 2.5 Schematic Of Bi-Axial Drage Gage

load cell (see Figure 2.5). Magnetic tape recording equipment, Consolidated Electrodynamic Corporation (CEC) VR-3300 and VR-3800 machines, recorded the signal from the transducers in an unmanned bunker at 1000 feet. Self-recording gages were used, to both supplement the electronic transducers at certain positions and to extend the blast line into the low pressure region.

2.3 Calibration

The electronic instrumentation was calibrated in place by the application of the particular forcing function, i.e., air pressure to the overpressure gage and force to the drag gages. Self-recording sensors were calibrated in the laboratory prior to their installation in the gage case. All pressure calibration equipment was checked for accuracy against a dead weight secondary standard. Dynamic tests were made with the sensors in the BRL Shock Tube prior to the field trial (see Reference 4).

3. RESULTS

3.1 Environmental Conditions

The environmental conditions prevailing at the time of detonation of Event 2A are presented in Table 3.1.

The high order detonation of the propane oxygen mixture is shown in Figure 3.1. A large amount of thermal energy, reminiscent of nuclear shots, was felt at the Technical Observation Point. The blackened tower mounts (see Figure 3.2) present direct evidence of a high thermal output. Also shown in Figure 3.2, are the remains of the balloon pipe anchoring system and the absence of any crater.

TABLE 3.1 ENVIRONMENTAL CONDITIONS, EVENT 2A

Firing Time	1315 MST, 27 July 1966
Ambient Pressure	13.71 psi
Temperature	118° F at surface 74° F at 2 meters
Wind	135° - 3.1 mph at 0.6 meters 165° - 4.2 mph at 2 meters 170° - 5.3 mph at 8 meters
Relative Humidity	46 percent
Sky Conditions	Clear with bright sunshine
Surface Conditions	Dry and clean

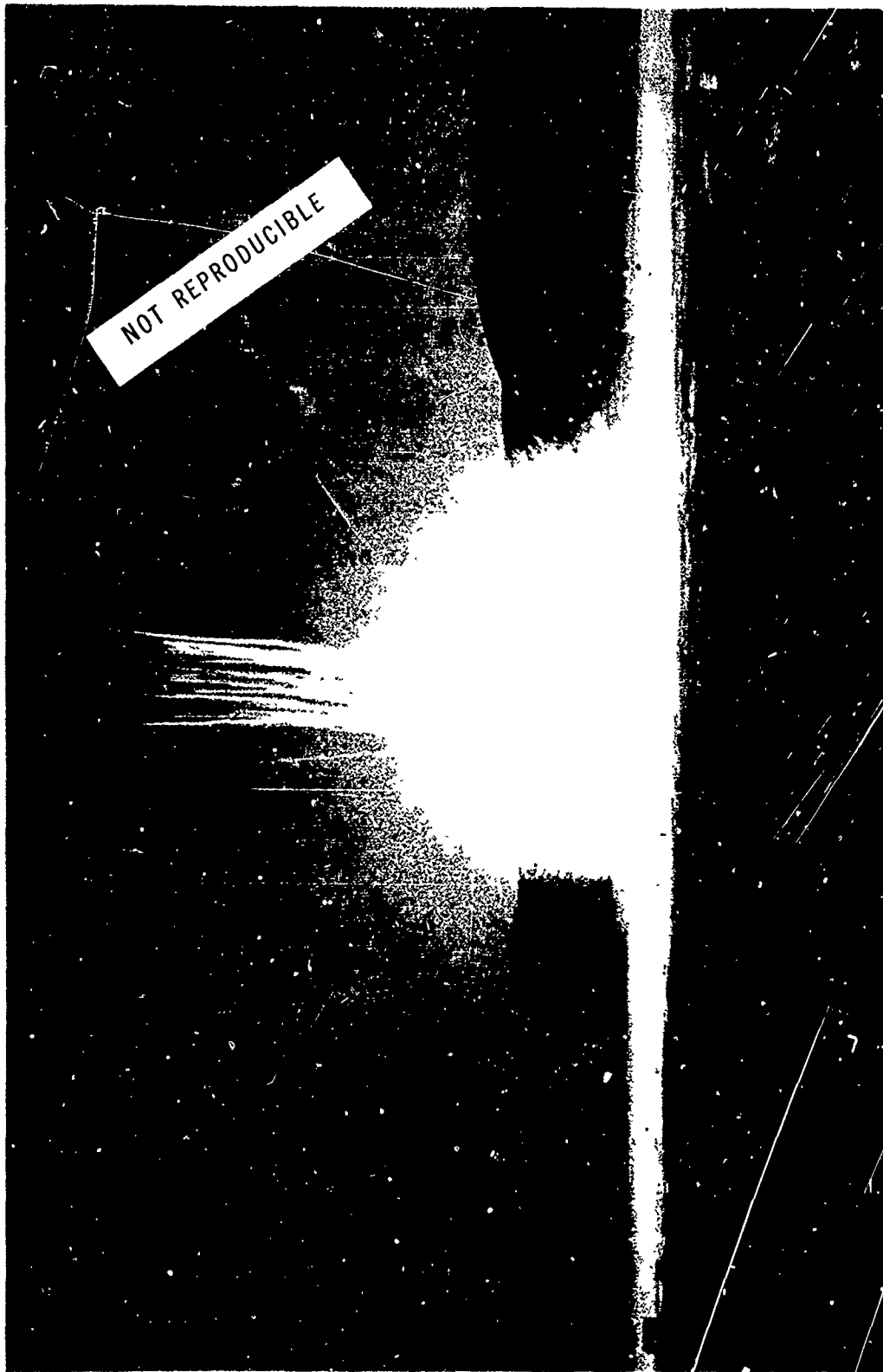


Figure 3.1 Detonation of Event 2A

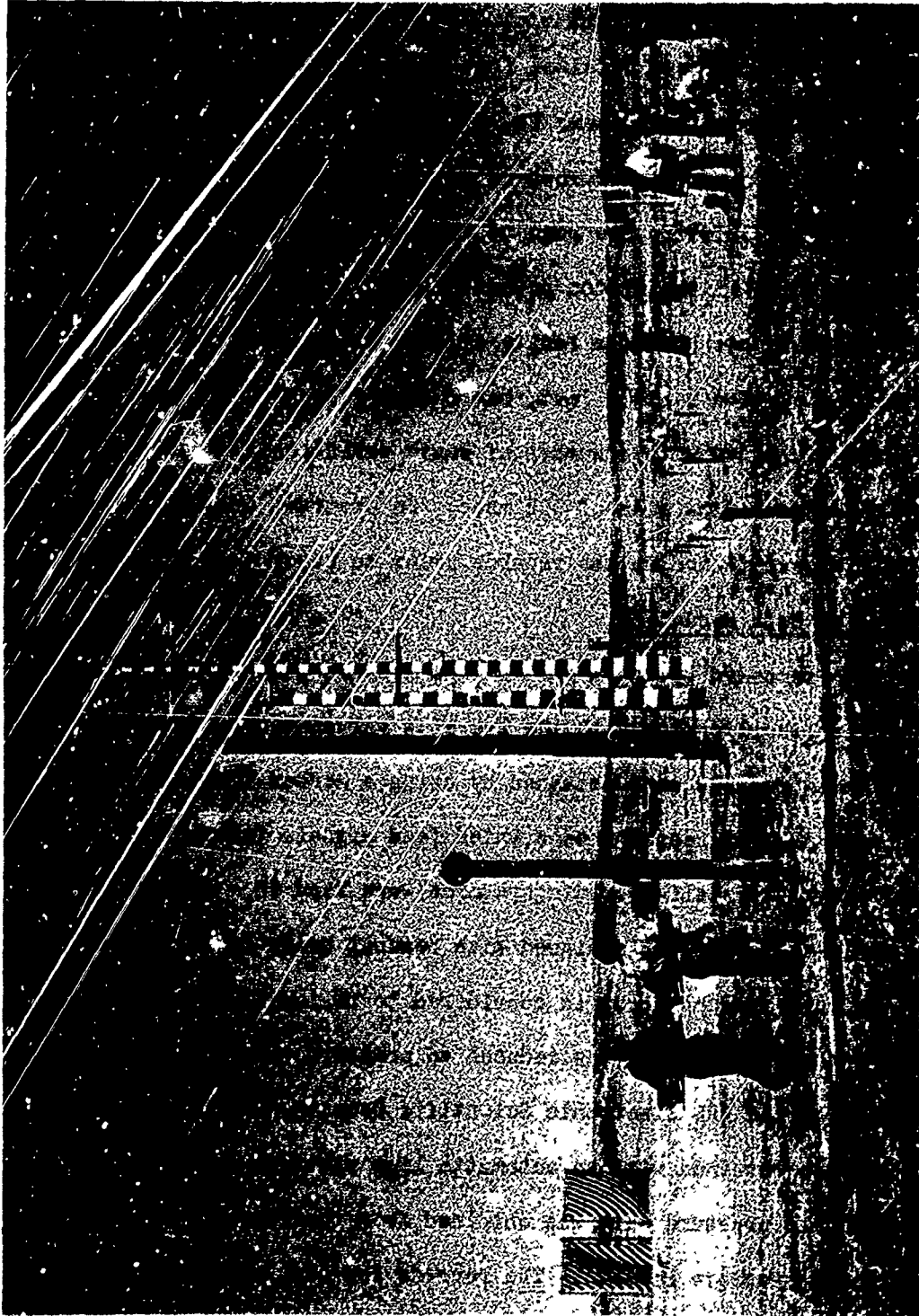


Figure 3.2 Post Shot View of Blast Line

3.2. Instrumentation Performance

Excellent records were obtained from the majority of the sensors used. Gages and recording systems functioned as planned with two exceptions. Two self-recording overpressure gages failed; one at the 201 foot range and one at 473 feet. The gage at 201 feet ran prematurely due to an electrical short in the piston actuator leads, while the gage at 473 failed to initiate because of a faulty arming switch. The record at the first station, Station 4 at 71 feet, has a slow rise of 0.1 msec to maximum pressure followed with a number of rapid variations. Station 5 at 116 feet also has a slow rise of 0.2 msec. In contrast to Event 1 there was no initial excitation on the records prior to shock arrival.

3.3 Method of Data Reduction

The data recorded by the magnetic tape systems was reproduced and recorded by an oscillograph with the use of a galvanometer driver. Digital data from these records were obtained by using a Gerber Chart Reader equipped with digital readout heads which feed signals into a Telecordex Accumulator System. Self-recording records were read in a similar manner, however a microscope reader equipped with readout heads replaced the chart reader. Overall reading error is considered to be less than one percent.

All of the digital data was reduced to pressure and time, and impulse was computed by the BRL Electronic Scientific Computer (BRL ESC). A plot of the data was obtained with an automatic line plotter.

The dynamic pressure data was obtained from the side-on overpressure and total head pressure records. The records for each station were read independently and reduced, then plotted on the same axes with an expanded

scale to emphasize any peculiarities that were common to each record. After manually correcting for such things as total head record spikes crossing the side-on pressure record, the two records were re-read. The BRLESC was used to process these final records, and compute corrected dynamic pressure versus time, dynamic pressure impulse versus time, and Mach number versus time. The method of computation is described in Reference 5. An example of the resulting plots is shown in Figure A. 12.

The drag records were read and processed in several steps. The first step converted analog data to digital and applied simple moving average smoothing techniques in the computer reduction process. The records, as presented in Appendix A (Figures A.19 and A.20), represent the drag records smoothed over an interval of one millisecond.

For comparison with each other and with pressure records still further smoothing was applied. The final step was to fit an exponential decay curve by eye through the record, remove the variation expressed by that curve from the data, and make a second plot. On this second plot the data consisted of oscillations about a horizontal or nearly horizontal line. A smoothing was made by eye on this second plot. This smoothed curve was combined with the variation previously removed from the data to obtain a final smoothed gage record. Oscillations with periods up to a maximum of from two to four milliseconds were removed in this smoothing process. Figure 3.2 shows this smoothing process as applied to the drag gage record obtained at an elevation of two feet at Station 6. The large oscillations were introduced by mount vibrations.

In the smoothing process the curves were extrapolated to shock arrival

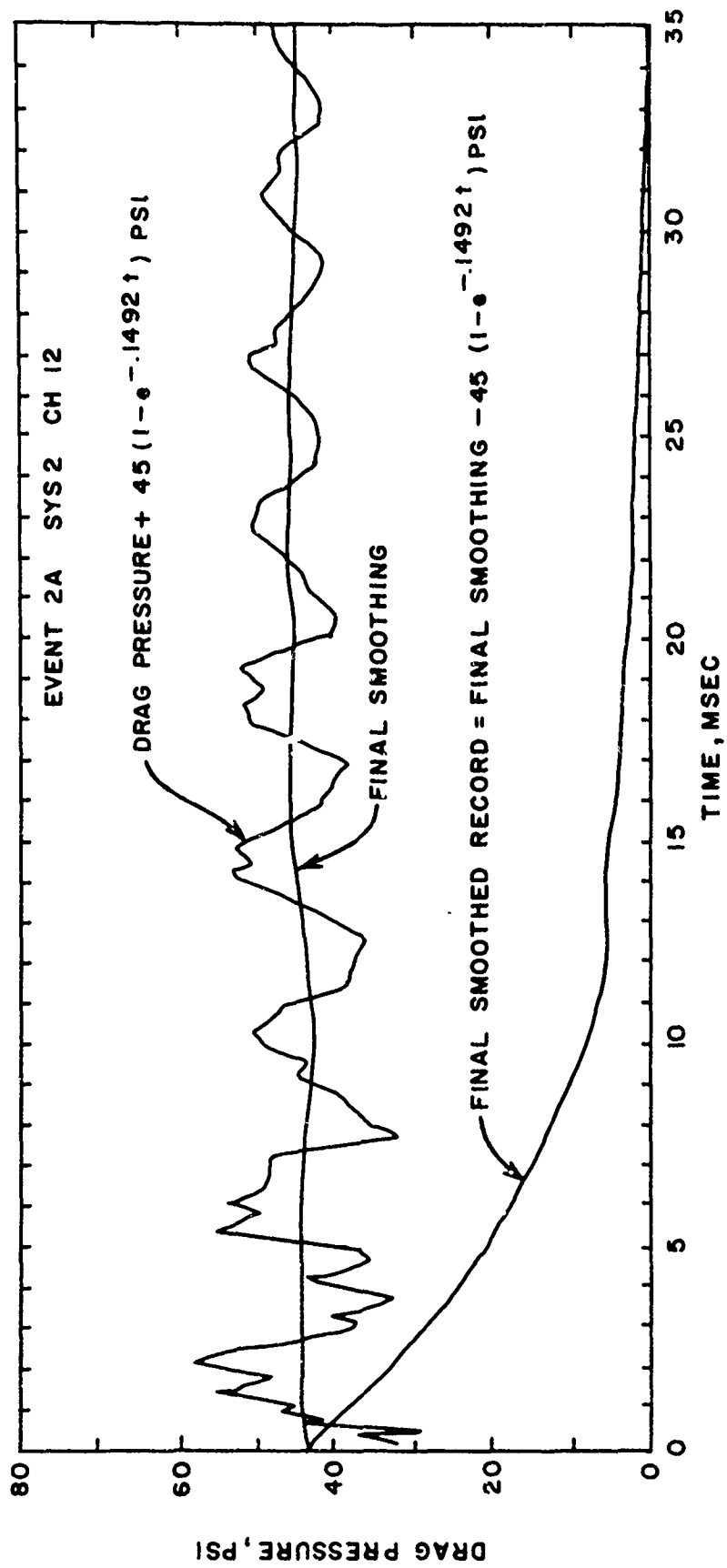


Figure 3.3 Final Smoothing Technique Applied to Drag Gage
Record Obtained at 2 Foot Elevation, Station 6

time, and the maximum values listed in Table 3.4 correspond to these smoothed extrapolated values.

The drag gages were bi-axial. The direction of the sensing axes listed in Table 3.5 and on the records in Appendix A were determined from the gage calibration data. The gages were installed with the axes nominally at 0, 90, +45 or -45 degrees elevation with respect to a level ground plane. The calibration data were examined to determine what deviation from the nominal axis direction would produce an equal decrease in gage output for a constant applied force as the angle of application of the force was varied in either direction about the axis. This angular deviation, usually small, was added or subtracted to the nominal axis direction to determine the actual direction of the gage sensing axis.

3.4 Presentation of Data

Air Blast data for Event 2A are listed in Tables 3.2 through 3.5. Maximum overpressure and positive duration were established by plotting the data on semi-logarithmic graph paper in accordance with the procedure set out in Reference 6.

The arrival time measured by the surface sensors is presented in Figure 3.4. The plots of maximum overpressure, maximum negative pressure, positive phase duration, negative phase duration, positive overpressure impulse, negative impulse, dynamic pressure, and dynamic pressure impulse are presented in Figure 3.5 through 3.13. Two plots of the duration data were made because of the secondary shock and its occurrence in the positive phase in some records and in the time shortly after the positive phase in others. Figure 3.7 presents the data where the secondary shock is

Table 3.2 Instrumentation Results, Event 2A

Station No.	Slant Range (ft)	Elevation (ft)	Gage No.	Arrival Time Pri. (msec)	Maximum Overpressure (psi)	Positive Duration Primary Shock (msec)	Positive Impulse Primary Shock (psi-msec)
4	71	0	1-3	9.98	178	40**	1221
5	116	0	1-4	24.86	47	46	649
6	156	0	12-11		35	42	454
	156	0	3-2	42.50	35	37	441
	156	2	2-13	42.55			
	156	10	2-11	42.70	36	42	655
	156	10	1-6	43.00			
	158	30	3-5	43.90	35	40	468
	158	30	3-6	43.85			
7	201	0	50-2		Gage Failed -- No Record		
	201	0	2-6	66.20	22	45	370
	201	2	3-9	66.55			
	201	22	3-11	66.85	23.2	47.5	400
	201	22	1-9	66.80			
	207	52	2-3	70.00	22.5	48	380
	207	52	2-2	69.95			
8	250	0	25-9				
8	250	0	1-11	96.50	16.5	58	323
	250	2	1-12	96.50	15.6	59	320

Table 3.2 Instrumentation Results, Event 2A (Continued)

Station No.	Slant Range (ft)	Elev- ation (ft)	Gage No.	Arrival Time Pri. (msec)	Maximum Overpressure (psi)	Positive Duration Primary Shock (msec)	Positive Impulse Primary Shock (msec)
9	295	0	25-5		11.7	80	341.7
10	382	0	25-12		7.2	73	203
11	473	0	10-15		Gage Failed --- No Record		
12	564	0	10-13		4.0	93	142.7
13	678	0	5-20		3.1		158.4
14	998	0	2-12		1.8		95
15	4190	0	48-4		0.36		23.8

Note:

** First value listed is derived from decay of primary shock.

*** Ranges of all elevated stations are slant ranges.

Table 3.3 Instrumentation Results, Secondary Shock and Negative Pressure, Event 2A

Station No.	Slant Range (ft.)	Gage No.	Arrival Time Secondary (Msec)	Positive Duration Primary & Secondary (Msec)	Positive Impulse Primary & Secondary (Psi-Msec)	Negative Pressure (Psi)	Negative Duration (Msec)	Negative Impulses (Psi-msec)
4	71	1-3	62	64	1295	5.6	311	998
5	116	1-4	74	70	689	2.7	295	422
6	156	12-11	--	65	496	3.07	241	351
	156	3-2	88	58	452	3.55	422	901
	156	2-11	88.7	64	713	2.3	241	204
	158	3-5	87.9	57	483	3.6	323	626
7	201	50-2		Gage Failed -- No Record				
	201	2-6	119	68	387	2.8	362	540
	201	3-11	119	66.5	418	2.0	364	466
	207	2-3	121.5	69	402	2.3	356	417
8	250	25-9		80	342	1.86	143	100
	250	1-11	156	81	342	1.9	319	332
9	295	25-5	--	96.5	377.9	1.26	318	215
10	382	25-12	--	100	214.5	1.51	309	278
11	473	10-15	--	Gage Failed -- No Record				
12	564	10-13	--	112	151.7	0.83	301	153
13	678	5-20	--	127		0.64	537	172
14	998	2-12	--	137		0.455	350	93
15	4190	48-4	--	180		0.116	350	25.5

TABLE 3.4 DYNAMIC PRESSURE RESULTS

<u>Station No.</u>	<u>Ground Range (ft)</u>	<u>Elevation (ft)</u>	<u>Maximum Dynamic Pressure (psi)</u>	<u>Dynamic Pressure Impulse (psi-msec)</u>
6	156	2	23.5	258
	155	10	24.0	94
	156	30	23.0	180
7	201	2	12.3	194
	199	22	13.7	141
	200	52	9.5	82
8	250	2	4.5	40*

* Extrapolated total head record crossover of side-on record at 20 msec.

Table 3.5 Drag Gage Results

Station No.	Ground Range (ft)	Elevation (ft)	Gage No. Axis Sy Ch	Arrival Time (msec)	Maximum Force (psi)	Axis** Angle	Maximum Resultant Force * (psi)
6	156	2	2 2 12	42.75	44	0°	44
	155	10	(x) 3 3	42.6	38.8	+46°	55.6
			(Y) 3 4	42.6	39.8	-43°	71***
	156	30	(x) 2 10	43.9	33.5	-51°	
7	201	2	(y) 2 9	66.75	21.5	0°	21.5
			3 10		17.5	56°	28.7
	199	22.4	(x) 2 5	66.8	20.1	-42°	24.1
			(y) 2 4	66.8	22.9	0°	
	200	52.3	(x) 3 12	69.9	7.4	90°	
			(y) 3 13	69.9			

* Simulated Extrapolated Values

** Positive force axis directed at listed angle with respect to ground plane

*** Calculated assuming flow direction along radius from G2

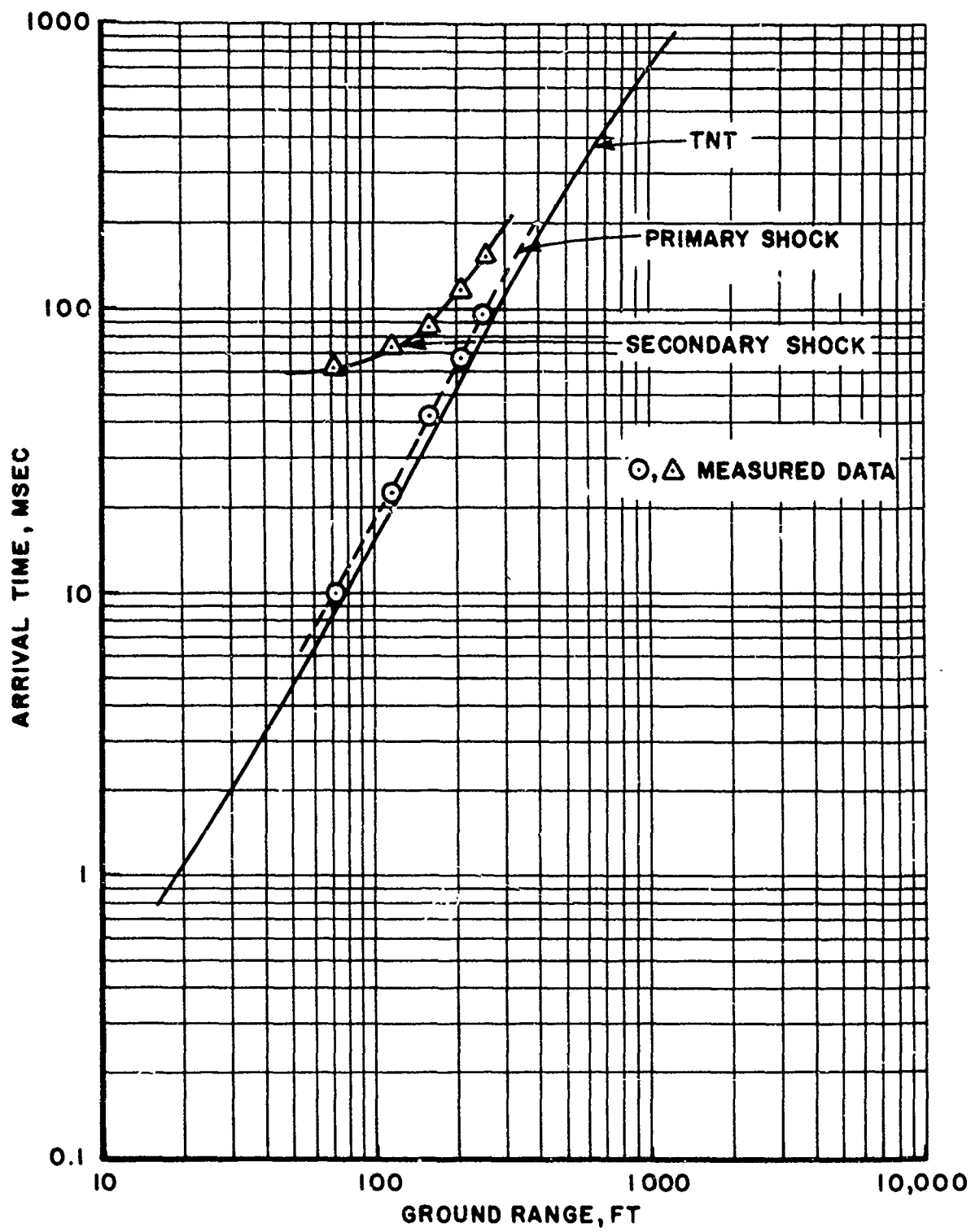


Figure 3.4 Arrival Time Versus Ground Range For Event 2A

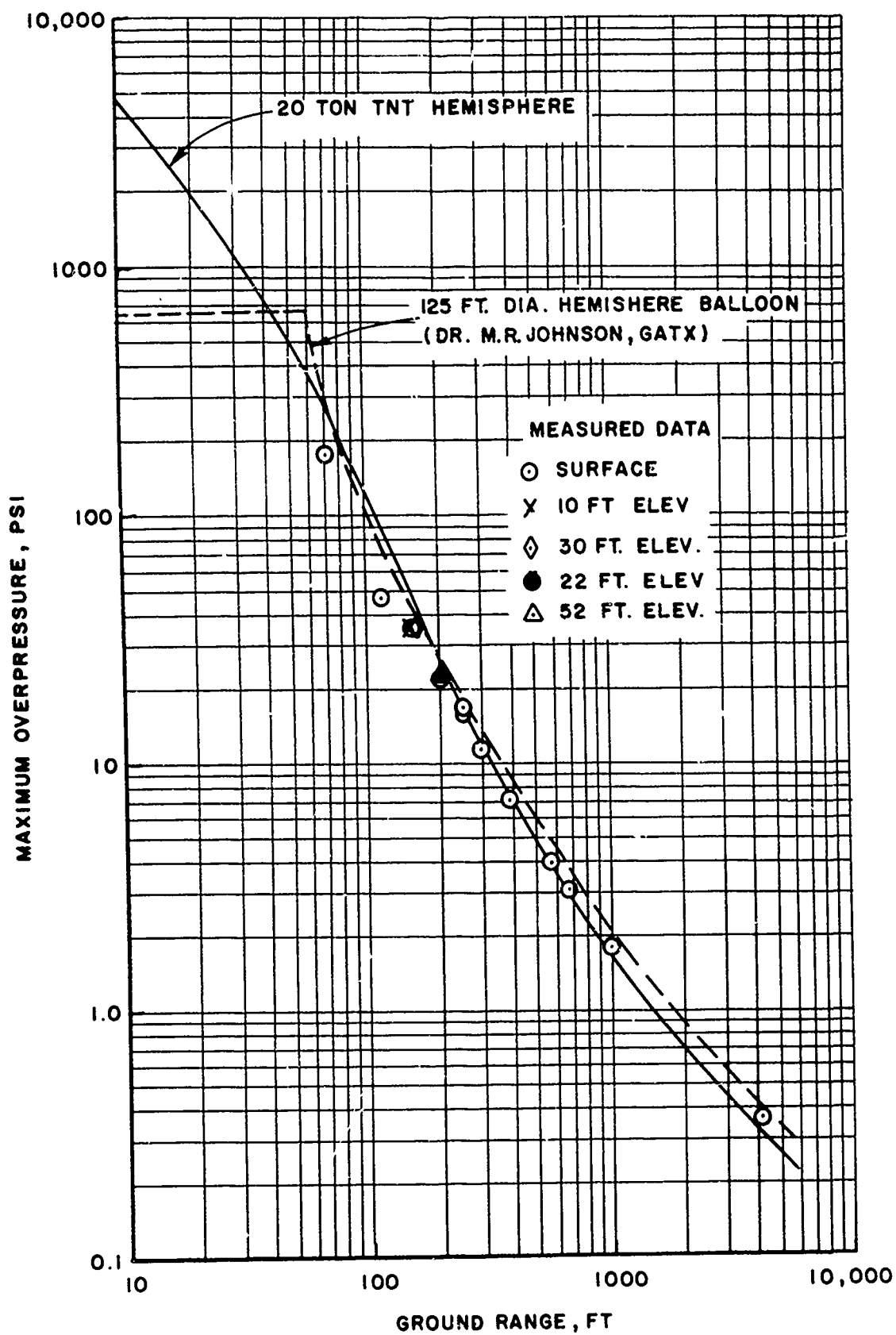


Figure 3.5 Maximum Overpressure Versus Ground Range For Event 2A

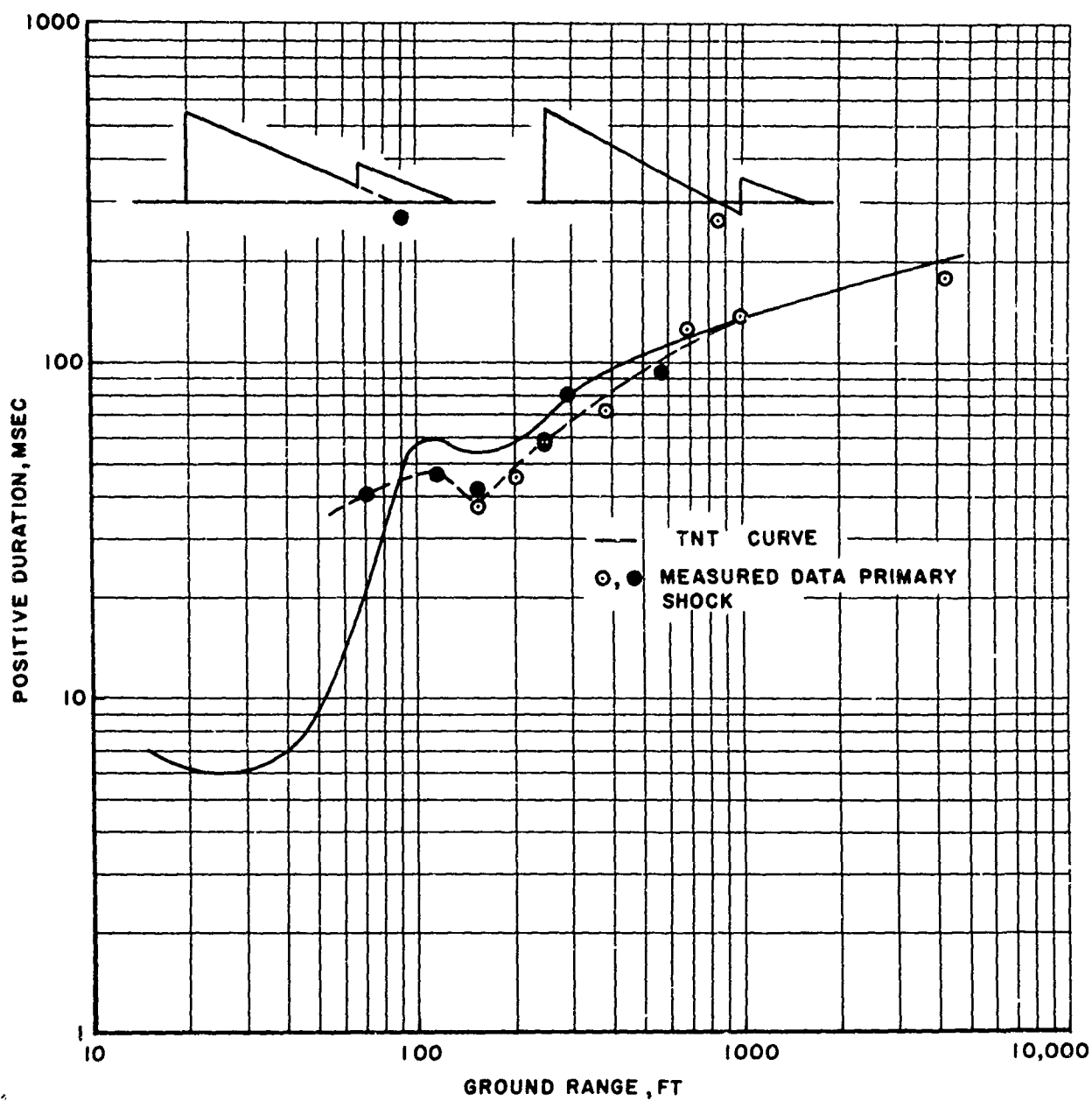


Figure 3.6 Positive Duration, Primary Shock Only,
versus Ground Range for Event 2A

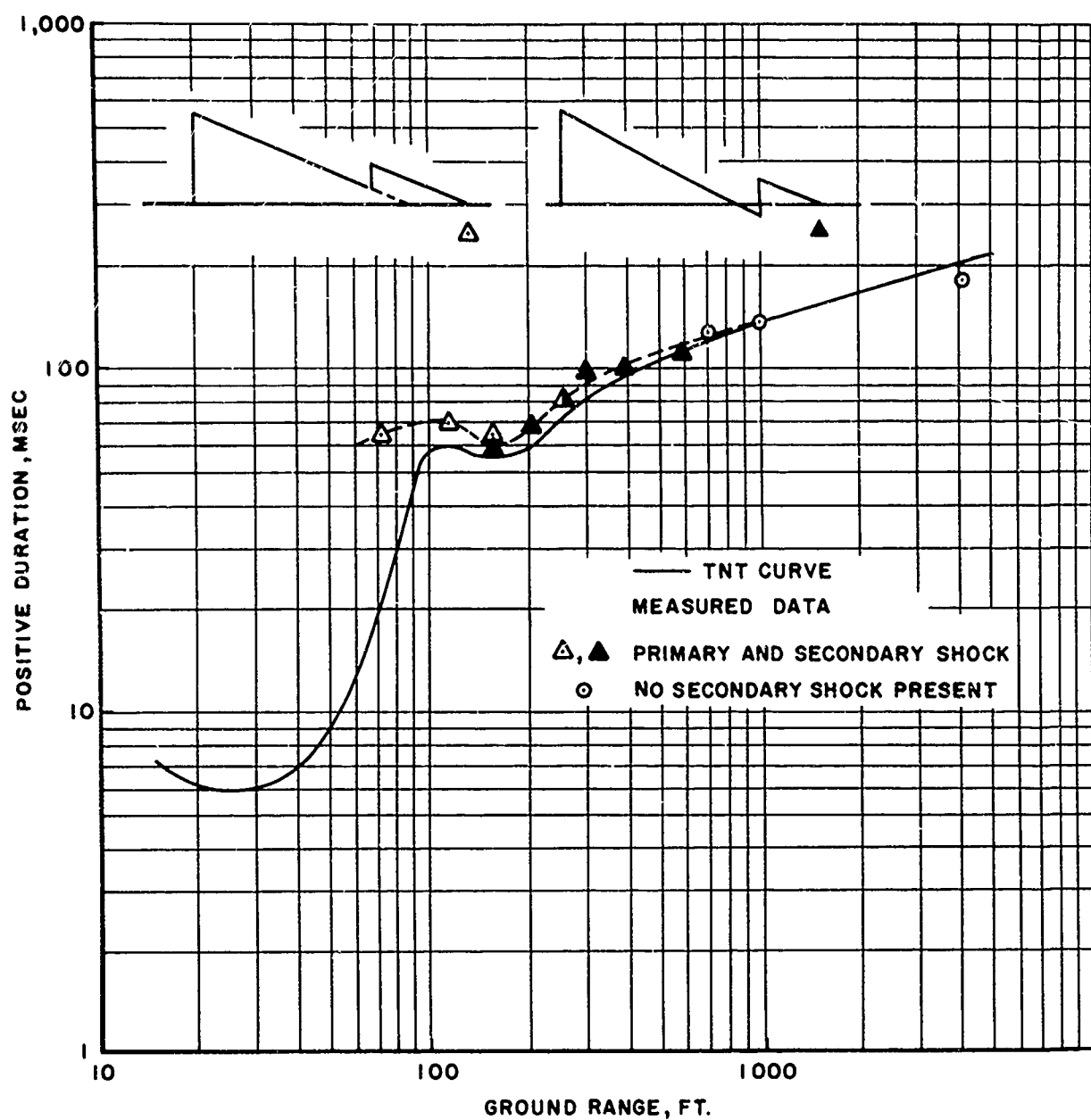


Figure 3.7 Positive Duration, Primary and Secondary Shock, versus Ground Range for Event 2A

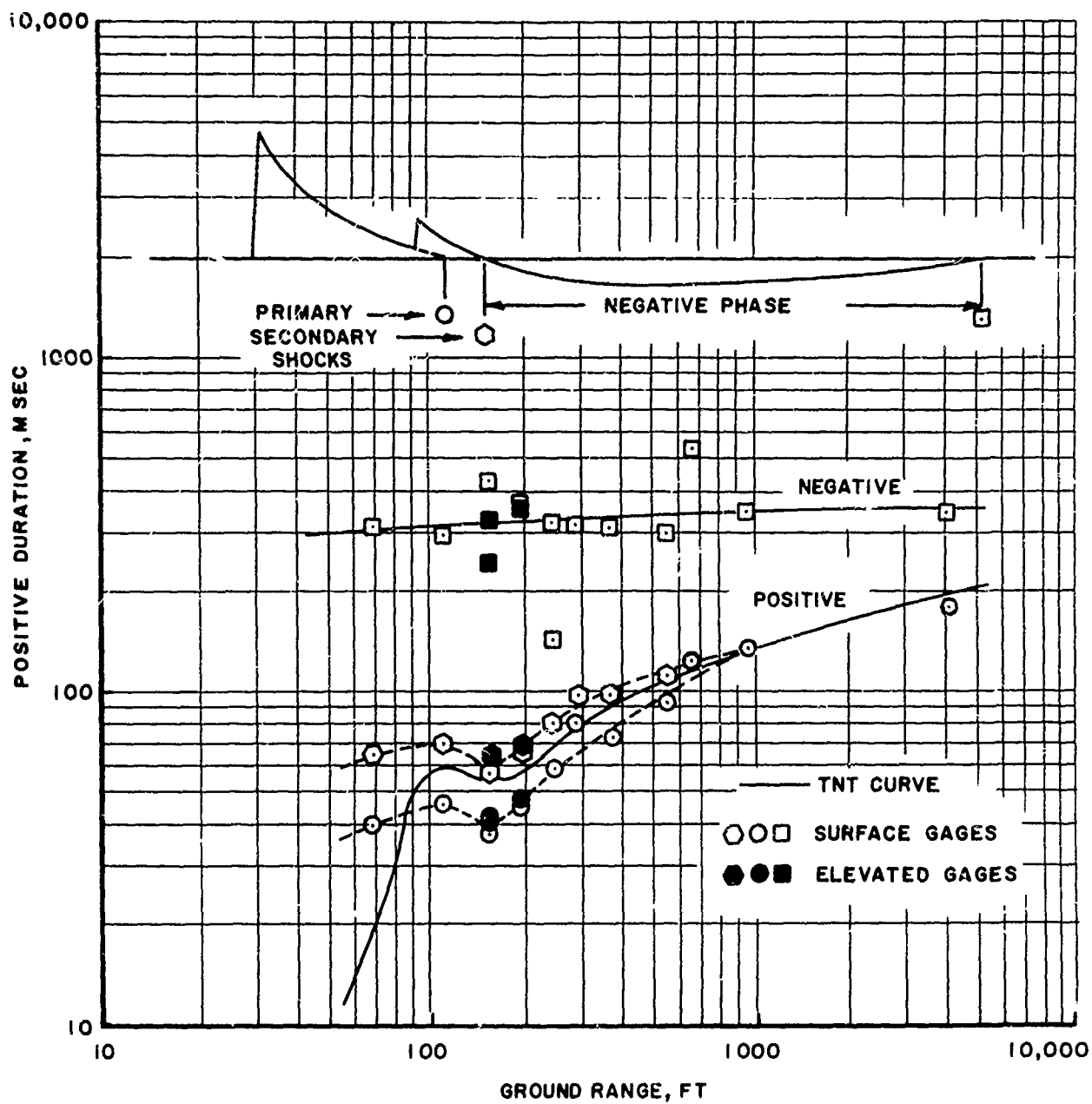


Figure 3.8 Positive and Negative Duration versus Ground Range for Event 2A

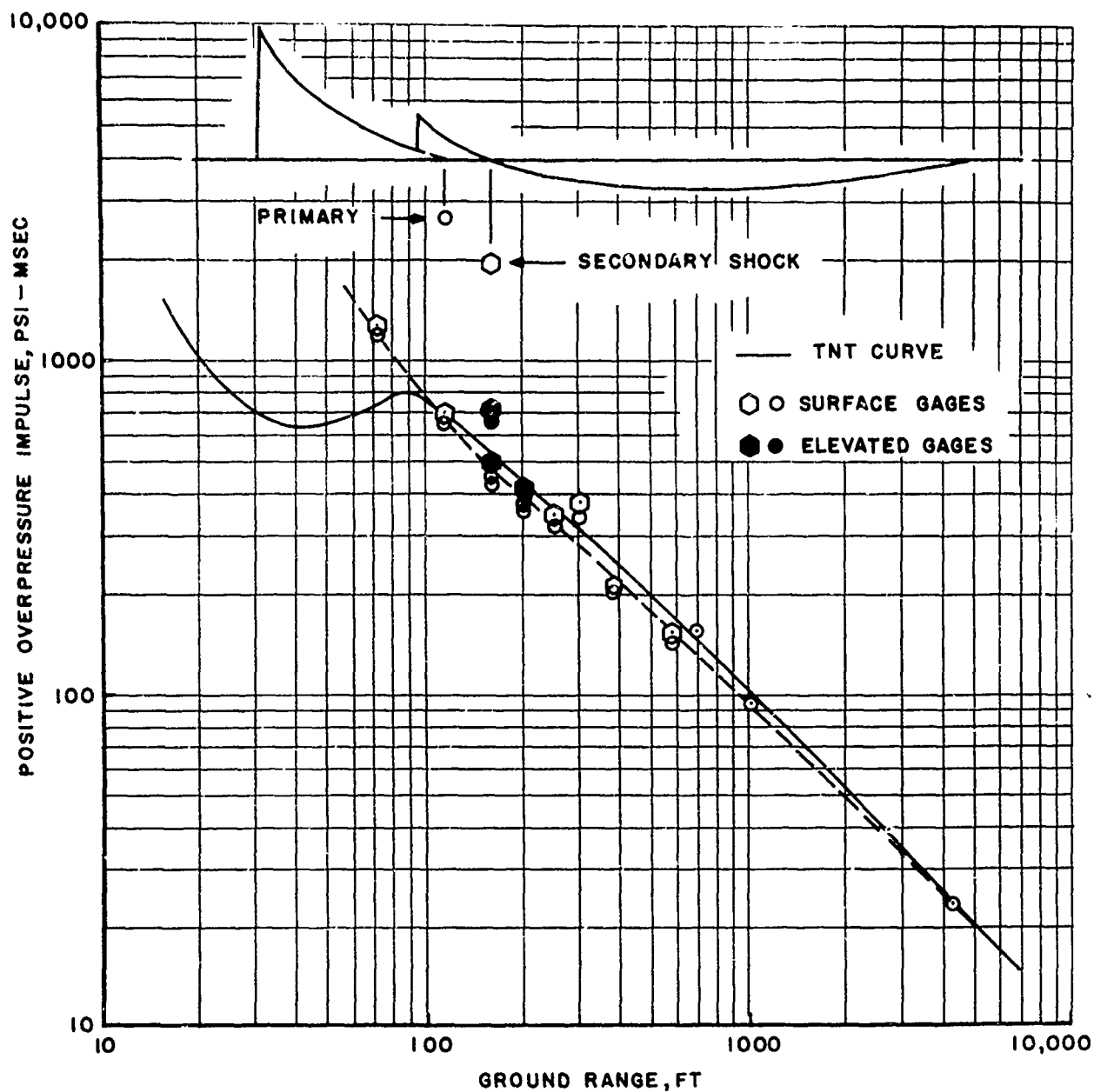


Figure 3.9 Positive Overpressure Impulse versus Ground Range for Event 2A

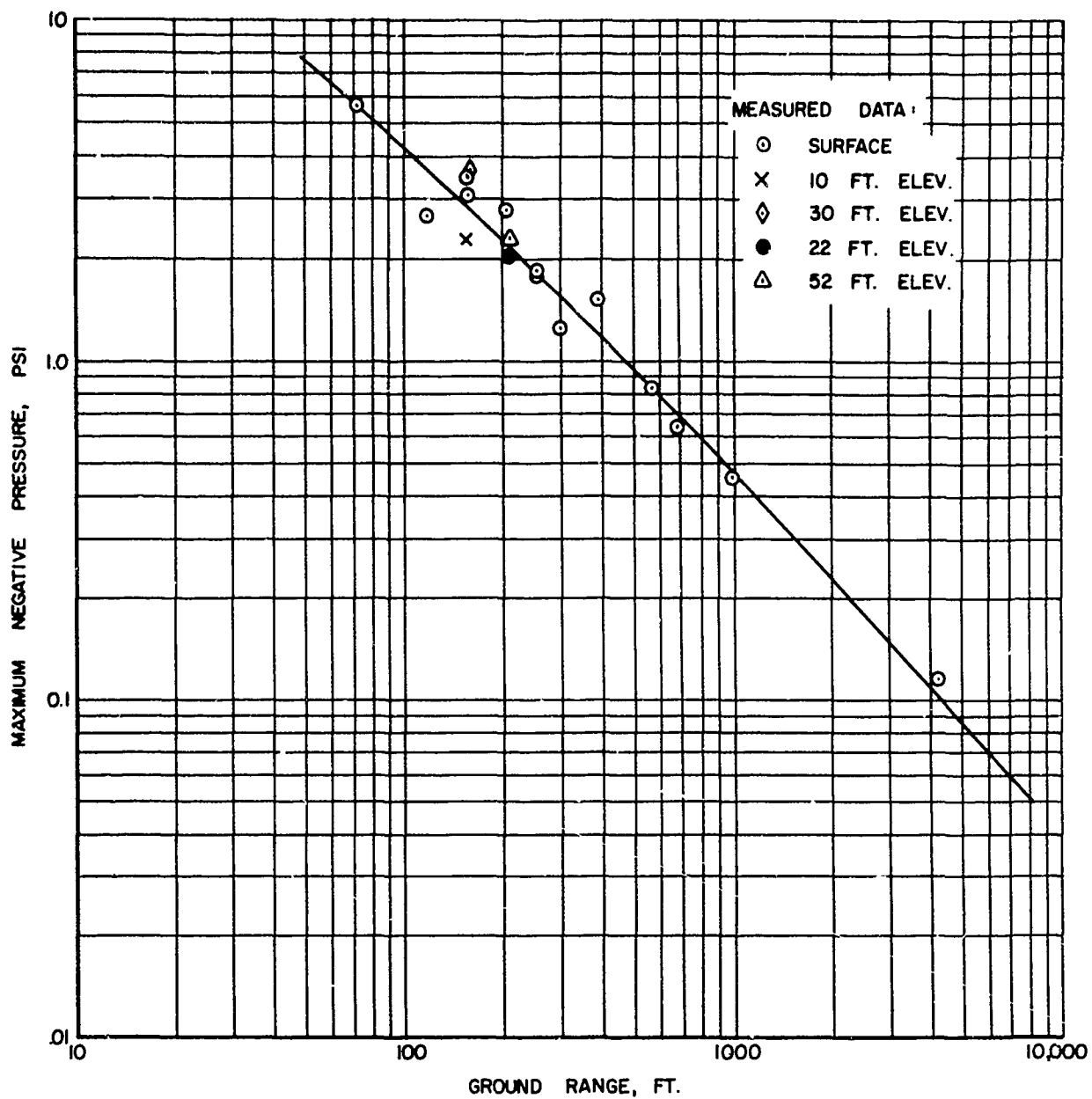


Figure 3.10 Maximum Negative Pressure versus
Ground Range for Event 2A

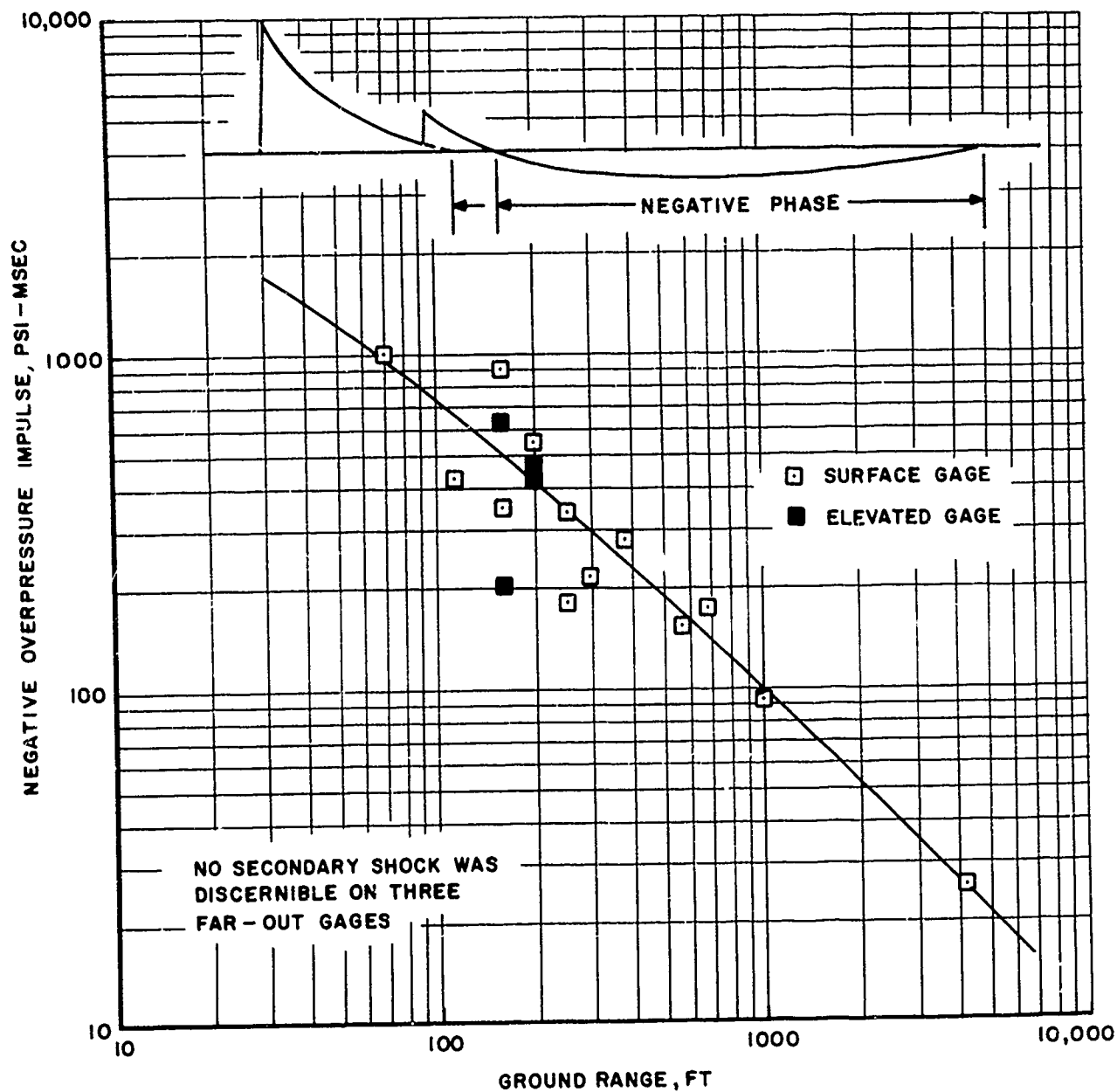


Figure 3.11 Negative Overpressure Impulse versus Ground Range for Event 2A

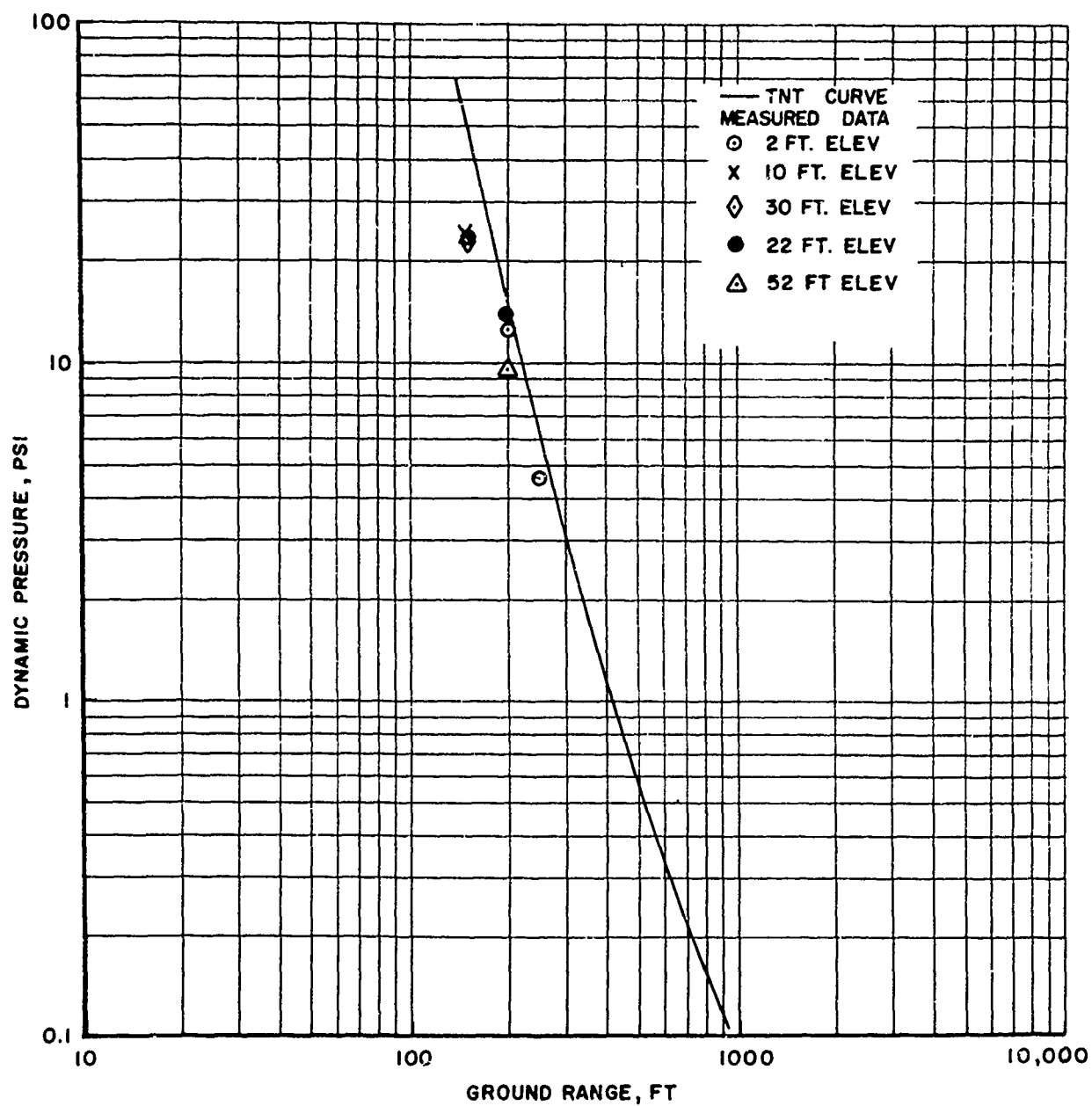


Figure 3.12 Dynamic Pressure versus Ground Range for Event 2A

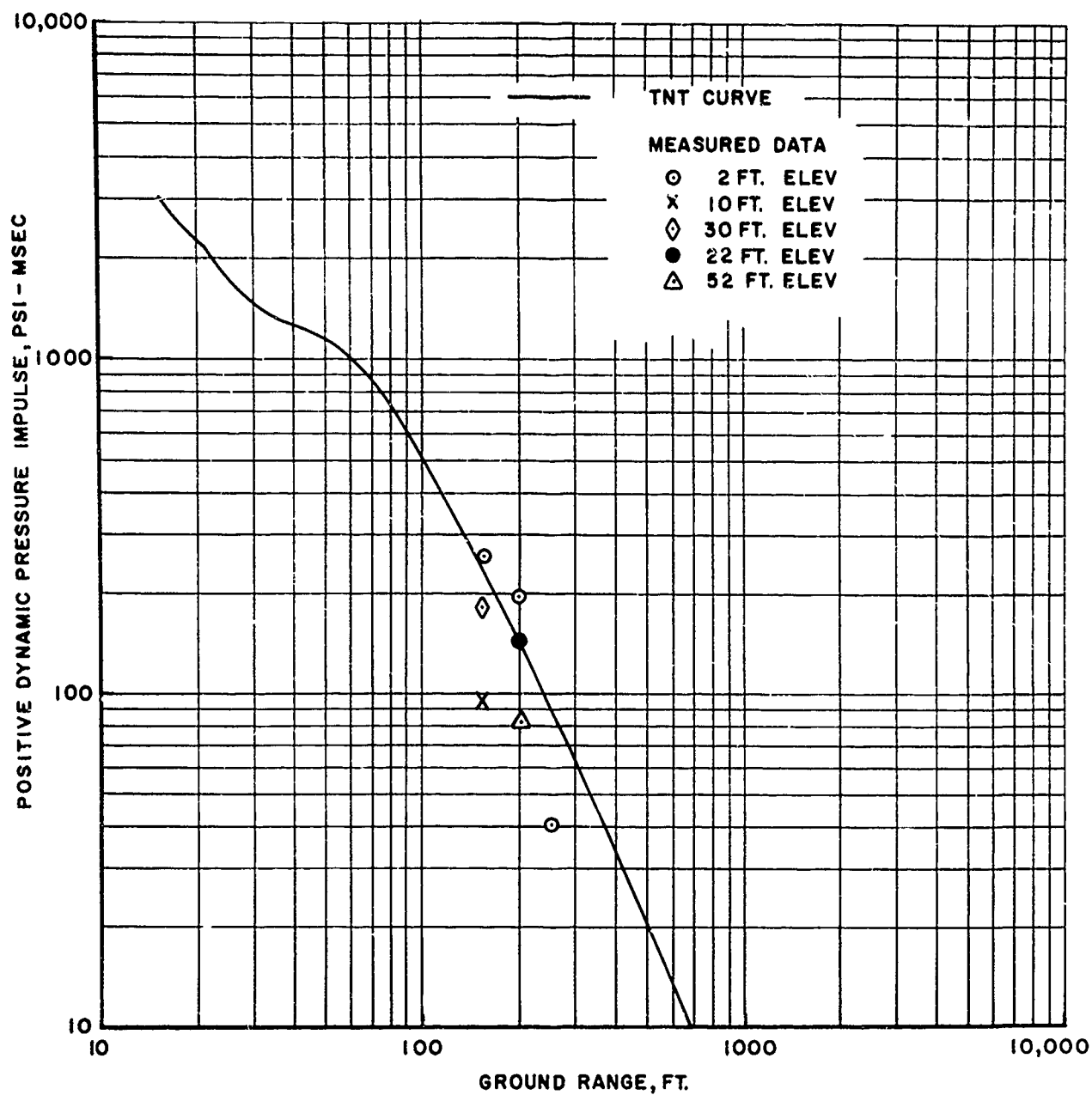


Figure 3.13 Dynamic Pressure Impulse
versus Ground Range for Event 2A

included whereas Figure 3.6 shows the data where the secondary shock is excluded. In some cases extrapolation was necessary in order to arrive at the duration of the primary shock.

Time histories of the waves are presented in Appendix A.

4. DISCUSSION

4.1 Gage Records

A very clean waveform is seen in the gage records over the ground range instrumented. Some perturbations, however, are evident at the closest stations, Stations 4 and 5, 70 and 116 feet from the center of the balloon. These variations may well be due to uneven breakup of the balloon panels.

Slower rise times than usual are evident at these stations. We feel these are real, that they result from the nearness of the gages to the balloon where the blast wave has not fully developed into a sharp shock.

A secondary shock seen developing around 45 msec at Station 5 at 116 feet and continuing beyond 500 feet influenced the positive phase duration measurements. In some instances the secondary shock occurred within the positive phase duration while in other cases it occurred as a positive shock after the wave had gone negative.

4.2 Comparison of Elevated and Surface or Near-Surface Gage Records

The elevated gages were very nearly at the same slant range from Ground Zero as the gages mounted on or near the ground surface. The elevated gages were at the same azimuth angle, but the surface or near-surface gages were located about 20 feet away from the base of the tower

supporting the elevated gages.

Figure 4.1 shows a comparison of overpressure records measured at station 6. The reflected wave from the tower appears on the elevated gage records beginning at about 3 milliseconds. Because of this reflection the gage record at 10 feet is significantly higher and different from the surface and the 30 foot gage record where the tower diameter is small and the station is located at the top of the tower.

Figure 4.2 shows the total head gage records obtained at Station 6. Here there is indeed very little difference between the records. The record at 10 feet does not show the peak before reflected shock arrival as occurred on the overpressure record. Since the total head gage does respond to the overpressure field, this suggests that the overpressure record at 10 feet is questionable, and hence any dynamic pressure calculated using it would be questionable.

Figure 4.3 shows the dynamic pressures as determined from overpressure and total head gage records for elevations of 2 feet and 30 feet. The value at 30 feet is lower than at 2 feet, although the rate of decay seems about the same. Since the elevated gages were affected by tower reflections, and the total head gage at 30 feet was measuring flow about 11 degrees off the gage axis, it is difficult to state how much the difference shown in Figure 4.3 is due to these effects and how much, if any, is real.

The drag records obtained at this station are shown in Figure 4.4. The records obtained at 10 feet and at 30 feet elevations are shown corrected to an assumed direction of flow corresponding to the angle of

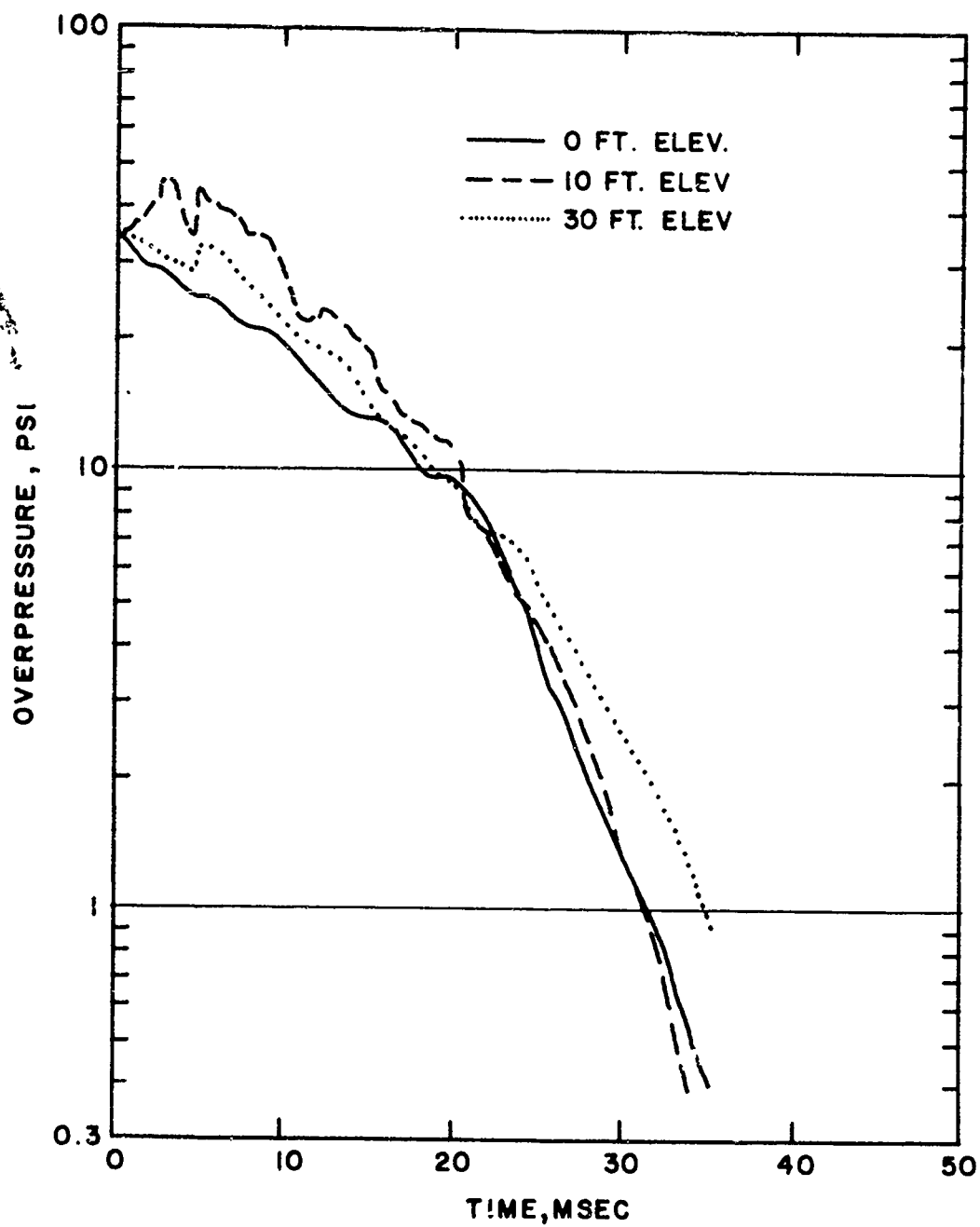


Figure 4.1 Overpressure versus Time Measured at Different Elevations
at Station 6, 156 feet

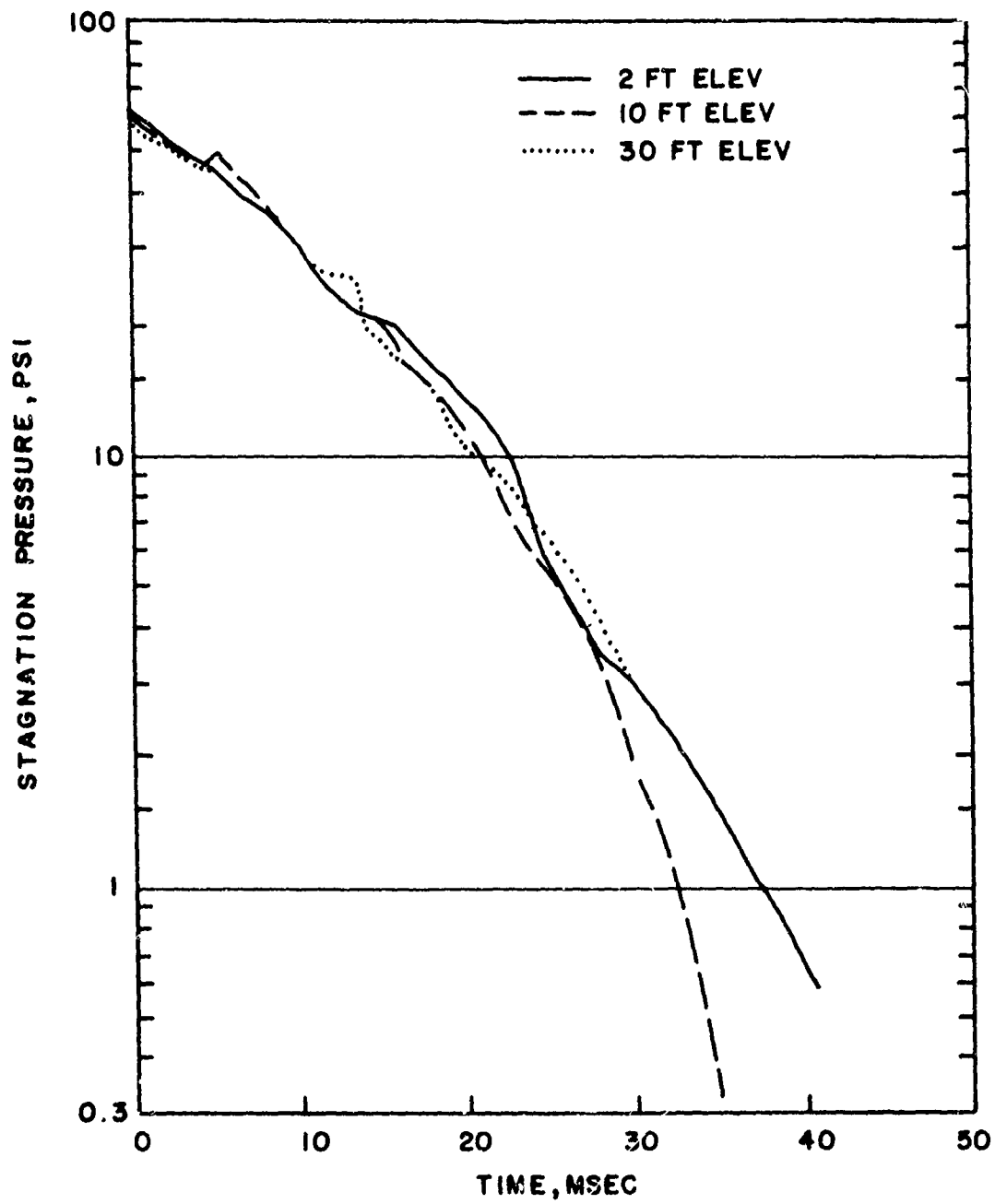


Figure 4.2 Stagnation Pressure versus Time Measured at Different Elevations at Station 6, 156 Feet

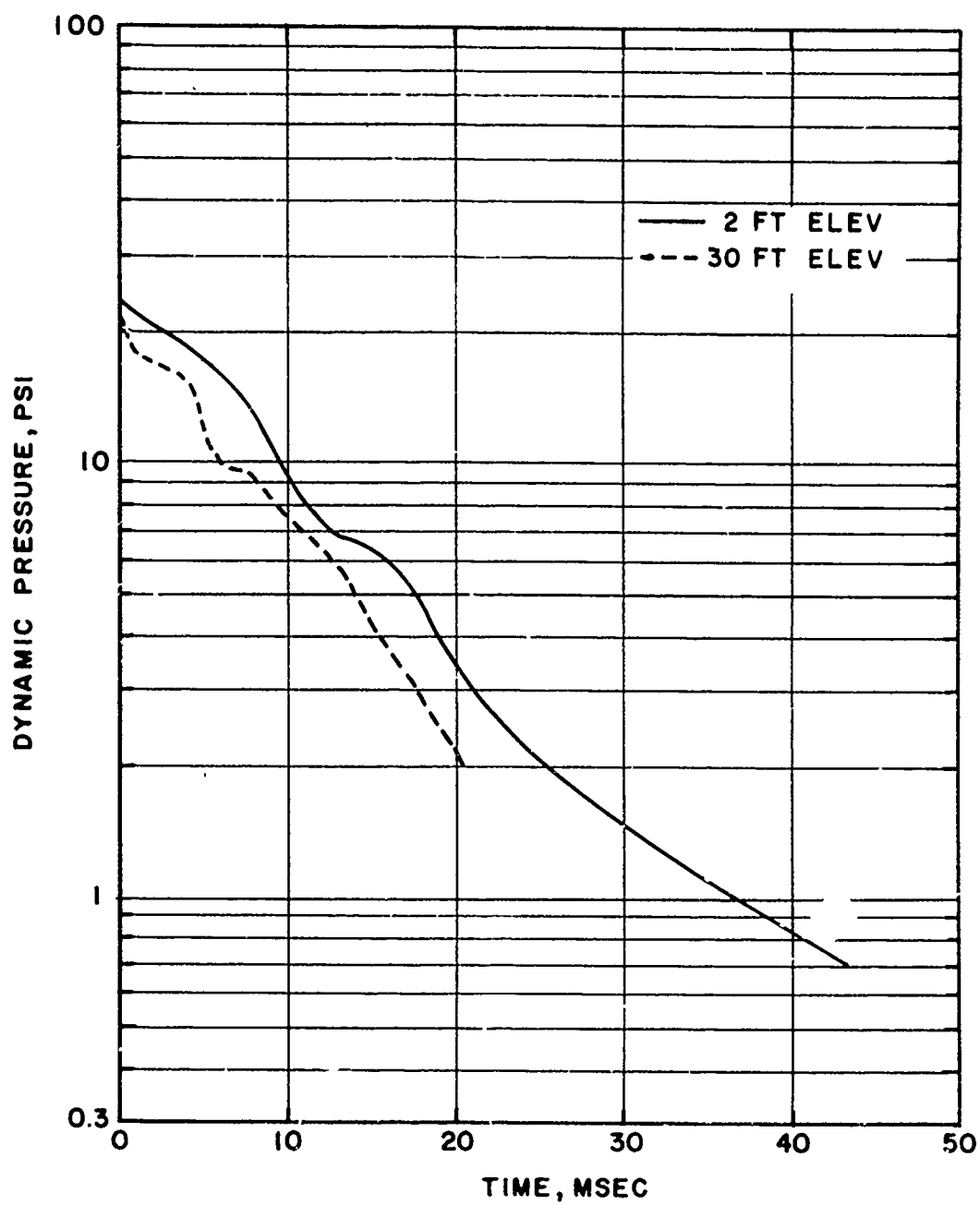


Figure 4.3 Dynamic Pressure versus Time for Different Elevations
at Station 6, 156 Feet

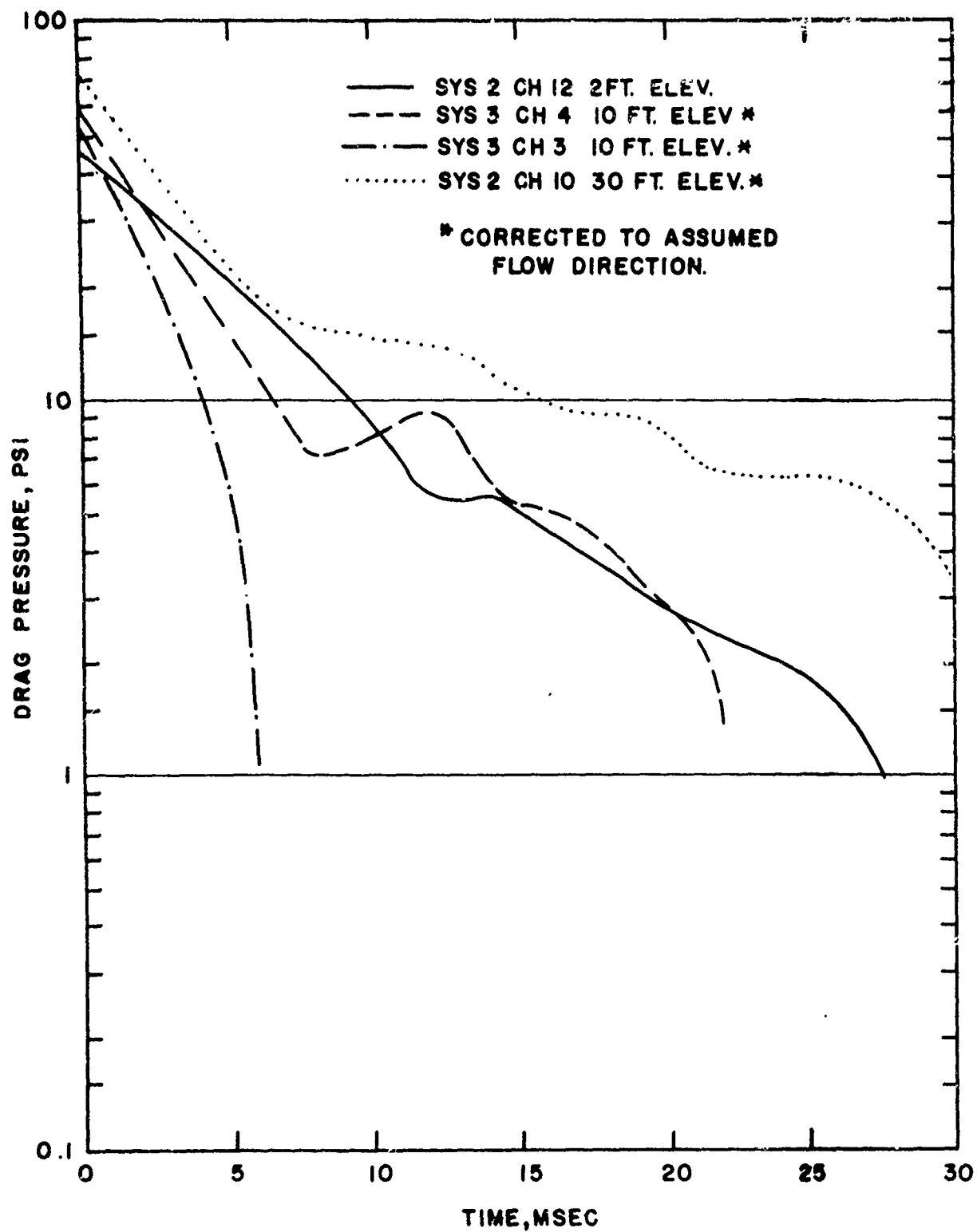


Figure 4.4 Drag Pressure versus Time Measured at Different Elevations at Station 6, 156 Feet

elevation of the radius from Ground Zero through the gage. Only one gage axis was active at 30 feet, and at 10 feet the record from one gage axis (channel 3, system 3) showed an abnormal rate of decay, thus no resultant force using data from two gage axes could be computed for either gage.

Correction to the assumed direction of flow involved dividing the gage data by the cosine of the angle between the gage axis and the assumed direction of flow. Since these angles were about 45 degrees, the additional percentage error introduced into the gage records by this process was about the same as the percentage error in the angles.

The records from each axis of the gage at 10 feet were treated independently, and the peak values obtained agree very well. The records at 10 feet and 30 feet elevations show higher peak values of drag pressure but a more rapid rate of decay than occurs at the two foot elevation.

Figure 4.5 shows a comparison of overpressure records measured at Station 7. The reflected wave from the supporting tower struck the elevated gages at about 4 milliseconds. The reflected wave was stronger at 22 feet because of the larger diameter of the tower at that elevation. The records agree very well at about 20 milliseconds. Beyond that time, the gage record at 52 feet seems to decay less rapidly than those measured at 22 feet and at the surface.

Figure 4.6 shows the total head gage records obtained at Station 7. The reflected wave from the tower arrived at the elevated gages at about 17 milliseconds. The peak on the two foot gage record is a reflection from the tower base. The records at two feet and 22 feet agree very well

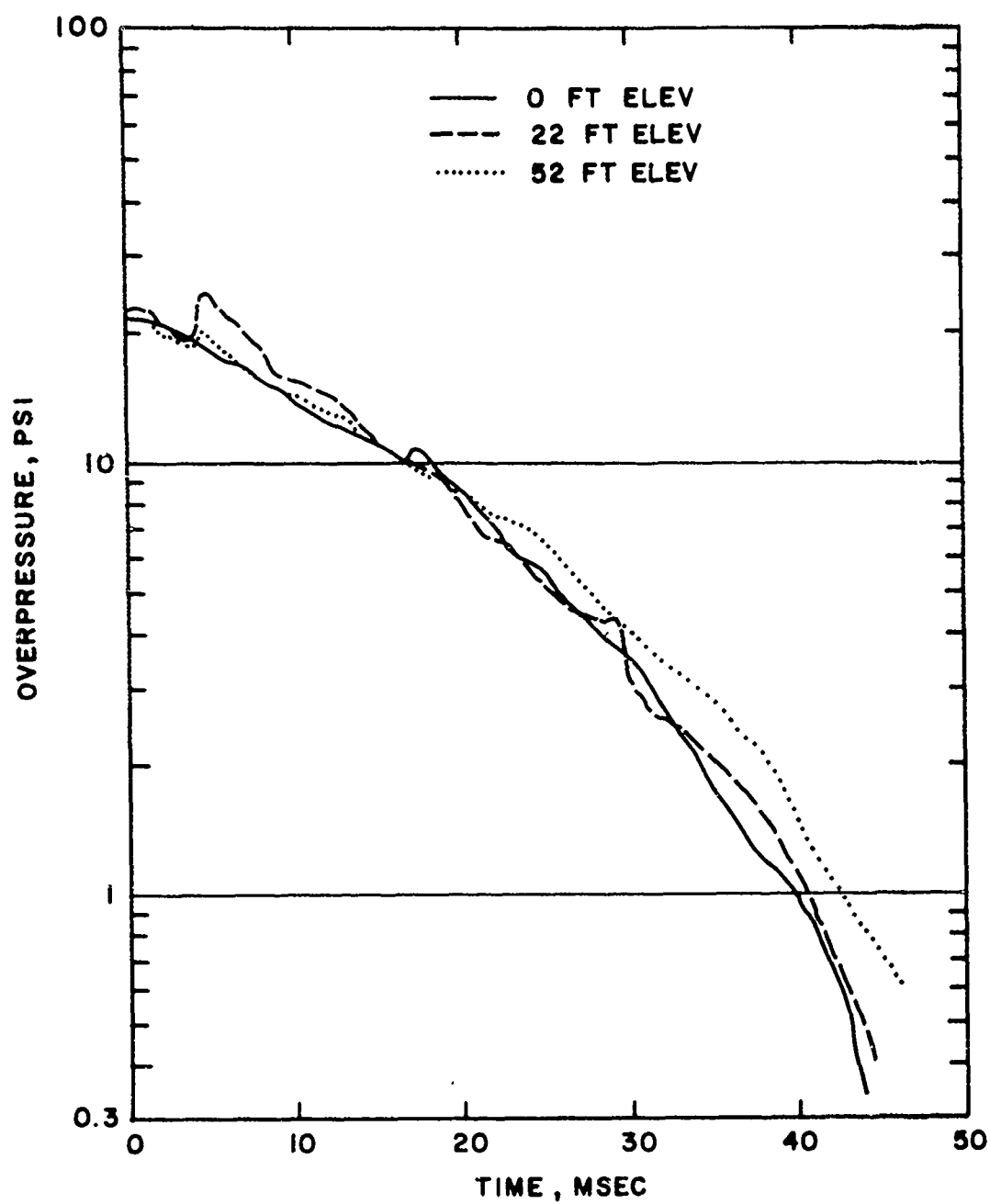


Figure 4.5 Overpressure versus Time Measured at Different Elevations at Station 7, 201' Feet

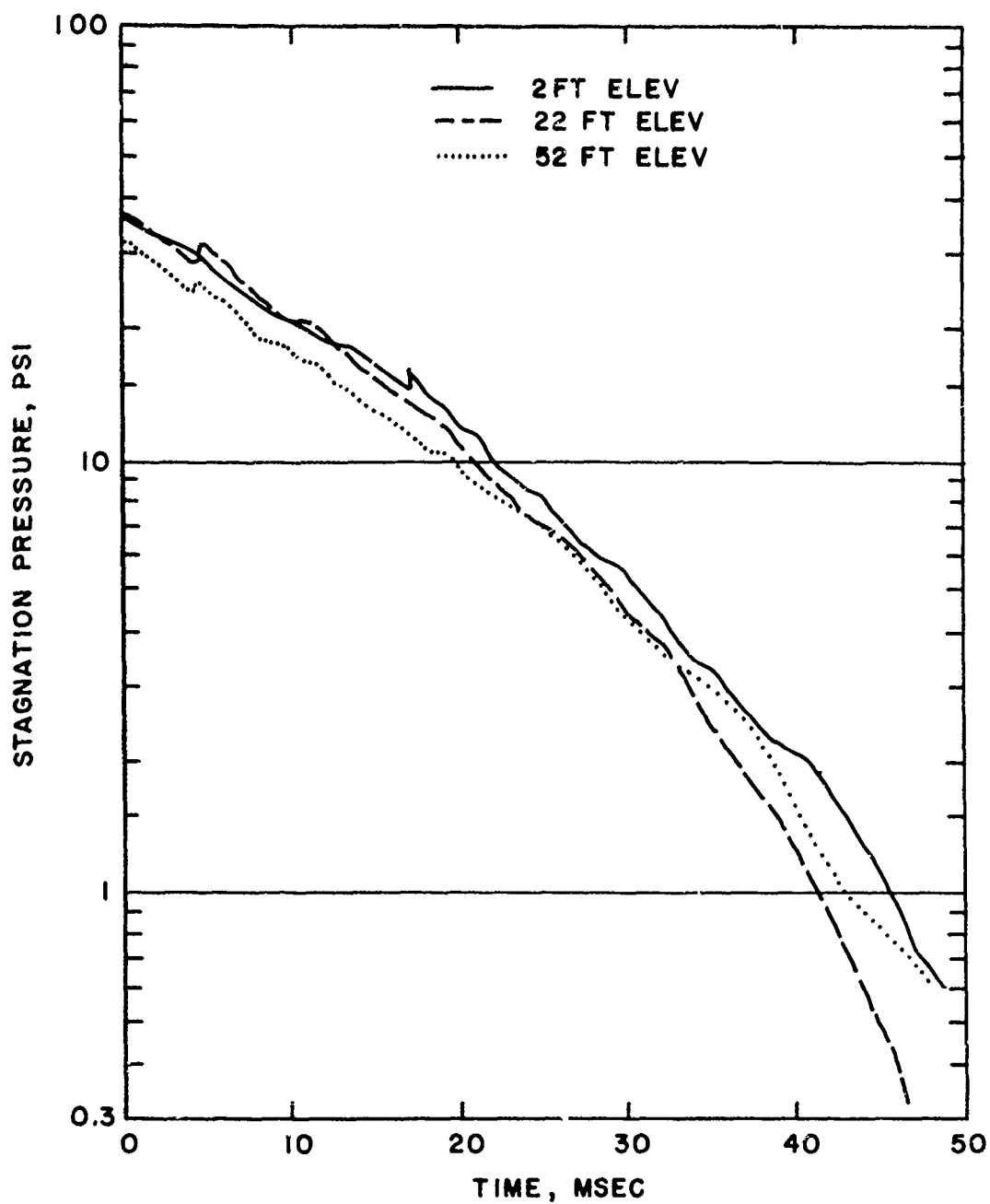


Figure 4.6 Stagnation Pressure versus Time Measured at Different Elevations at Station 7, 201 Feet

initially. The angle of elevation of a radius from Ground Zero through the gage at 22 feet is 6.4 degrees, while for the gage at 52 feet, the angle is about 15 degrees. The total head gages were mounted parallel to a level ground plane, so that these angles indicate the inclination with respect to the flow if the blast wave were symmetric. The 15 degree off-axis flow may account for the lower magnitude of the record obtained at the 52 foot elevation. There is a slight indication in Figure 4.6 that the rate of decay of the elevated gage records may be more rapid than for the gage record obtained at 2 feet.

Figure 4.7 shows the dynamic pressure calculated using the overpressure and total head gage records at each gage station. The surface overpressure record was used in conjunction with the total head gage record at two feet for the calculation. The dynamic pressures agree initially at two feet and at 22 feet, but at 52 feet the record is low at all times. As at Station 6, it is difficult to determine how much, if any, of the reduction is real because of the off-axis flow and the reflection from the gage tower.

The drag records obtained at this station are shown in Figure 4.8. Here both gage axes were active and provided reasonable records at 22 feet and at 52 feet. The records plotted in Figure 4.8 for these elevations are the resultant drag pressures computed using records from the two axes of each gage. The peak magnitudes are higher for the gages on the tower, although not radically so. The initial rate of decay seems to match for the two elevated gages for about the first three milliseconds. After three milliseconds all the gage records differ.

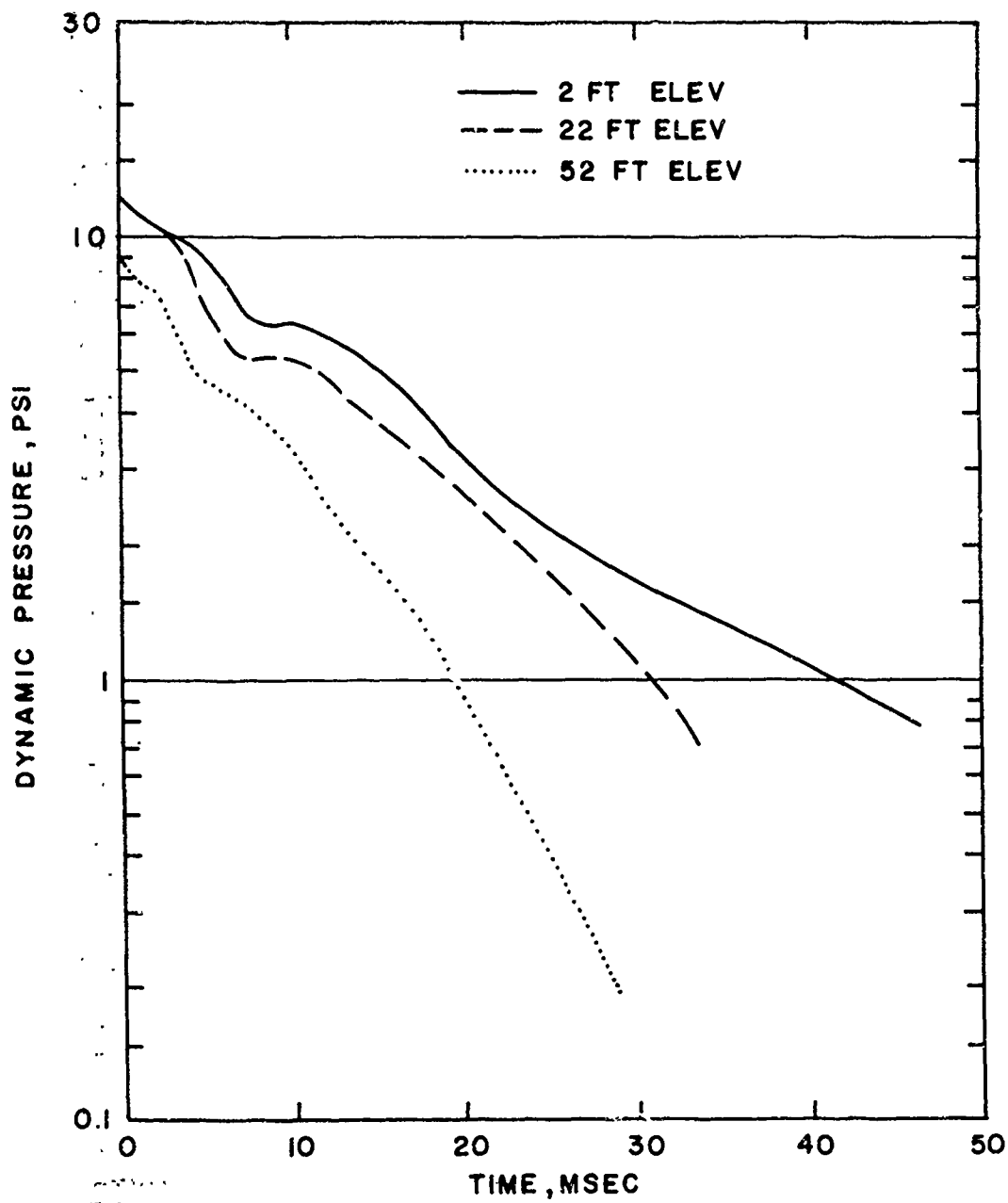


Figure 4.7 Dynamic Pressure versus Time at Different Elevations
at Station 7, 201 Feet

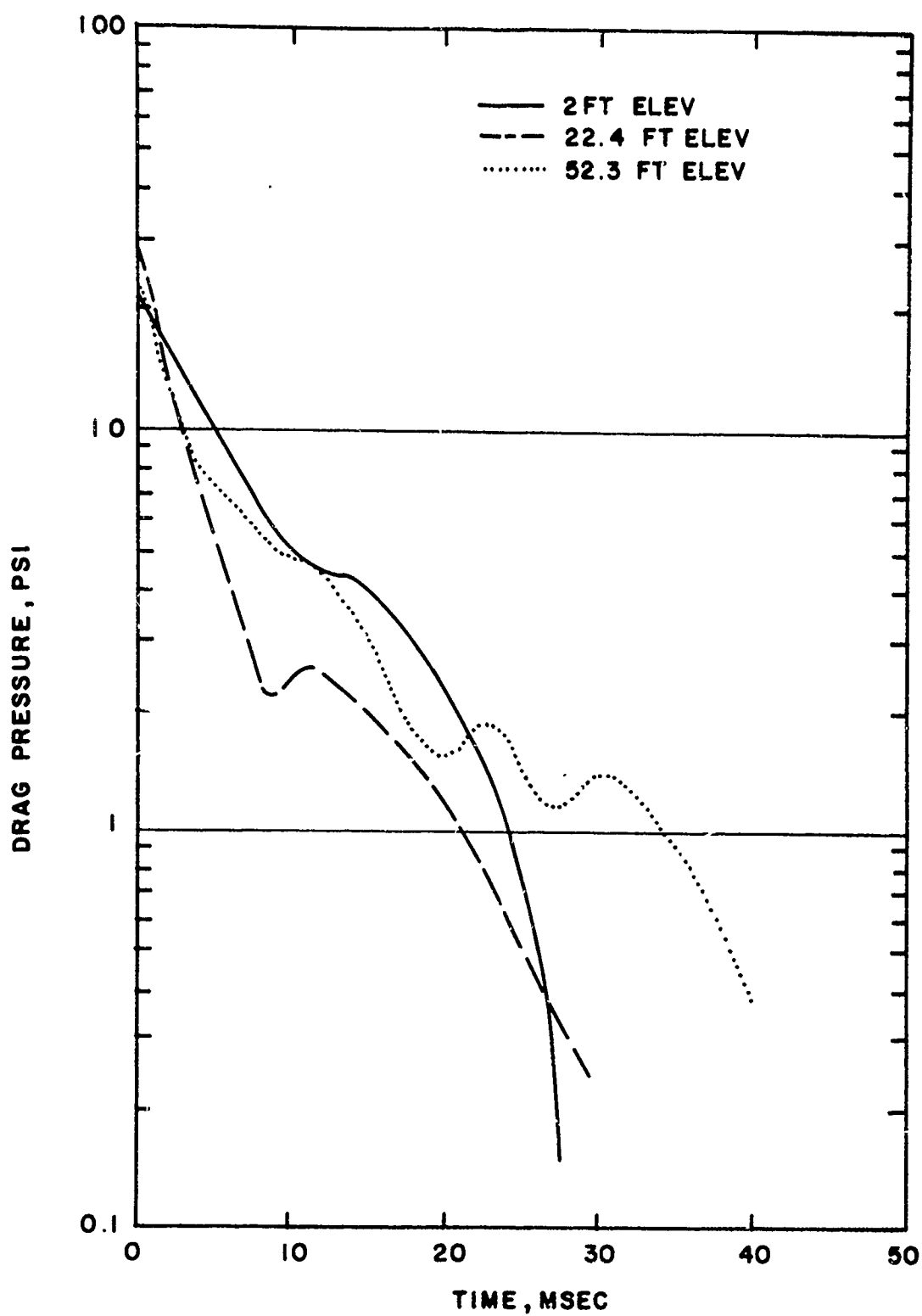


Figure 4.8 Drag Pressure versus Time Measured at Different Elevations at Station 7, 201 Feet

The elevated gage records at this station were used to calculate flow direction. The results obtained are shown in Figure 4.9 for the gage at 22 feet and in Figure 4.10 for the gage at 52 feet. The dashed horizontal line is the flow angle with respect to the horizontal plane, predicted assuming a symmetrical blast wave. Both gages show a flow angle which is off in the predicted direction, but the variation in angle is large. Since the gage records themselves have large oscillations, a slight mismatch in oscillations between records will produce large oscillations in the computed angle of flow. Thus these gage records do not seem to provide a reliable indication of the direction of flow versus time.

Figure 4.11 shows drag coefficients calculated using the resultant drag pressure and the dynamic pressure measured at the gage locations, except for Station 6, where dynamic pressure for the two foot elevation was used with the drag gage record at 10 feet. All drag coefficients show a rapid decay from an initial peak, with the rapid decay ending in times ranging from 3 to 10 milliseconds. The greatest differences at each station are for the highest gage, where the measured dynamic pressure records were quite low compared to the other gage locations.

Figure 4.12 shows drag coefficients computed using the dynamic pressure records obtained at the two foot elevation. Here the drag coefficients more nearly agree. The greatest deviation occurs for the gage record at 30 feet at Station 6 and the gage record at 22 feet at Station 7.

The agreement noted between surface and near-surface overpressure

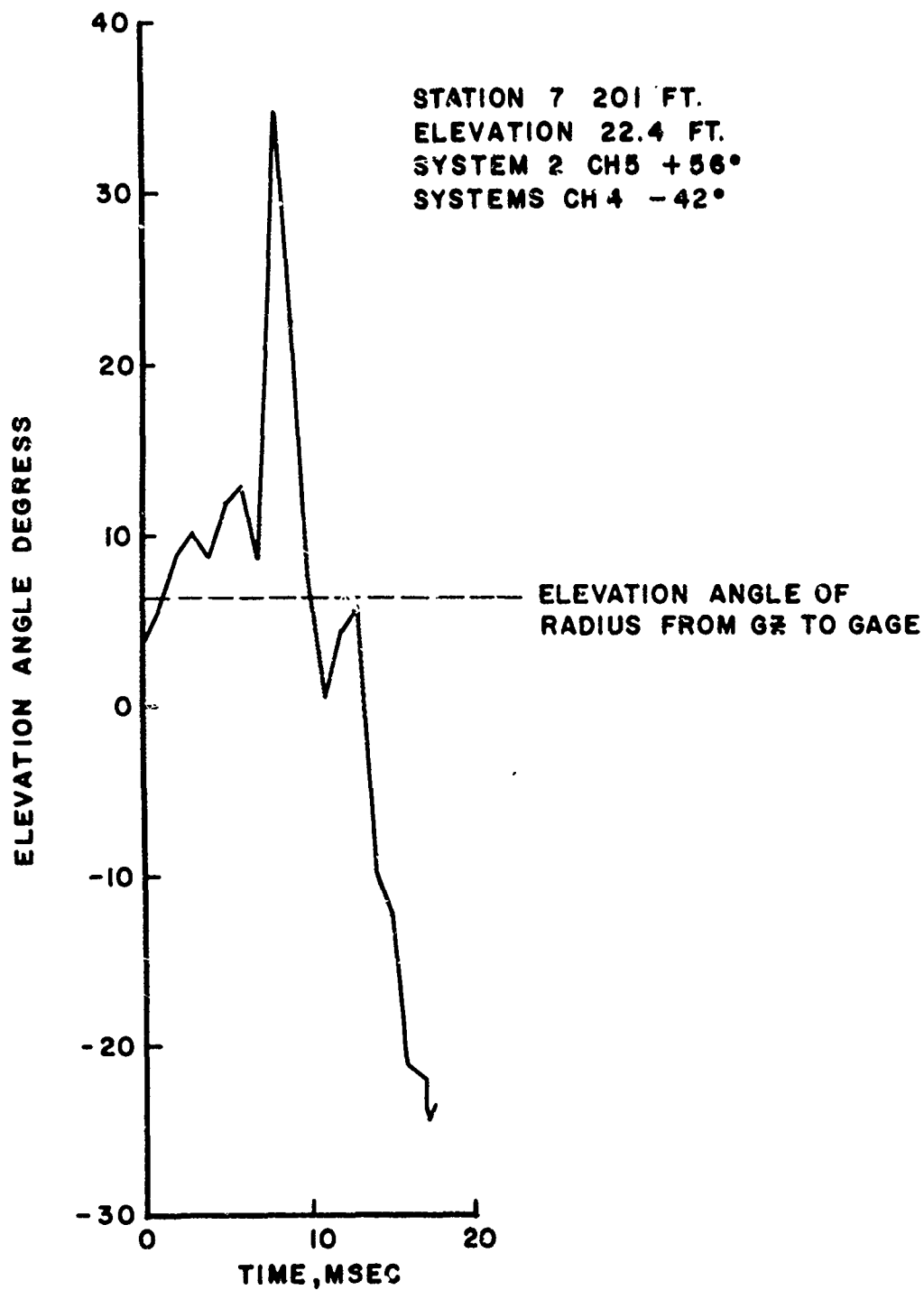


Figure 4.9 Direction of Flow as Derived from Drag Gage at 22 Foot Elevation, Station 7, 201 Feet

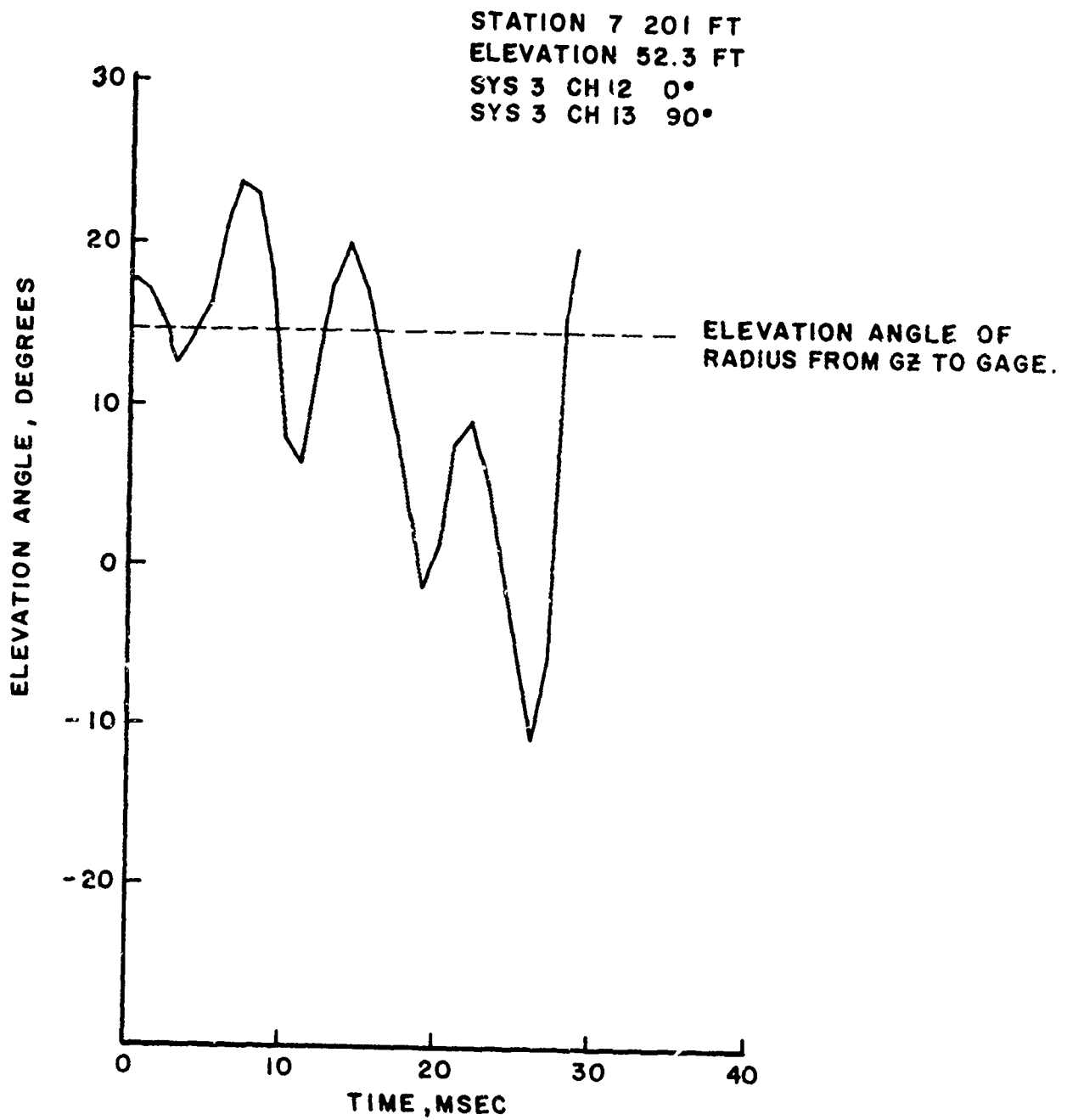


Figure 4.10 Direction of Flow as Derived from Drag Gage at
52 Foot Elevation, Station 7, 201 Feet

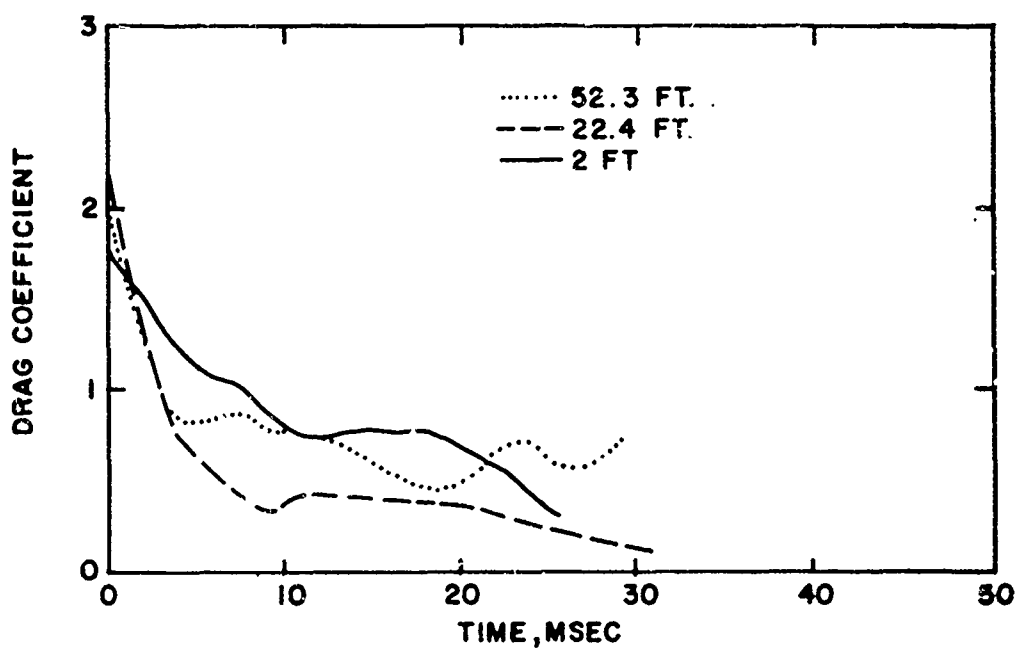
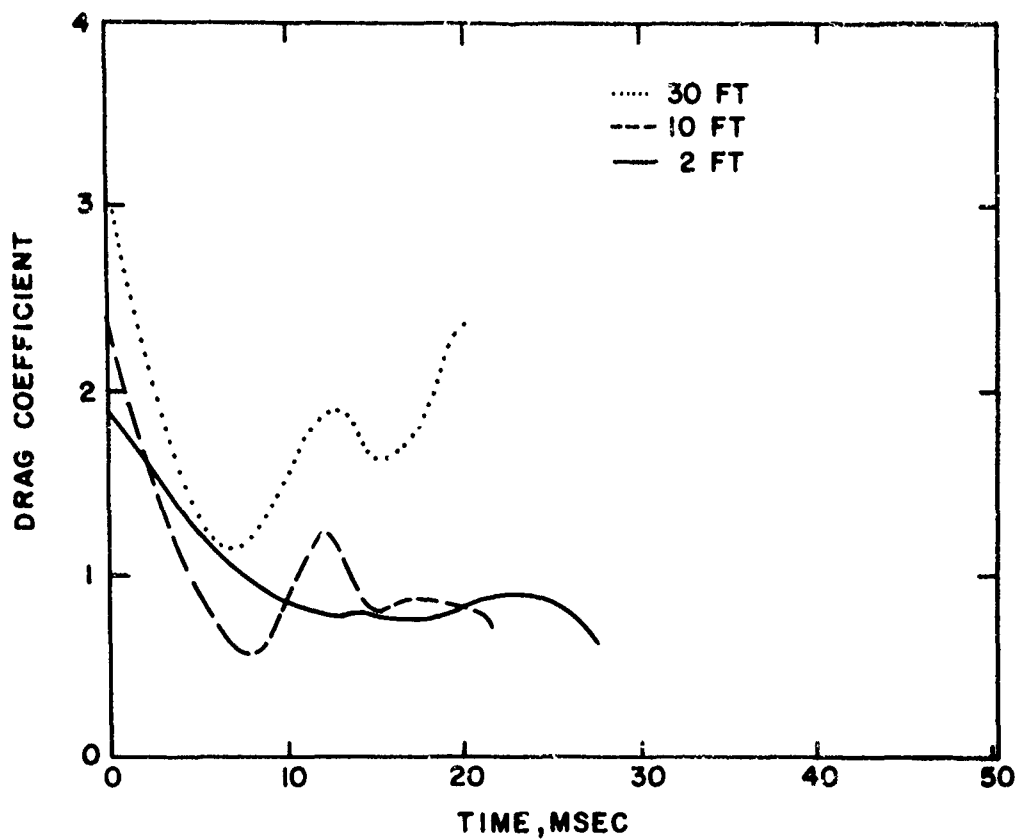


Figure 4.11 Drag Coefficients versus Time at Stations 6 and 7 Using the Dynamic Pressure Measured at the Gage Locations

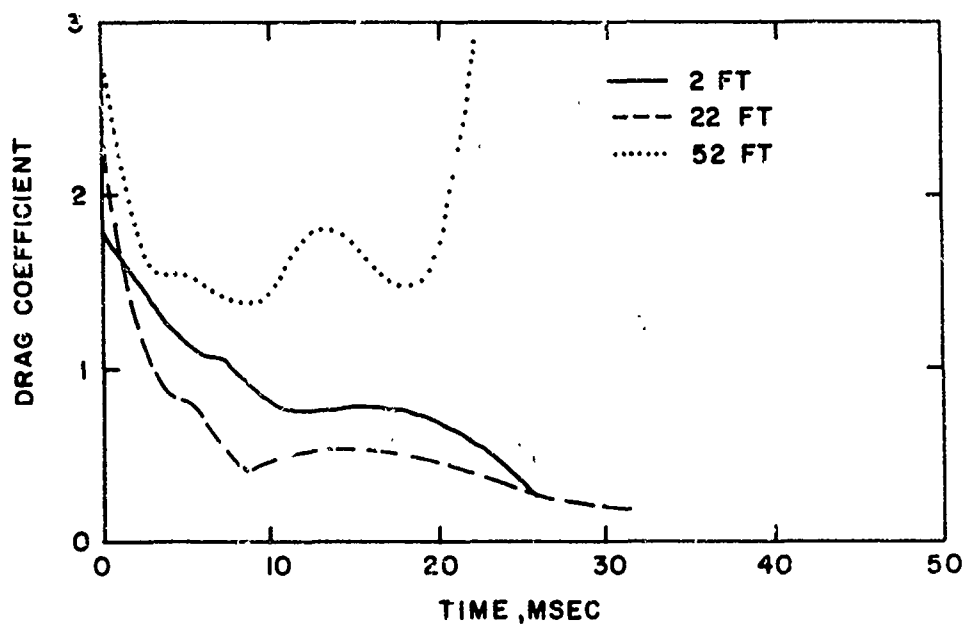
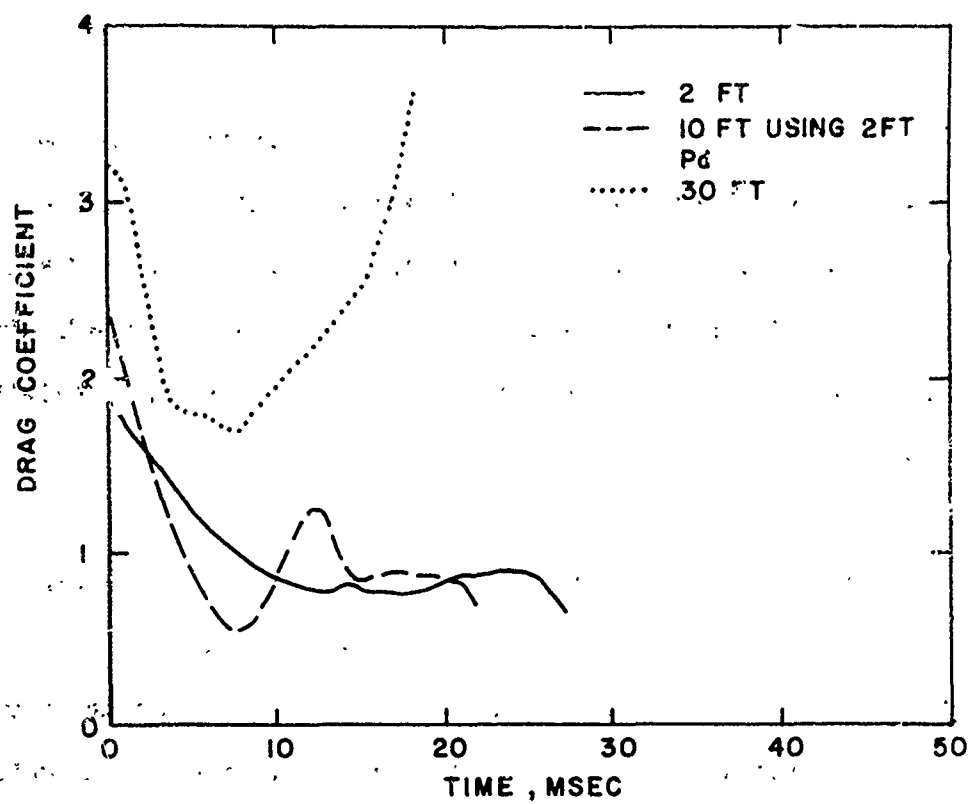


Figure 4.12 Drag Coefficients versus Time at Stations 6 and 7 Using the Dynamic Pressure Records Obtained at the 2 Foot Elevation

and total head gage records at Stations 6 and 7 indicate that the blast wave was reasonably symmetric. The difference in total head records and dynamic pressure records which were noted were probably caused by off-axis flow effects and tower reflections. The drag gage records differed significantly at each location, and did not provide a reliable indication of flow direction.

4.3 Scaling

The scaling laws, developed by Sachs while at BRL (Reference 7) were used to scale blast parameters to a standard explosion of 1 lb. of TNT in an atmosphere of 14.7 psi and at a temperature of 15°C, better known as the sea level standard. The three items that are needed to determine the scaling factors are ambient pressure, ambient temperature, and yield. For this shot, the ambient pressure was 13.71 psi, the ambient temperature 23.4°C, and the yield was 20 tons.

The scaling factor formulas and definitions are:

$$S_p = \frac{14.7}{P_o}$$

$$S_d = \left[\frac{P_o}{14.7 \times W} \right]^{1/3}$$

$$S_t = \left[\frac{T_o + 273}{288} \right]^{1/2} = S_D$$

$$S_I = S_p \times S_t$$

where:

S_p is the pressure scaling factor

S_d is the distance scaling factor
 S_t is the time scaling factor
 S_I is the impulse scaling factor
 P_o is the ambient pressure
 W is the yield in pounds
 T_o is the temperature in $^{\circ}C$

The numerical scaling factors are:

$S_p = 1.0723$
 $S_d = 0.0286$
 $S_t = 0.0290$
 $S_I = 0.0311$

These numerical scaling factors were used to calculate the standard sea level conditions from the measured values, see Tables 4.1 and 4.2.

4.4 Comparison of Data

In order to show how the measured data compares with the standard, both measured data and the standard have been plotted on log log graph paper. The measured data and the standard are at sea level conditions i.e. an atmospheric pressure of 14.7 psi and a temperature of $15^{\circ}C$. The standard curve is for a hemispherical detonation of TNT, (see Reference 8).

Figure 4.13 is the arrival time versus ground range curve. As can be seen, the gas balloon data shows a later arrival time when compared to the standard and generally follows a parallel line to the standard. The low detonation velocity and largeness of the bag (gas vs. TNT) results in

Table 4.1 Measured Overpressure Data Scaled to 1 lb. Sea Level Conditions

Station No.	Ground Range (ft)	Elevation (ft)	Arrival Time (msec)	Maximum Overpressure (psi)	Positive Duration		Positive Impulse (psi-msec)	
					Primary (msec)	Primary & Secondary (msec)		
4	2.03	0	0.296	191	1.16	1.856	40.27	
5	3.32	0	0.716	50.4	1.334	2.03	21.42	
6	4.46	0	1.2325	37.5	1.218	1.885	15.42	
		0		37.5	1.073	1.682	14.05	
		0.286	1.238	39.7	1.218	1.856	22.17	
		0.856	1.273	37.5	1.16	1.653	15.02	
7	5.75	0	1.931	23.6	1.305	1.972	12.03	
		0	Gage Failure -- No Record					
		0.629	1.937	24.9	1.378	1.928	12.99	
		1.487	2.030	24.1	1.392	2.001	12.50	
8	7.15	0	2.7982	16.7	1.711	2.349	10.64	
		0		17.7	1.682	2.320	10.64	
9	8.44	0		12.5	2.320	2.798	11.75	
10	10.93	0		7.7	2.117	2.900	6.67	
11	13.53	0	Gage Failure -- No Record					
12	16.15	0		4.29	2.697	3.248	4.72	
13	19.39	0		3.32		3.683	4.93	
14	26.54	0		1.93		3.973	2.95	
15	119.83	0		0.39		5.220	0.74	

Table 4.2 Measured Dynamic Pressure Data Scaled to
1 Lb. Sea Level Conditions

<u>Station No.</u>	<u>Ground Range (ft)</u>	<u>Dynamic Pressure (psi)</u>	<u>Dynamic Pressure Impulse (psi-msec)</u>	<u>Dynamic Pressure Impulse Australasian Data (psi-msec)</u>
6	4.46	25.19	8.02	
	4.46	25.73	2.69	
	4.52	24.67	5.15	
7	5.75	13.08	6.03	6.0
	5.75	14.7	4.03	
	5.92	10.19	2.34	
8	7.15	4.82	1.24	4.04
9	8.44			2.58
10	10.93			1.2

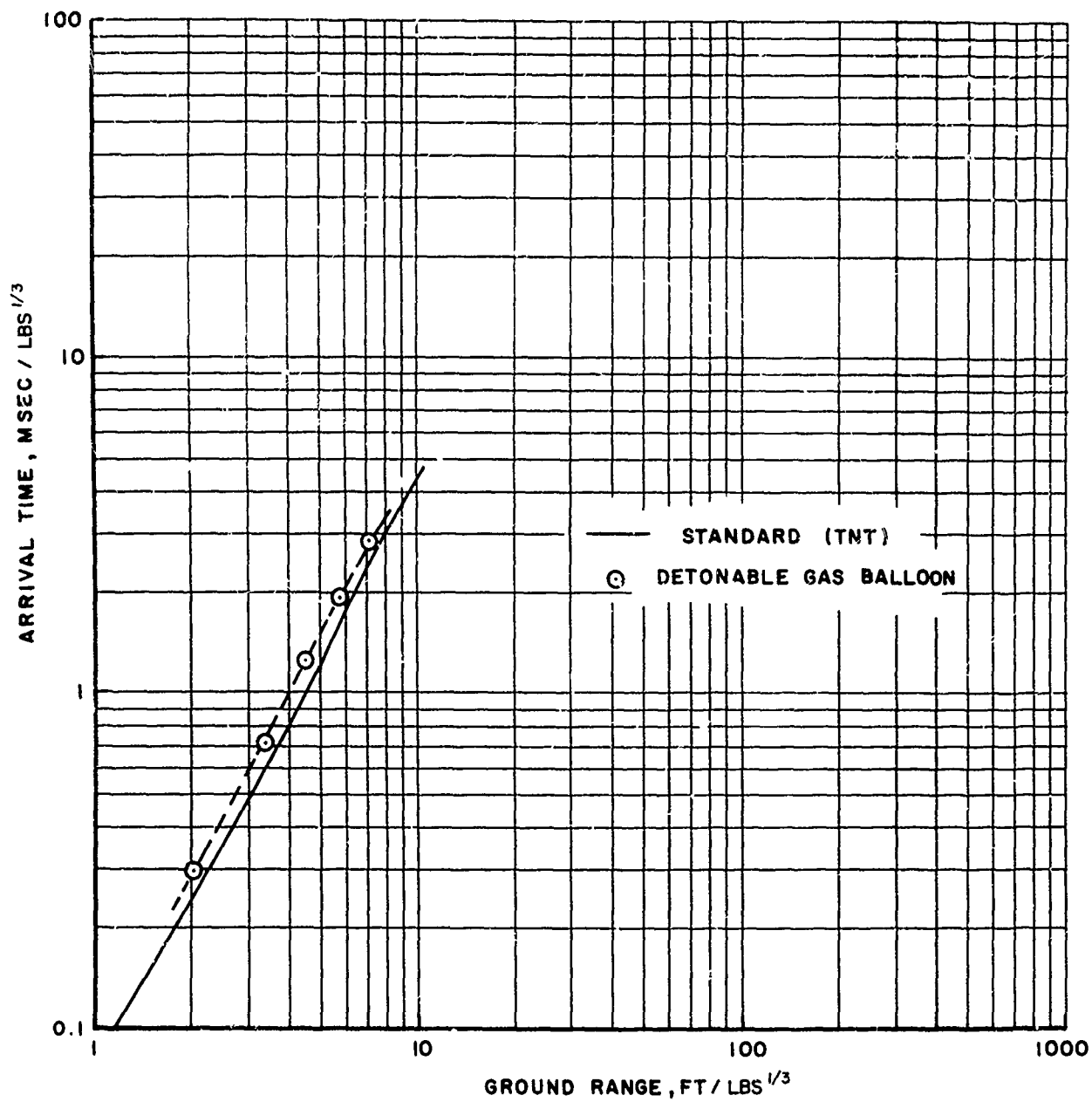


Figure 4.13 Measured Arrival Time for Event 2A, Scaled

a later arrival time and a delay in the formation of a true shock front.

Figure 4.14 is the overpressure versus the ground range. From the scaled ground range of 7.1 feet (station 8) outward the balloon data is in good agreement with the standard. From this point inward the measured data is less than the standard, establishing a curve of overpressure corresponding that of a 10 ton TNT charge. Comparison with the prediction made by the computer code of GATX as shown in Figure 3.5 indicates the measured data to be lower than their prediction, although a similarity in shape of the curve is shown.

The positive duration versus ground range curve is shown in Figure 4.15. The second shock has been included in the duration times extracted from the records. Because of the presence of the second shock in these times, the values are 15 to 20 percent higher than the standard. If one extrapolates the curve ignoring the secondary shock, the measured curve will fall below the standard by approximately the same percentage.

The measured data compares favorably with the standard over the major area instrumented for the positive impulse as seen in Figure 4.16. Differences occurred at those stations closest to the charge.

Dynamic pressure data are plotted in Figures 4.17 and 4.18. Dynamic pressure impulse as obtained from mechanical gages by the Defence Standards Laboratory, Melbourne, Australia (Reference 9) is plotted with the project data in Figure 4.18. Except for the extrapolated project data point at Station 8, the data derived from the two instrumentation systems agree and are larger in magnitude than the standard TNT curve.

It was noted in Figure 4.14 that the overpressure curve for the

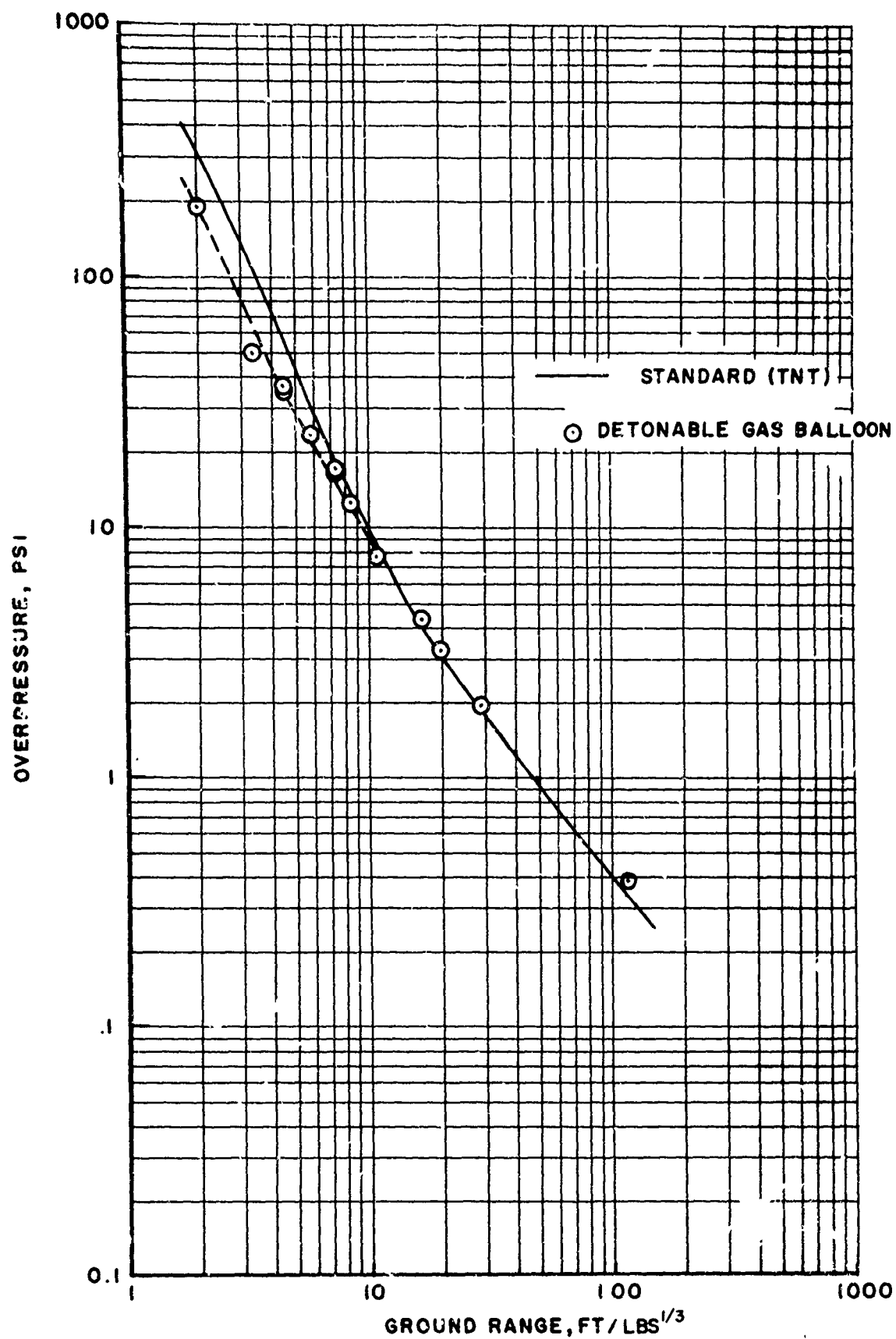


Figure 4.14 Measured Overpressure for Event 2A, Scaled

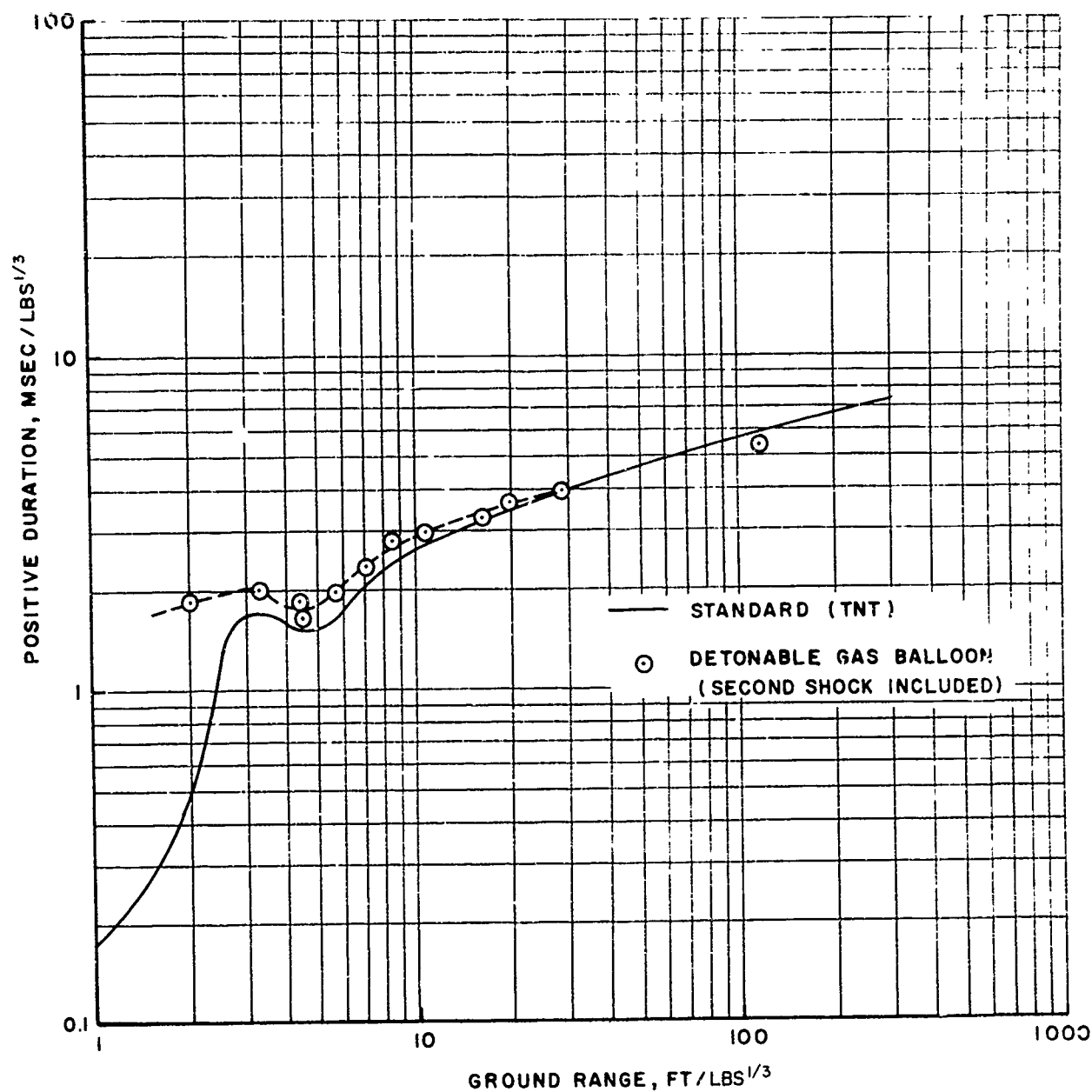
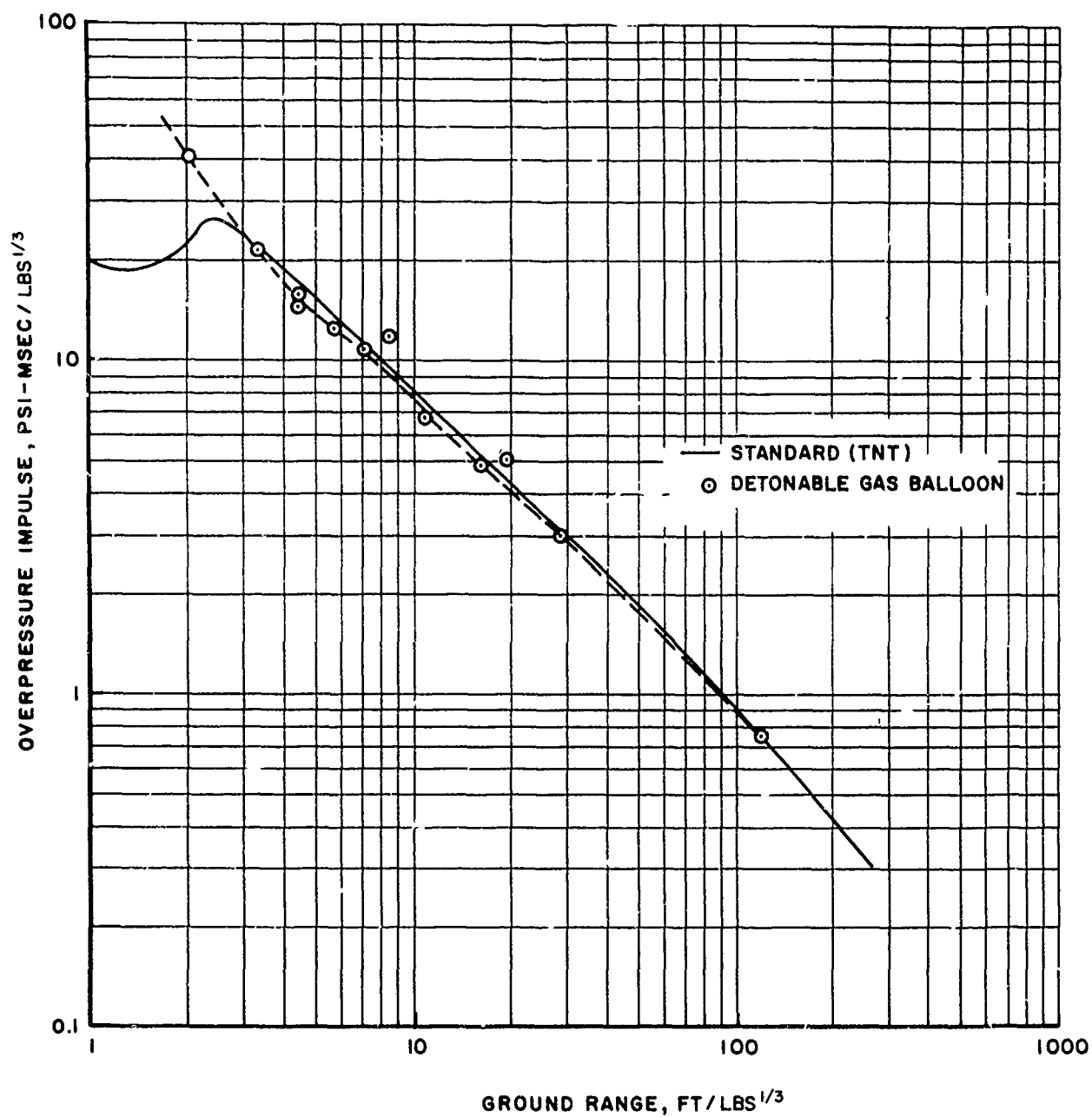


Figure 4.15 Measured Positive Phase Duration for Event 2A, Scaled



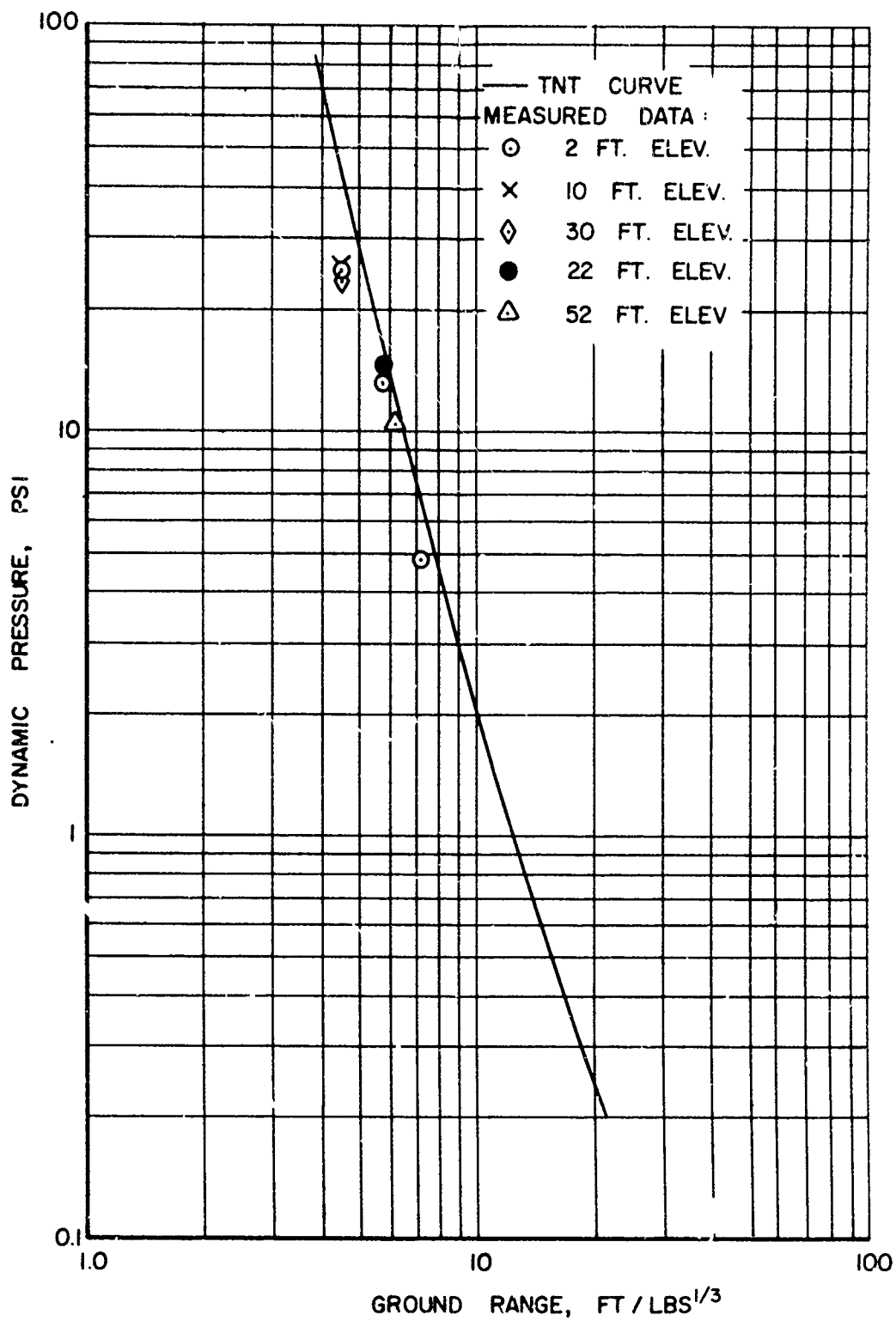


Figure 4.17 Dynamic Pressure for Event 2A, Scaled

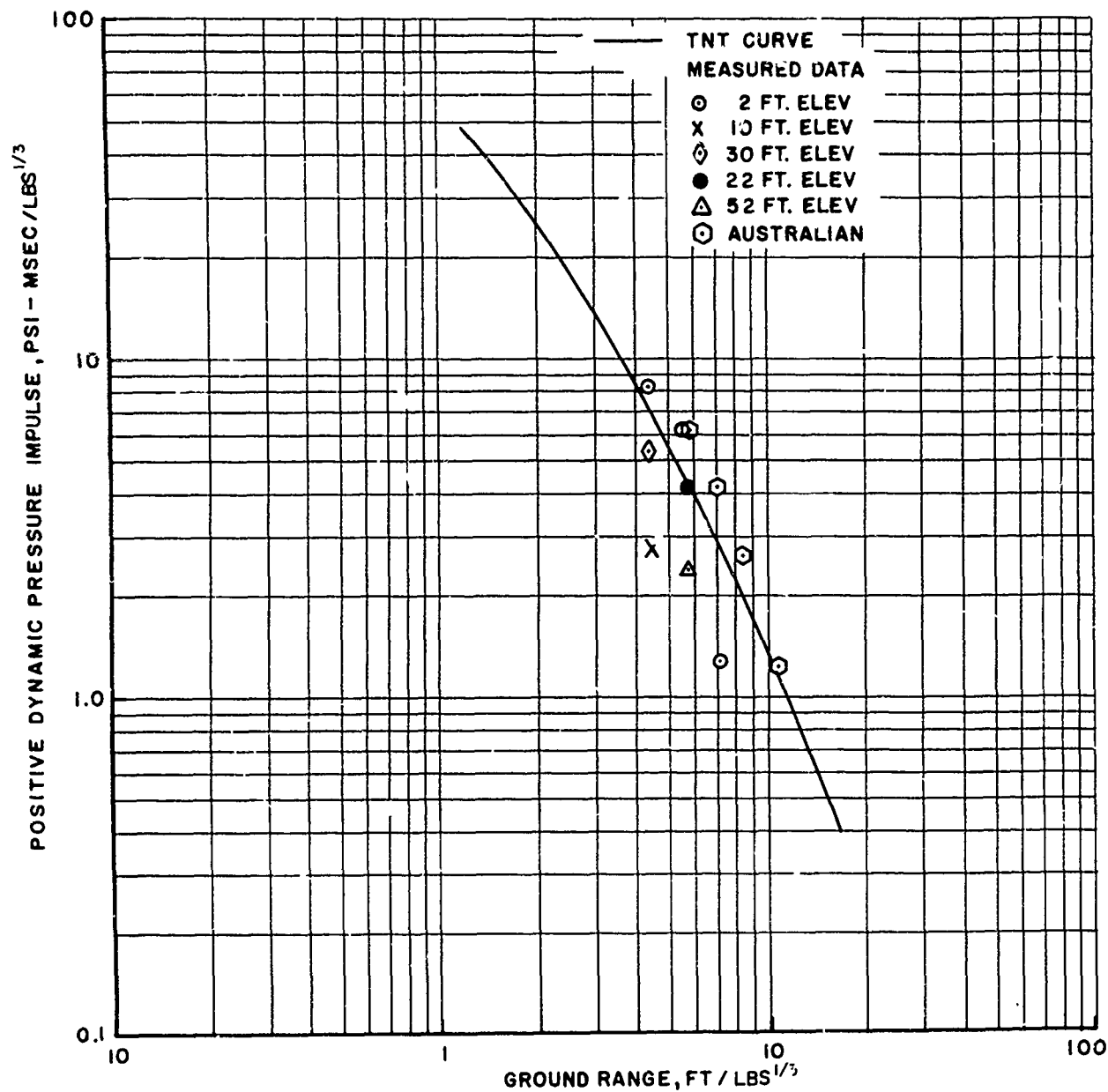


Figure 4.18 Dynamic Pressure Impulse Compared with Australian Data, Scaled

balloon explosion produced a pressure-distance curve that initially corresponded to a 10 ton TNT hemispherical charge explosion. However, for simulation purposes the wave shape produced for a given maximum overpressure is of greater interest. Figure 4.19 shows a plot for Event 2A of the decay constant C in the relation $P = P_m e^{-Ct}$, where P_m is the maximum overpressure. The value of C was obtained by plotting the pressure record on semi-logarithmic paper and fitting a straight line by eye to the initial portion of the record as described in Reference 6. The value obtained was then scaled to correspond to 1 lb. at sea level conditions. For comparison, Figure 4.19 indicates the C values obtained in a similar fashion for TNT hemispherical charges by C. Kingery in Reference 10. The higher the value of C the more rapid the decay of overpressure with time.

As shown in Figure 4.19 the agreement in the decay constants is very close in the region below about 15 psi. The data do indicate a somewhat lower value of C and therefore a slower decay at higher pressures. This implies that though the pressure distance curve in Figure 4.14 would correspond to a lower yield than 20 tons at overpressures above 10 psi, the wave shape is that for a 20 ton or slightly larger charge.

Figure 4.20-scaled overpressure impulse plotted versus maximum overpressure. The solid curve is that for a TNT hemispherical charge of 1 lb at sea level, and was derived using data in Reference 8. Here the overpressure impulse agrees very well up to about 20 psi. Above 20 psi the overpressure impulse is somewhat higher than for the corresponding TNT charge. This indicates that the balloon data corresponds to at least a 20

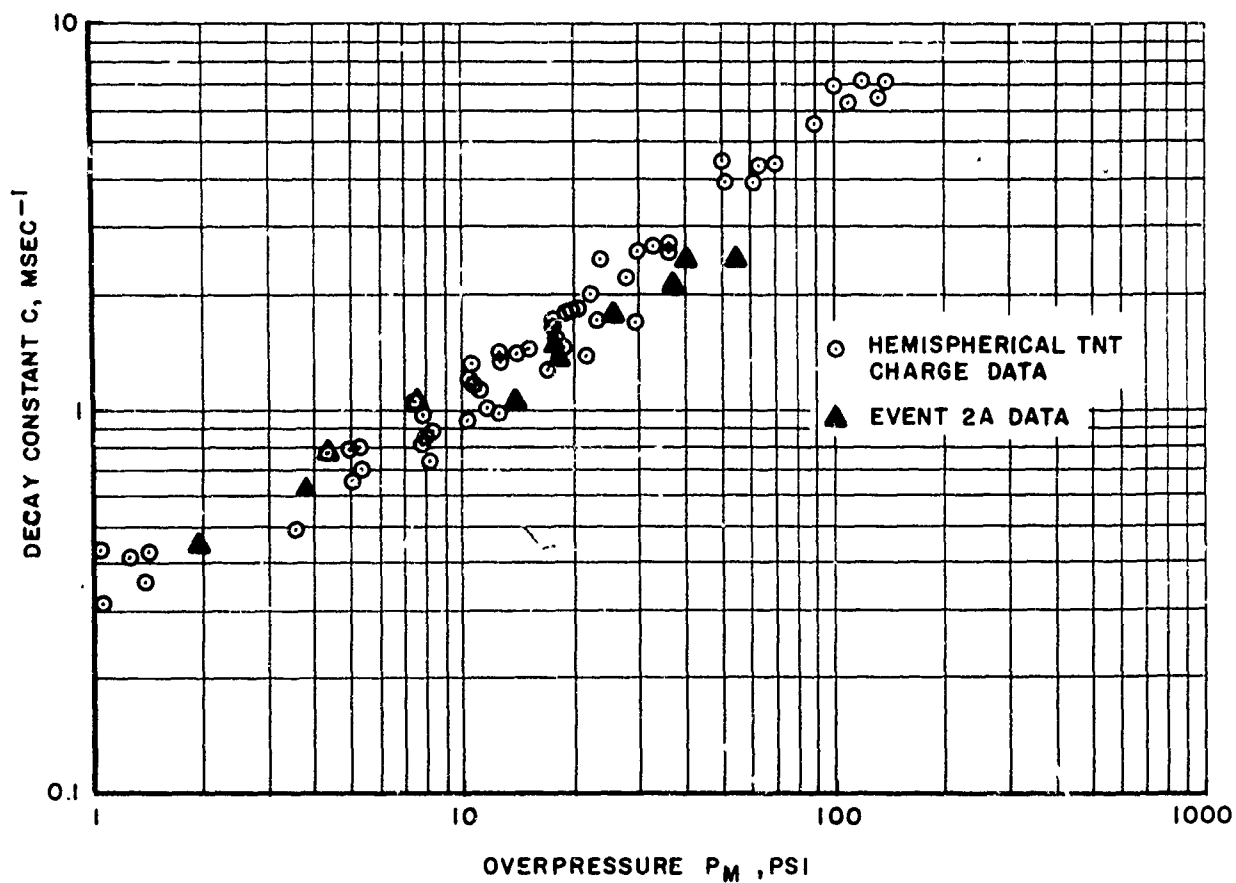
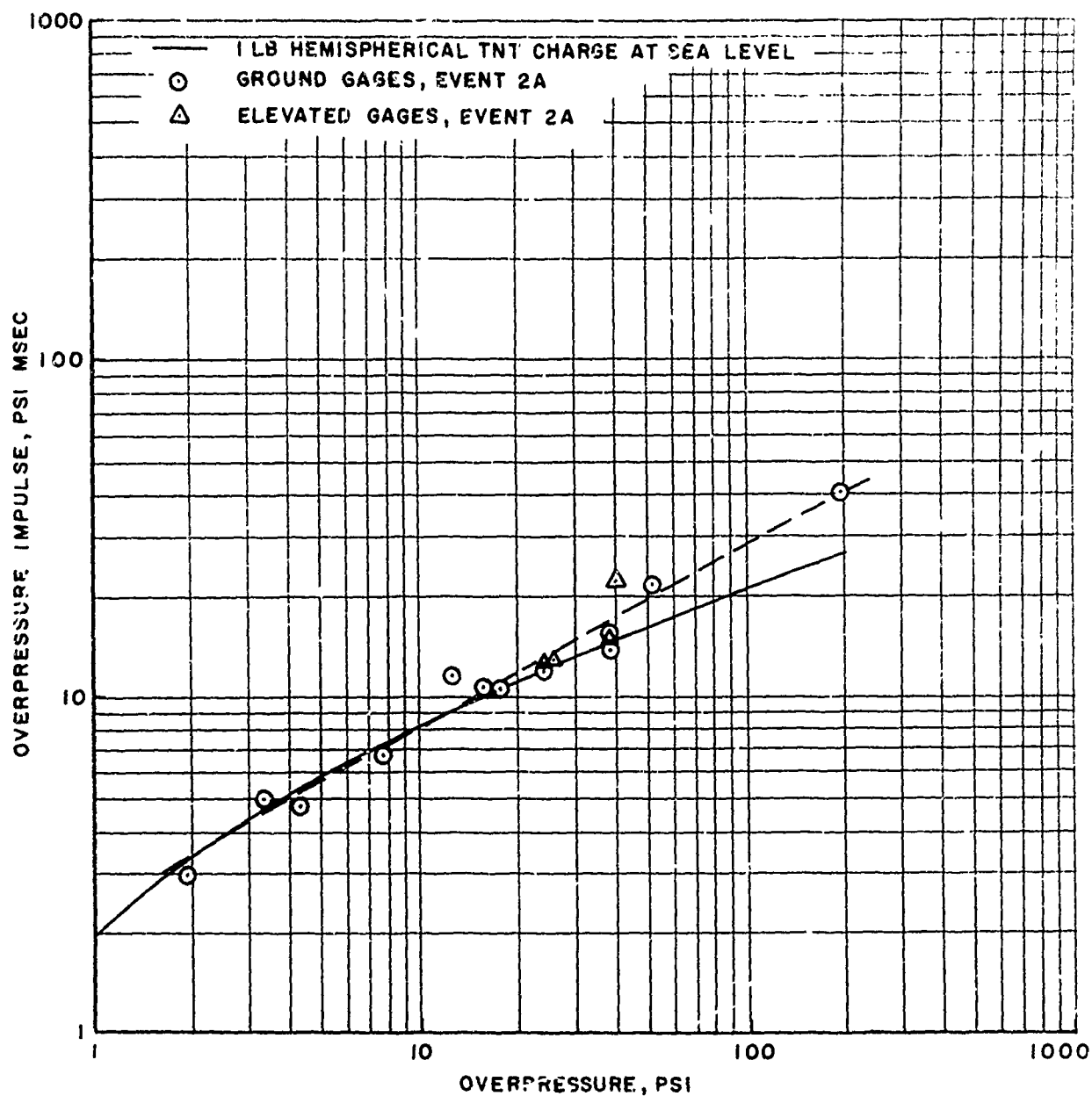


Figure 4.19 Exponential Decay Constant C versus Shock Front Overpressure for Event 2A and a 1 pound Hemispherical TNT Charge at Sea Level



ton TNT charge, and somewhat more at shock overpressures above 20 psi.

Figure 4.21 shows a comparison of scaled dynamic pressure impulse for the balloon explosion compared with that predicted for a 1 lb hemispherical TNT charge at sea level versus shock front overpressure. The figure shows that the dynamic pressure impulse was about 60 percent larger than that for a corresponding TNT explosion. Thus, although the overpressure impulse was not very greatly different, the dynamic pressure impulse was disproportionately large. Another difference is that the dynamic pressure impulse data do not approach the curve for TNT at the lower shock front overpressures as one would expect. However, the data shown in Figure 4.21 for the lower pressures were obtained with the Australian mechanical dynamic pressure impulse gage which has an error band of about ± 20 percent, and it is possible such a trend is obscured by large errors in this case. More accurate dynamic pressure impulse measurements on additional detonable gas balloon experiments are required to determine dynamic pressure impulse versus distance from such explosions.

The blast parameters as a function of distance indicate less than 20 tons yield for the balloon explosion when compared to a TNT surface hemispherical charge, however, comparisons on the basis of matching shock front overpressure indicate that the wave shape and overpressure impulse were that of a charge of at least 20 tons. The dynamic pressure impulse was about 60 percent larger for a given shock front overpressure than for the corresponding TNT charge.

5. CONCLUSIONS AND RECOMMENDATIONS

Mean pressure waveforms with little noise or distortion were recorded

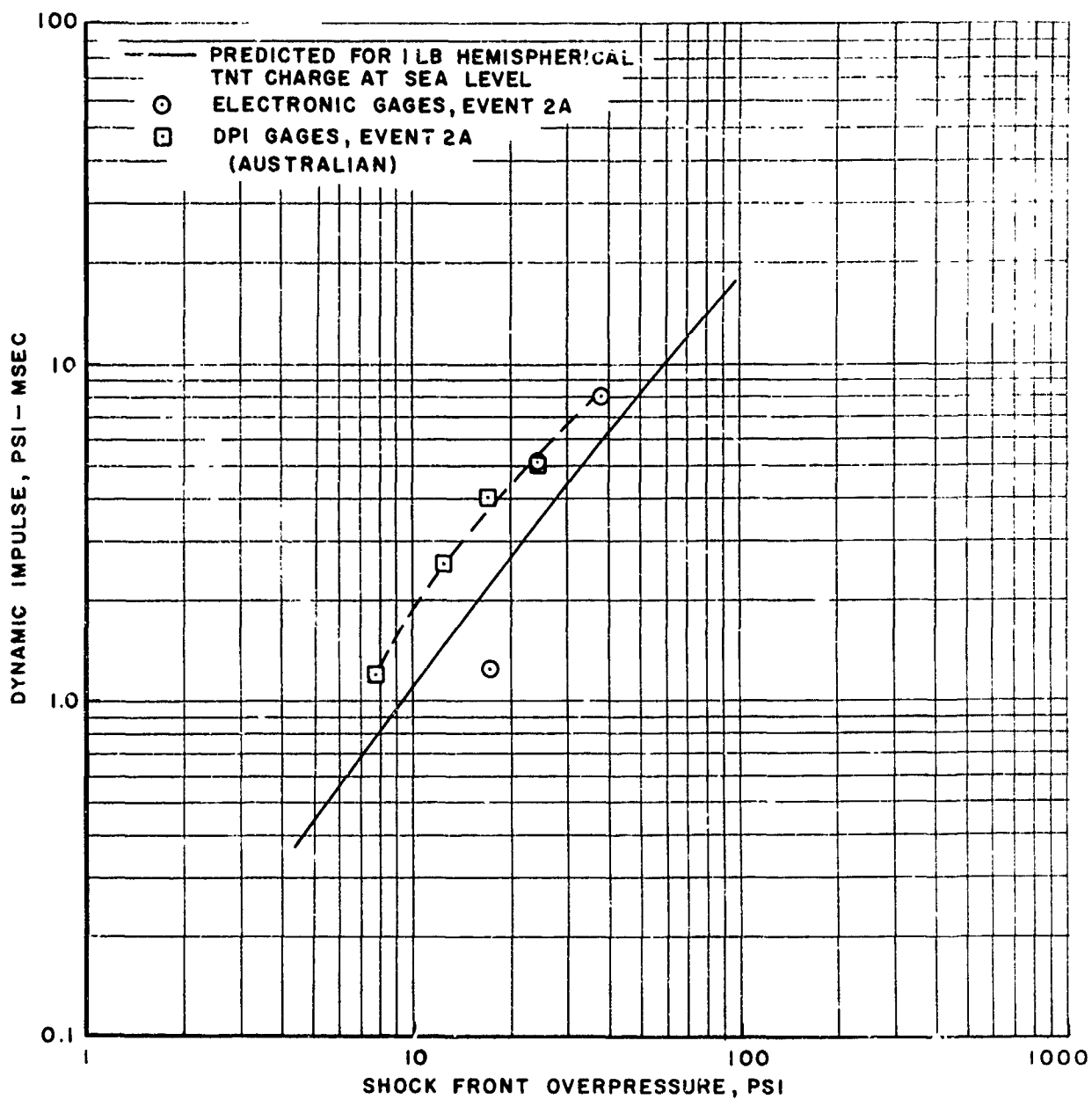


Figure 4.21 Dynamic Pressure Impulse versus Shock Front Overpressure for Event 2A and a 1 Pound Hemispherical TNT Charge at Sea Level

over the major stations instrumented. The slower burning rate and large size of the charge influenced the arrival times, resulting in later times compared to those from a TNT charge. Other blast parameters compared well with that of TNT, especially below 30 psi. Above 20 psi, the radius for a given overpressure was less than that of TNT, approaching the pressure-distance curve corresponding to 10 tons of TNT. The occurrence of the secondary shock late in time influenced the positive phase duration.

Measurements made with surface, near-surface, and elevated pressure gages indicated that no major differences occurred with elevation, although dynamic pressures differed, these differences may have been due to off-axis flow effects from the supporting tower. Drag gage records differed considerably and did not provide a clear indication of flow conditions or flow direction at the gage locations.

Comparison of overpressure wave shape and impulse as a function of shock front overpressure indicated an equivalent yield of 20 tons or slightly larger, and a dynamic pressure impulse (based on limited data) about 60 percent larger than for a corresponding 20 ton TNT charge. Thus the balloon explosion simulated a 20 ton TNT charge or larger.

The thermal energy radiated was larger than for a corresponding TNT charge. Cratering common to TNT explosions on the ground surface did not occur.

Additional detonable gas balloon experiments are required to improve prediction capability parameters, particularly for dynamic pressure impulse.

ACKNOWLEDGEMENTS

The authors gratefully acknowledge the field support provided by the staff of the Defence Research Establishment, Suffield, and especially the helpful discussions with Mr. John Anderson of the Technical Staff.

The support and technical assistance given by the Distant Plain Technical Director, Mr. Charles Kingery, and the Distant Plain Program One Director, Mr. John Keefer, is also gratefully acknowledged.

REFERENCES

1. Operation Distant Plain Preliminary Report Vol. I (u) DASA 1876-1 December 1966.
2. J. R. Keefer, Air Blast Predictions for Operation Distant Plain, BRL Technical Note No. 1612, June 1966
3. N. Spackman, Survey and Meteorological Data and Details of Charge, Suffield Technical Note No. 179 December 1966
4. L. Giglio-Tos et al, Air Blast Instrumentation, Operation Distant Plain, BRL Memorandum Report to be published.
5. C. N. Kingery, et al, Surface Air Blast Pressure Measurements from a 100 Ton TNT Detonation, BRL Memorandum Report No. 1410 June 1962
6. N. H. Ethridge, A Procedure for Reading and Smoothing Pressure Time Data from H.E. and Nuclear Explosions, BRL Memorandum Report No. 1691 September 1965
7. R. G. Sachs, The Dependence of Blast on Ambient Pressure and Temperature, BRL Report No. 466, 15 May 1944.
8. C. N. Kingery, Air Blast Parameters versus Distance for Hemispherical TNT Surface Bursts, BRL Report No. 1344.
9. Private Communication from J. Howe, Defence Research Standards Laboratory, Melbourne, Australia, TDY at Washington, D.C. to R. E. Reisler BRL, Aberdeen Proving Ground, Maryland
10. Private Communication from C. N. Kingery, BRL, Aberdeen Proving Ground, Maryland

APPENDIX A

Gage Records, Event 2A

CAPTION NOTATIONS

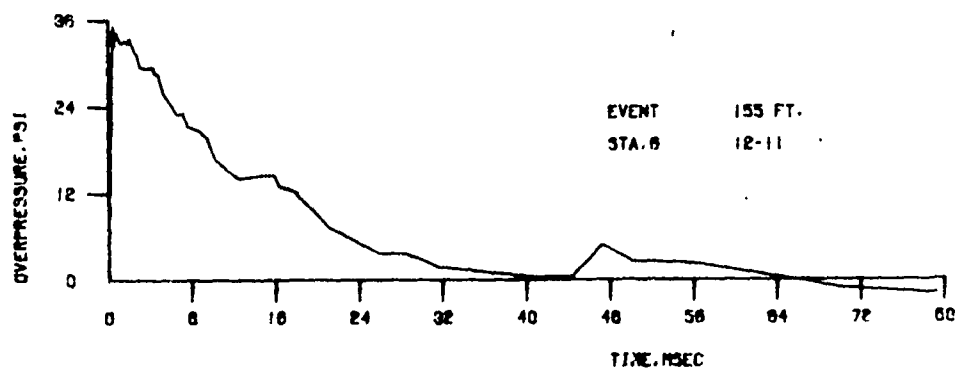
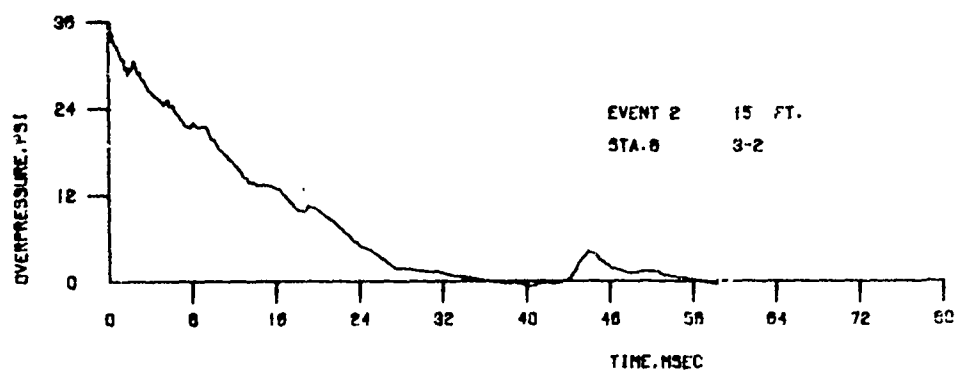
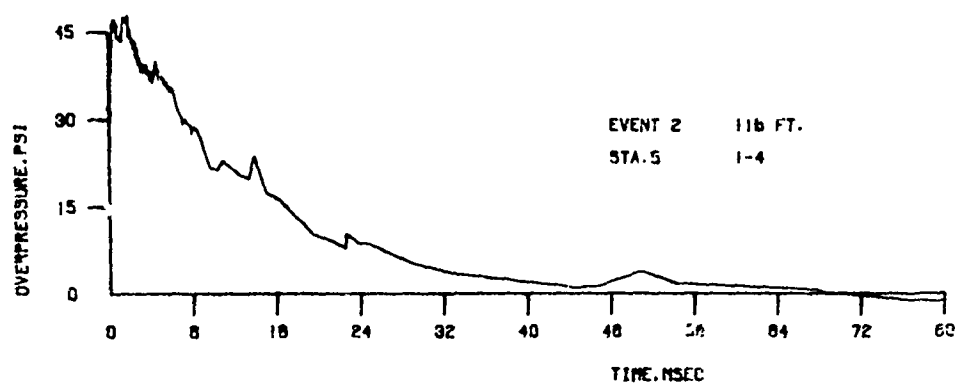
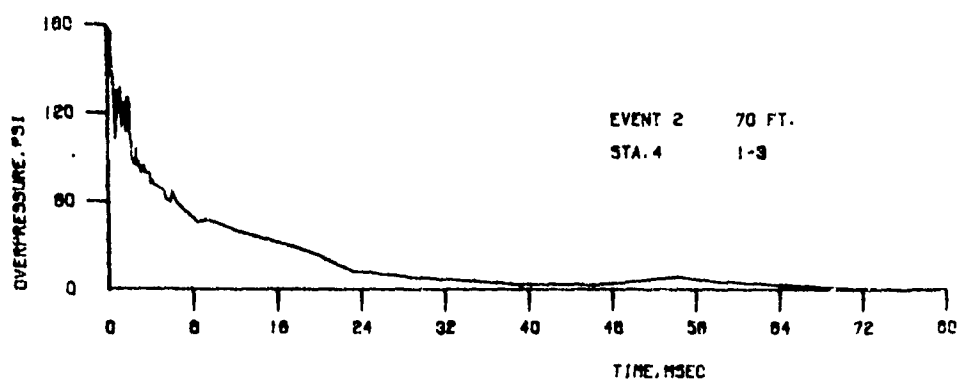
The captions associated with each pressure record contain the event number, the distance, the station number (the first digit indicating the particular blast line, succeeding digits indicating the particular station number) and the system and channel number or self-recording sensor number. In the case of the dynamic pressure the following information identifies the notations:

P_T - Total Head Pressure

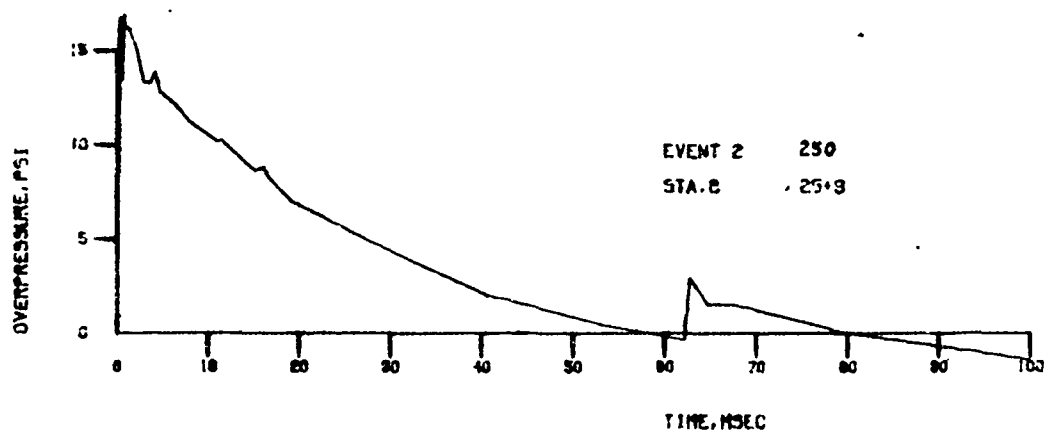
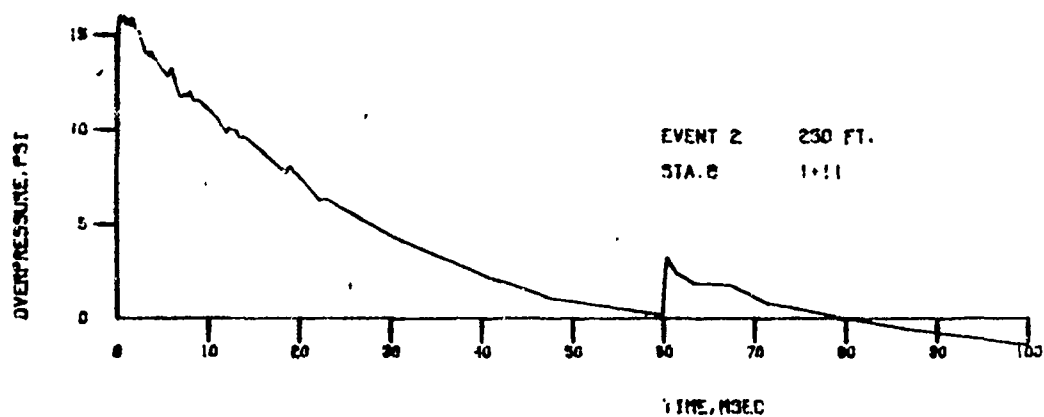
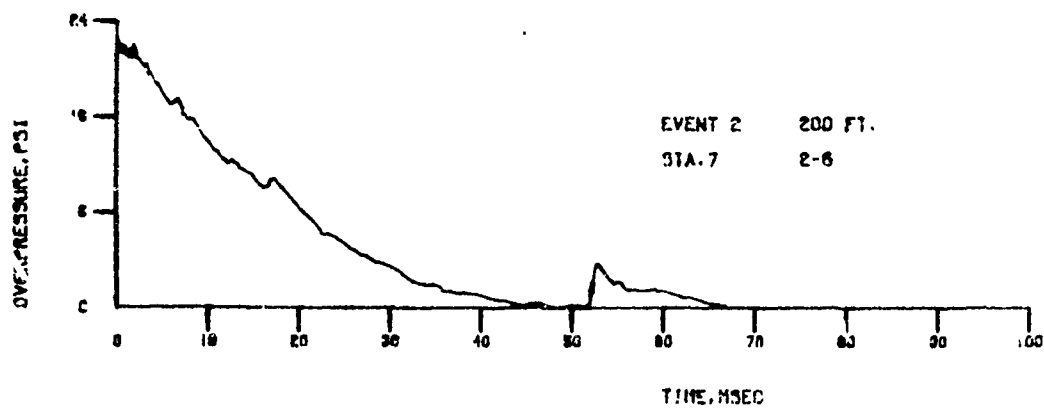
P_S - Side-On Overpressure

P_{DC} - Corrected Dynamic Pressure

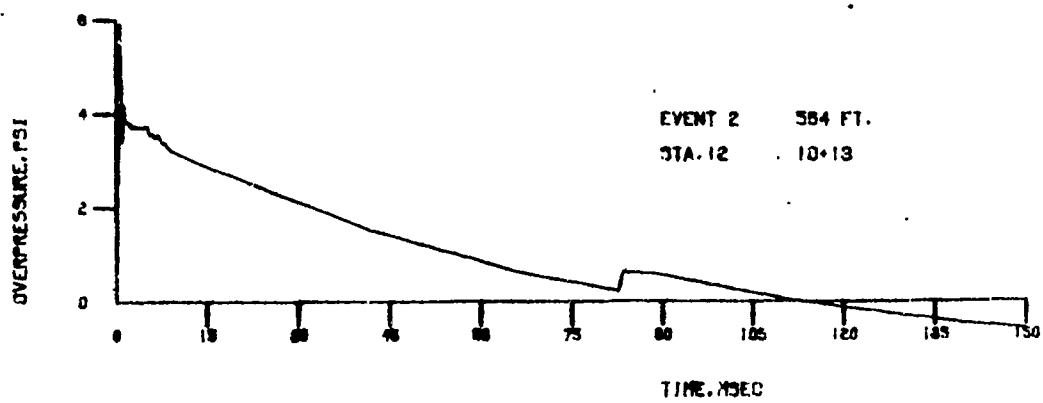
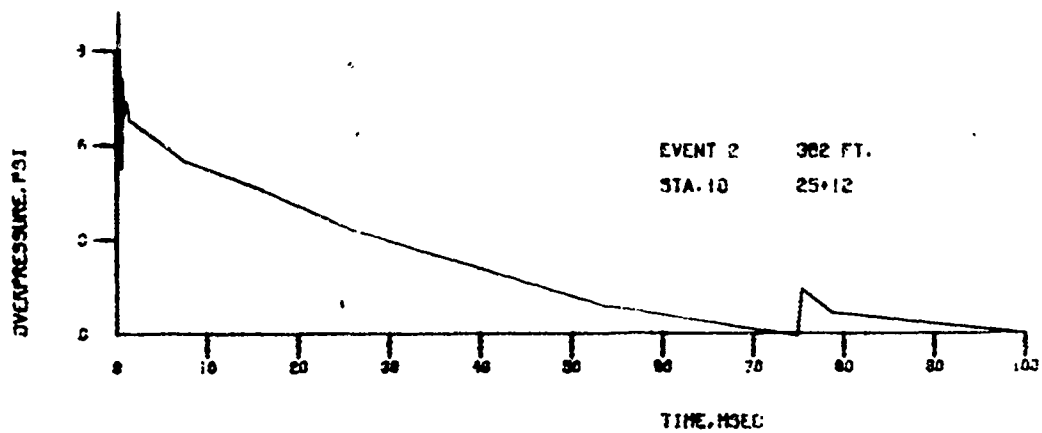
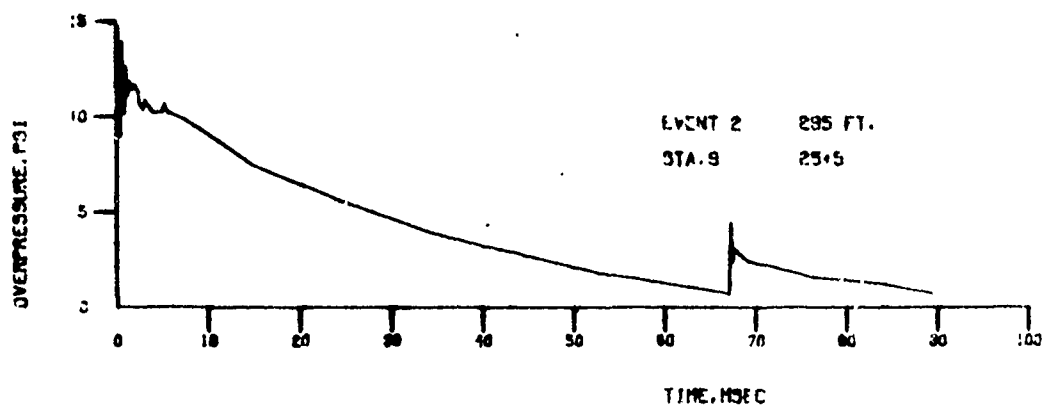
Mach - Mach Number



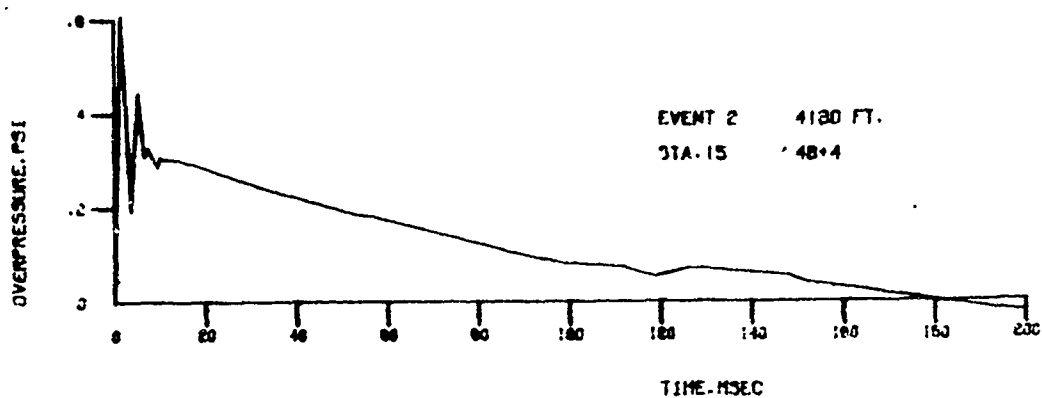
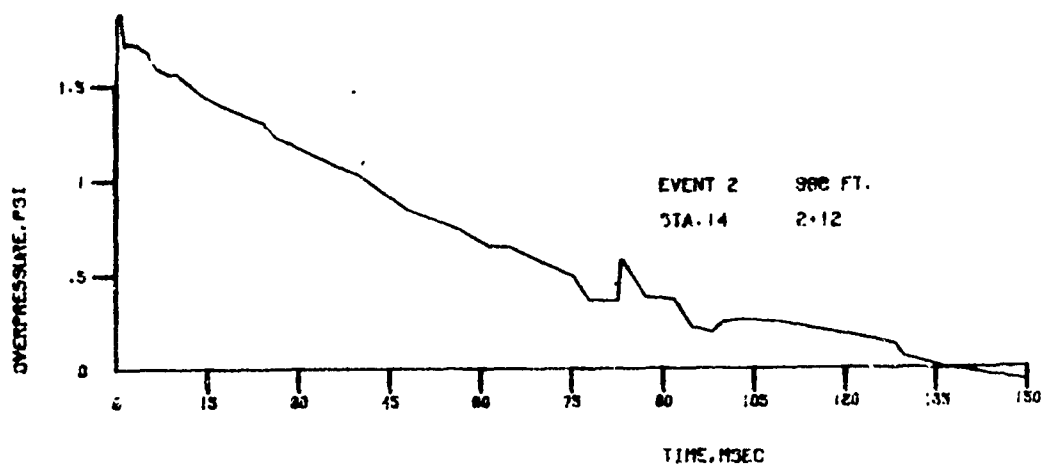
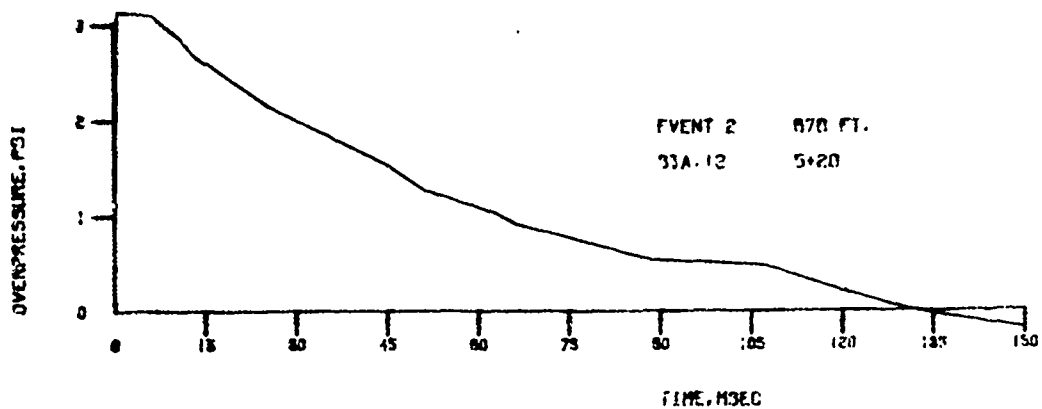
A.1 Pressure-Time Records, Stations 4-6



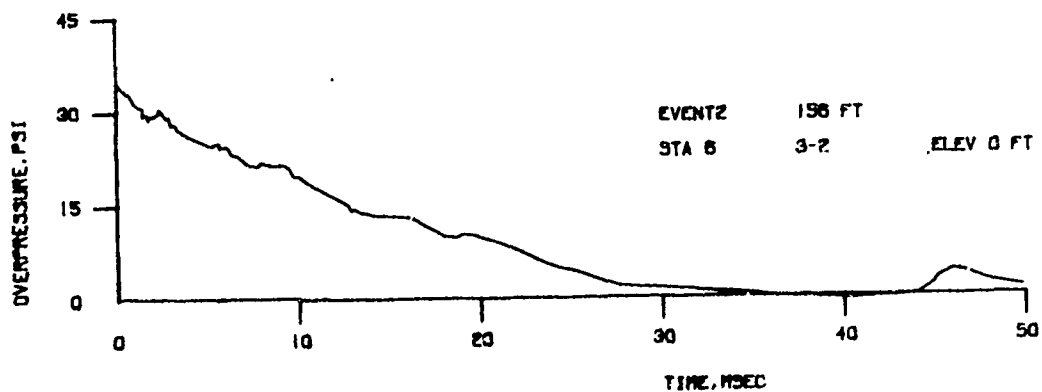
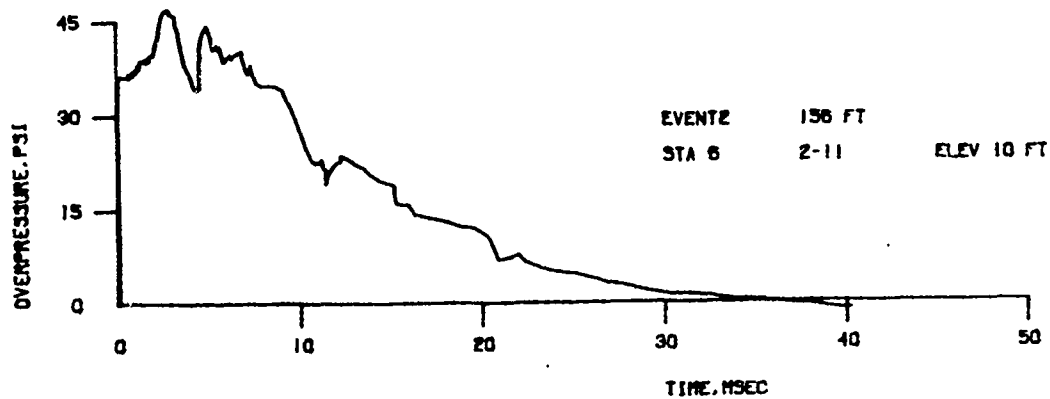
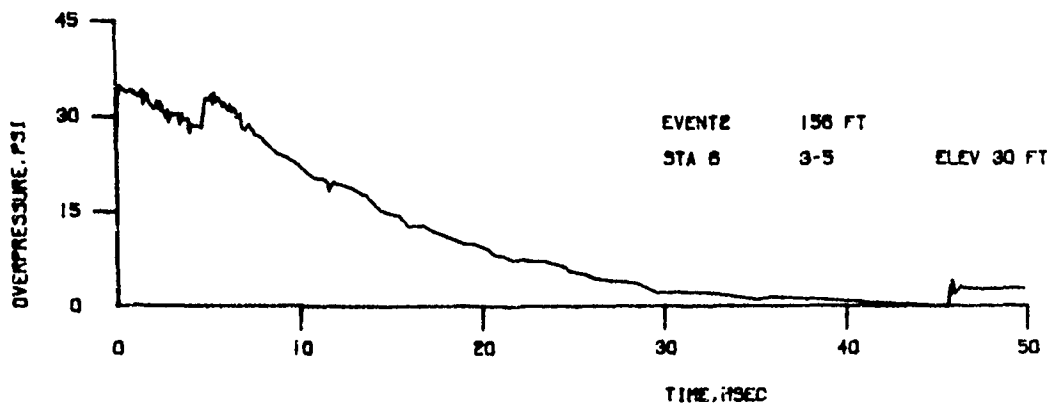
A.2 Pressure-Time Records, Stations 7 and 8



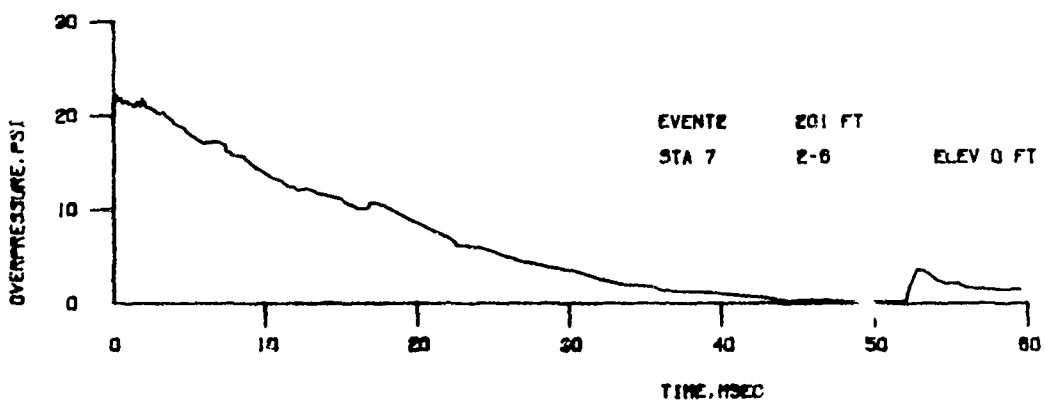
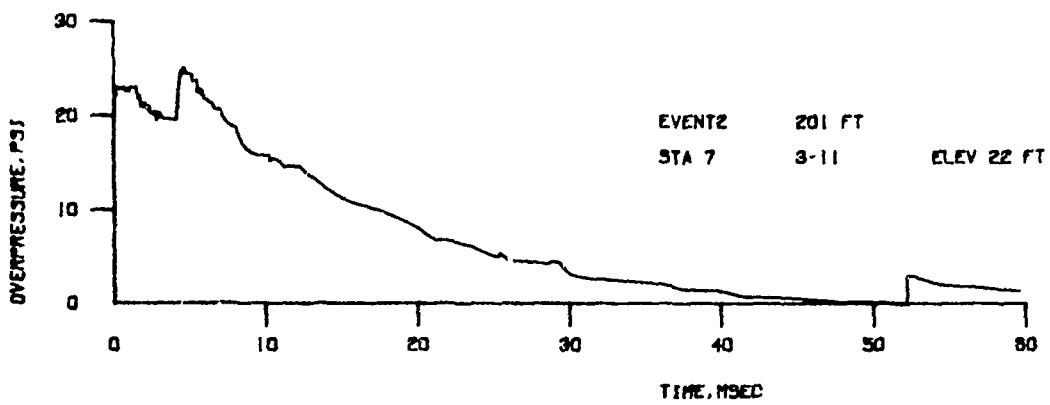
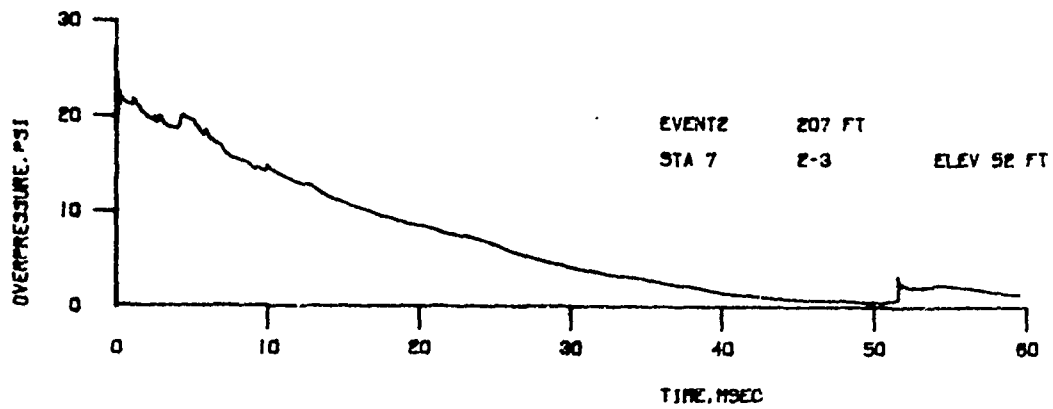
A.3 Pressure-Time Records, Stations 9-12



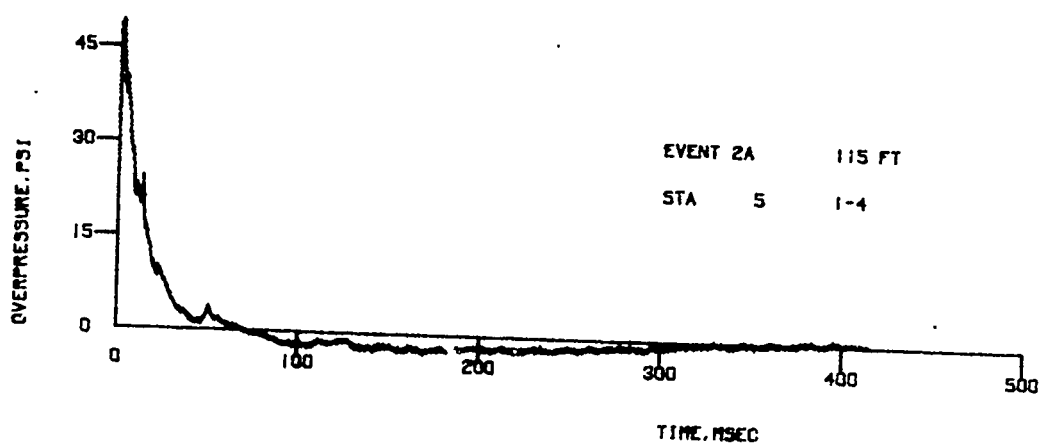
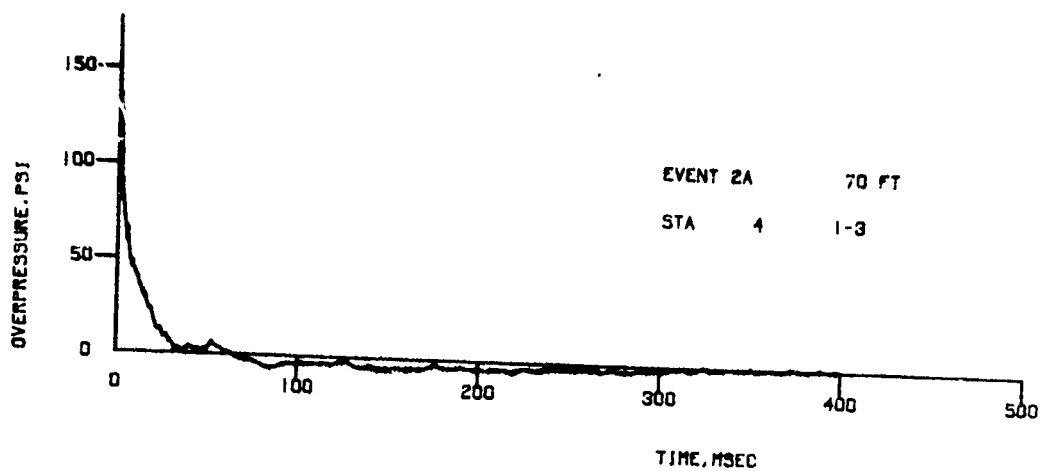
A.4 Pressure-Time Records, Stations 13-15



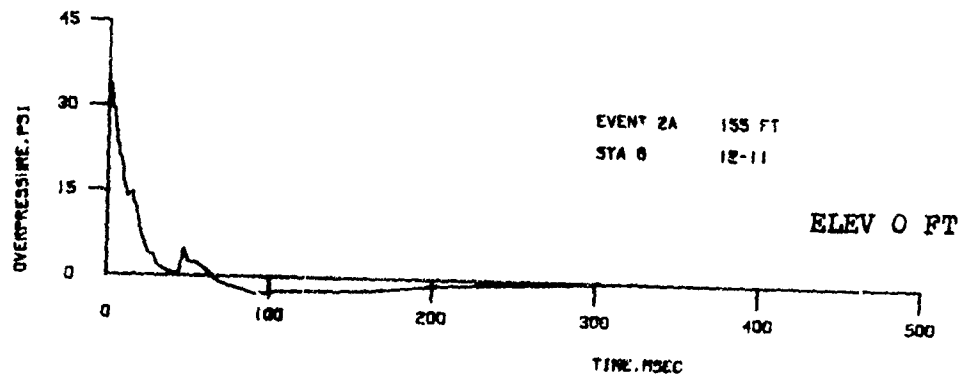
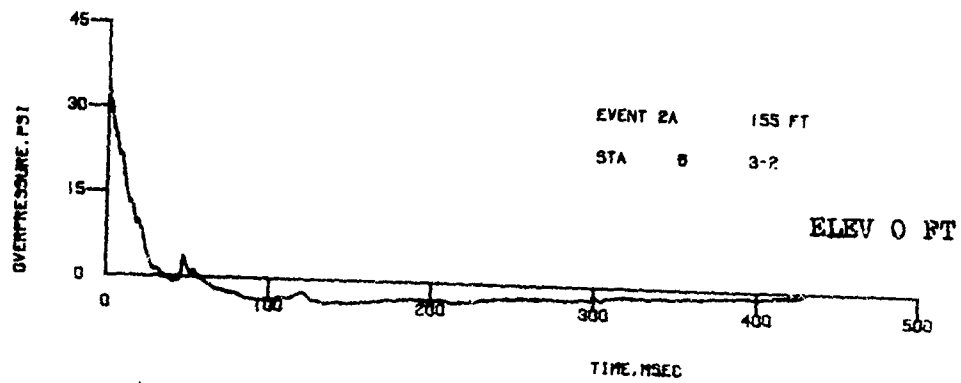
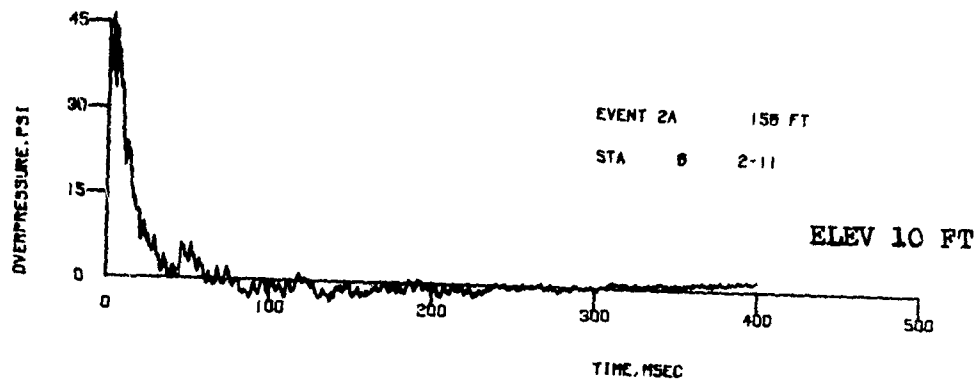
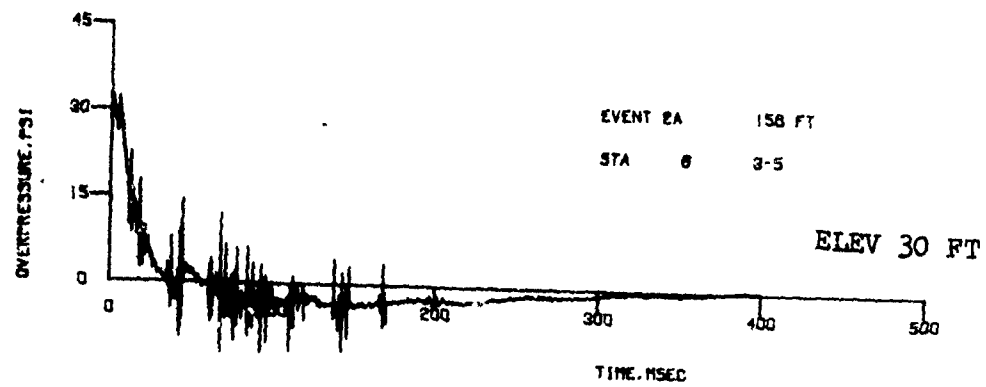
A.5 Pressure-Time Records, Elevated Positions, Station 6



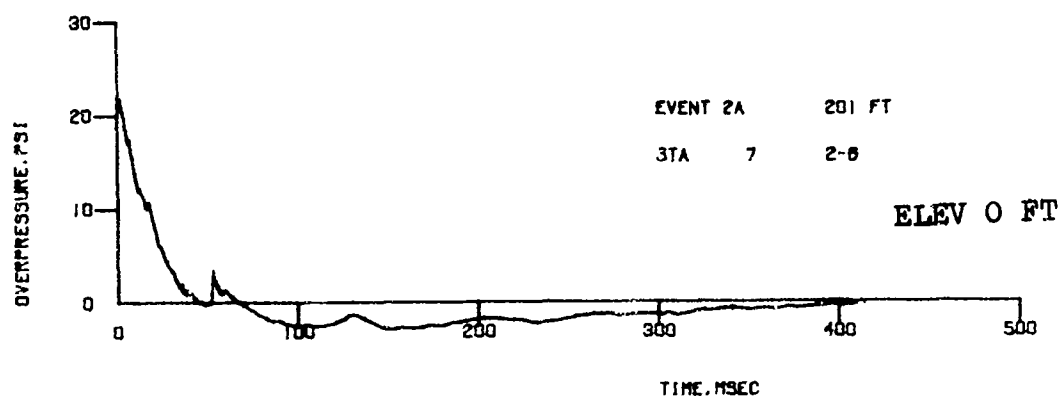
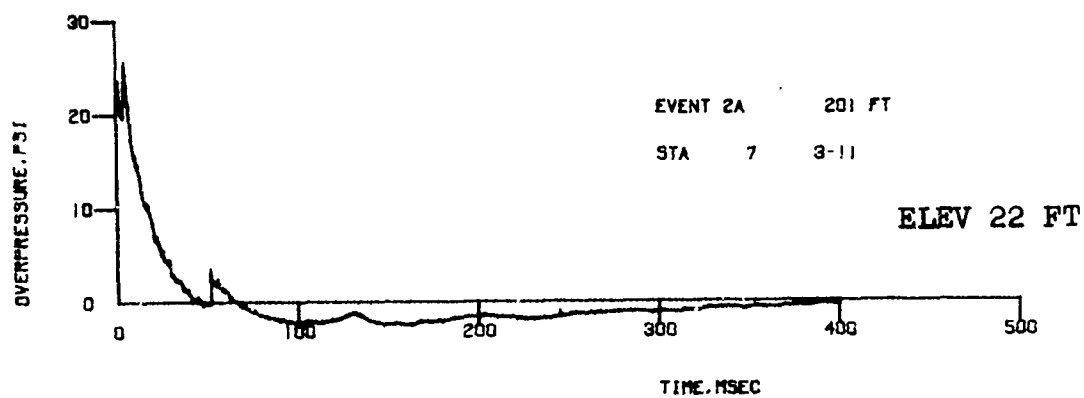
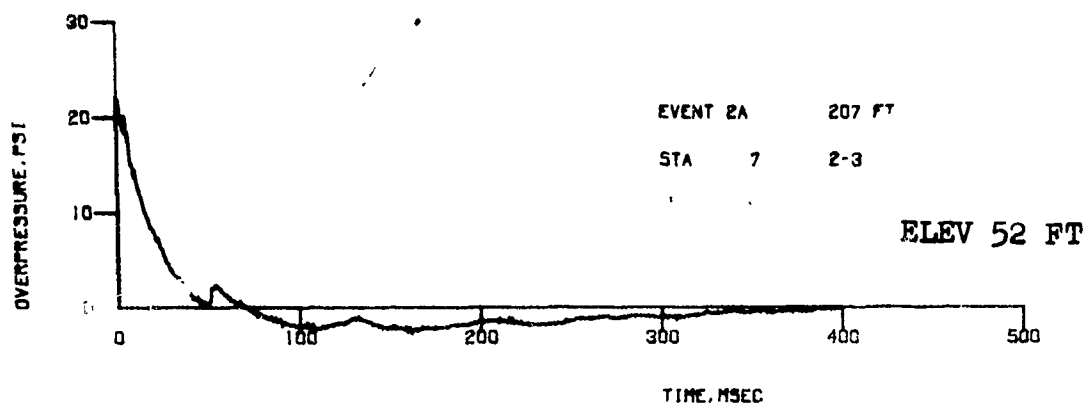
A.6 Pressure-Time Records, Elevated Positions, Station 7



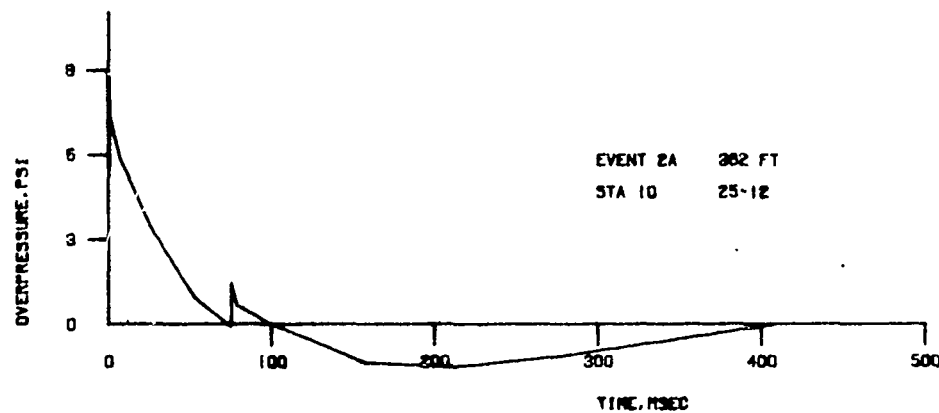
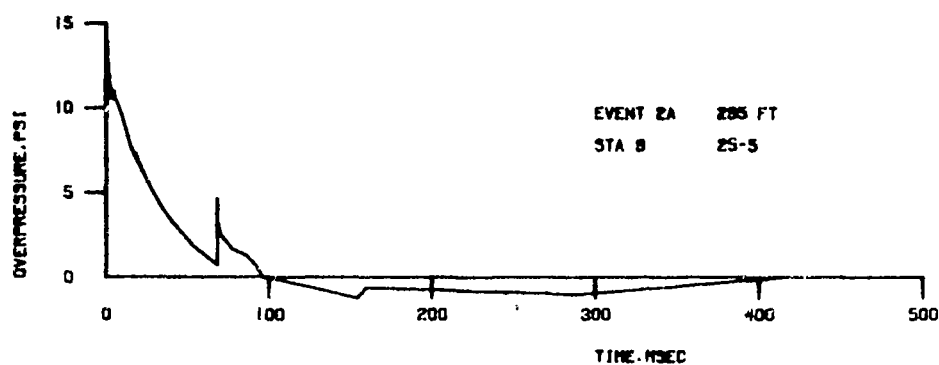
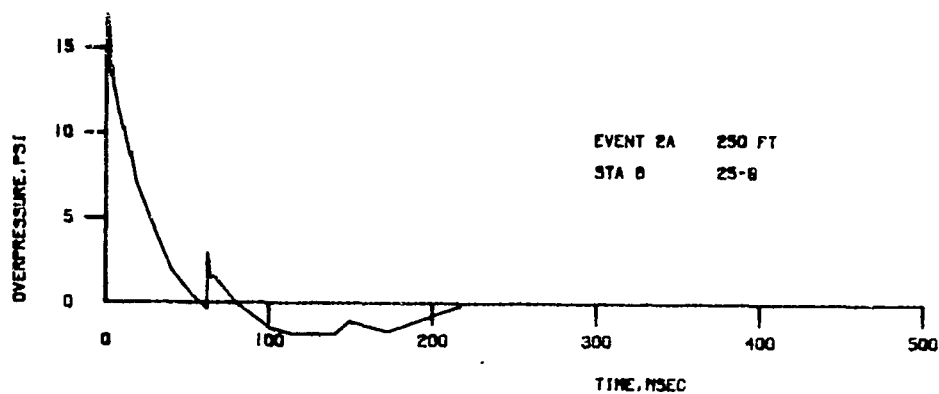
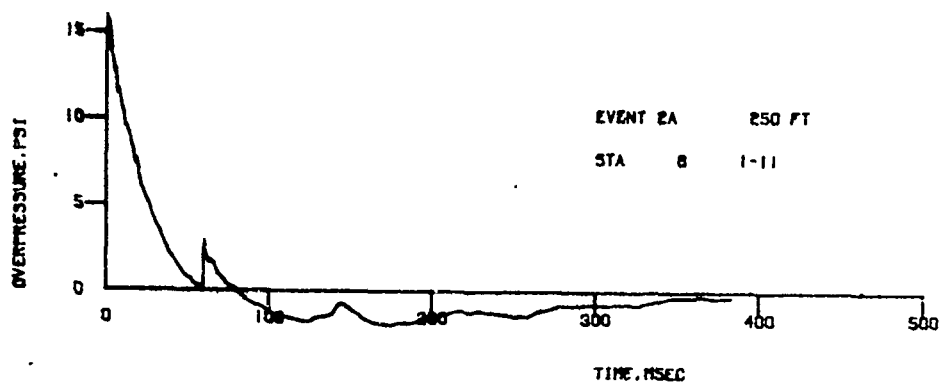
A.7 Pressure-Time Records Showing Negative Phase,
Stations 4 and 5



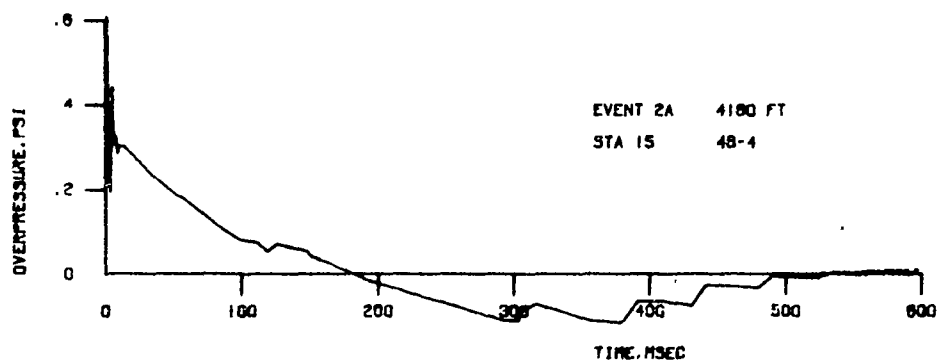
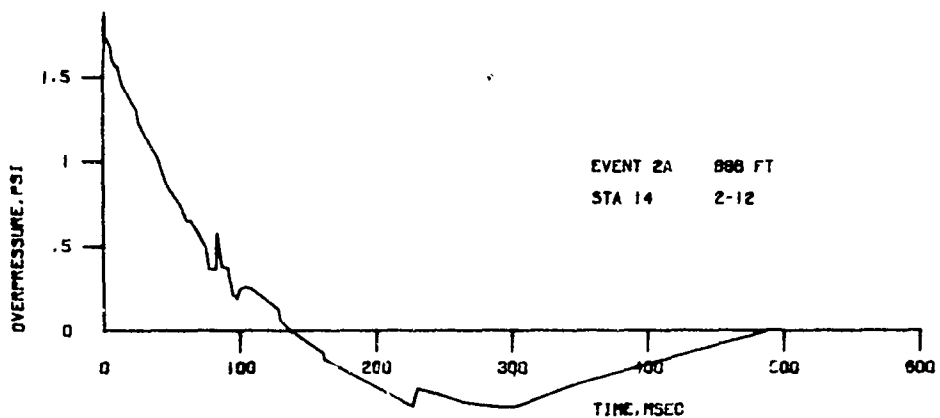
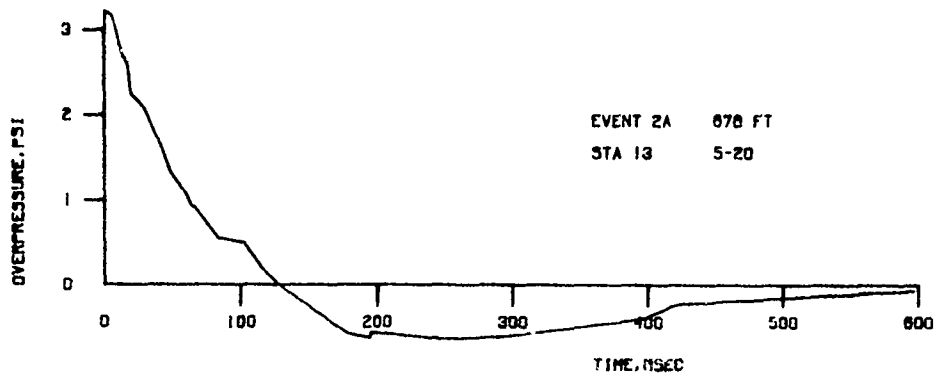
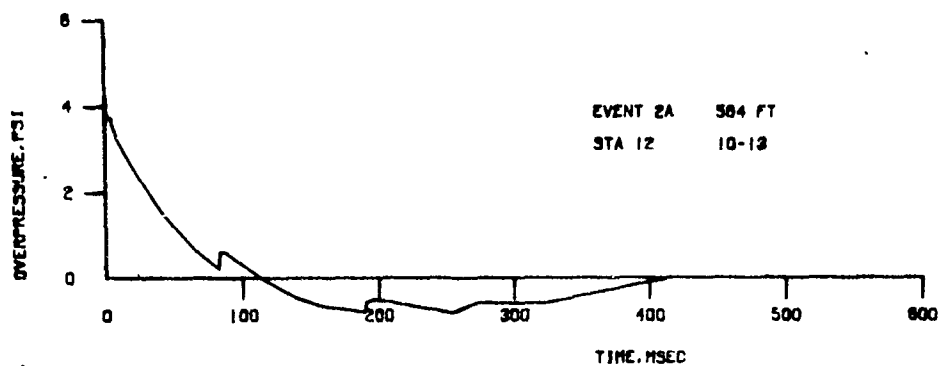
A.8 Pressure-Time Records Showing Negative Phase, Station 6



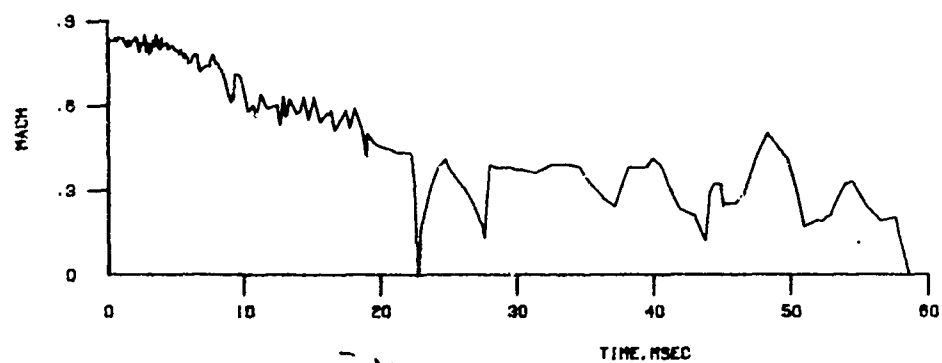
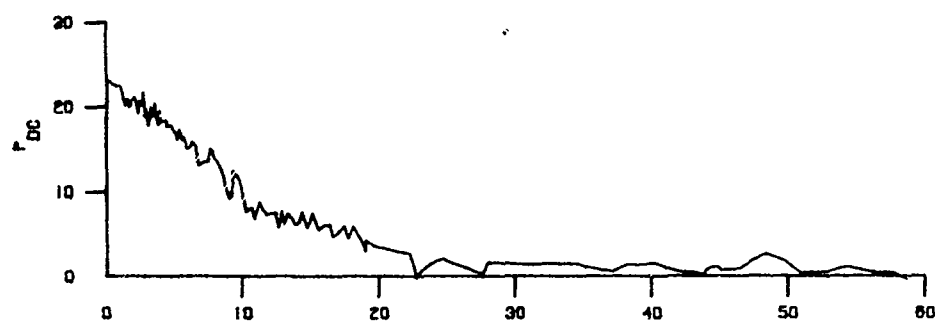
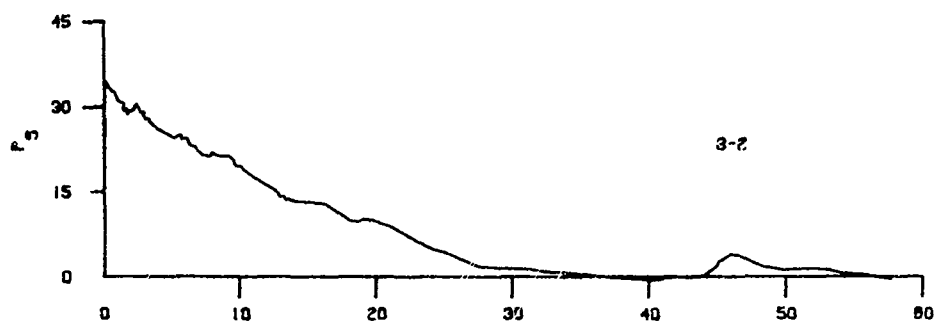
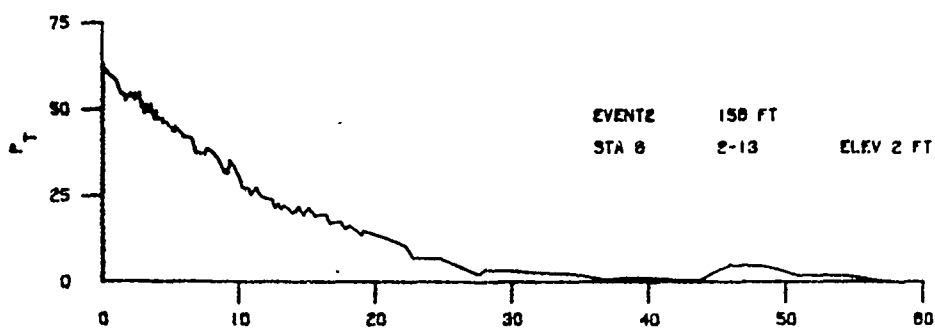
A.9 Pressure-Time Records Showing Negative Phase, Station 7



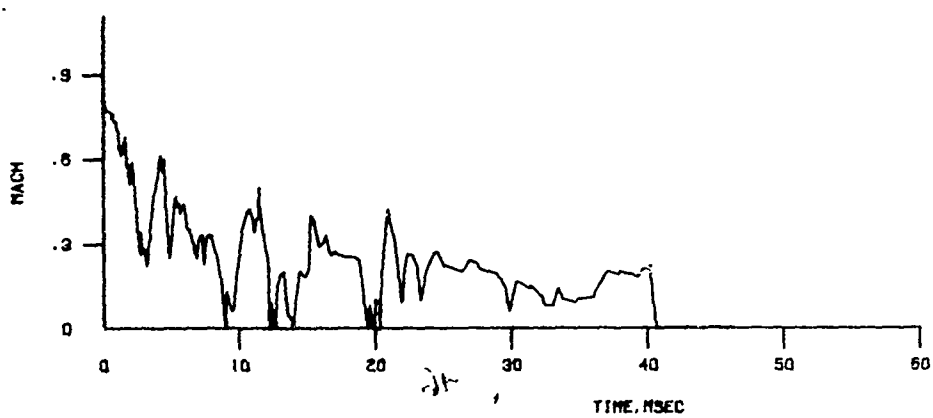
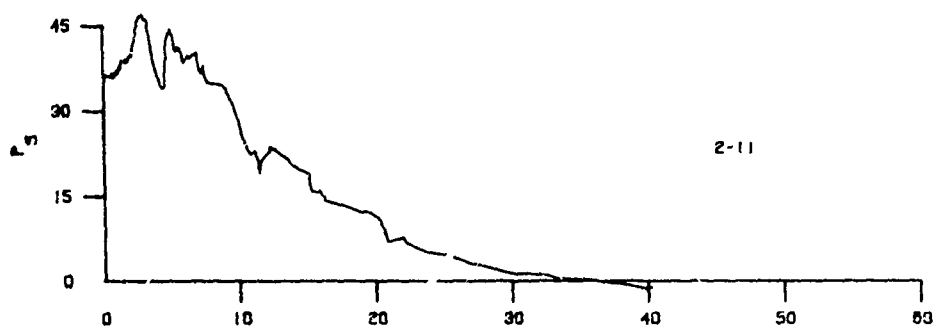
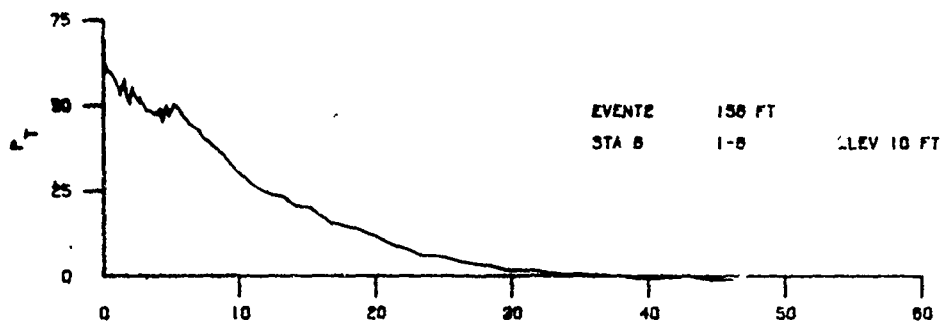
A.10 Pressure-Time Records Showing Negative Phase, Stations 8-10



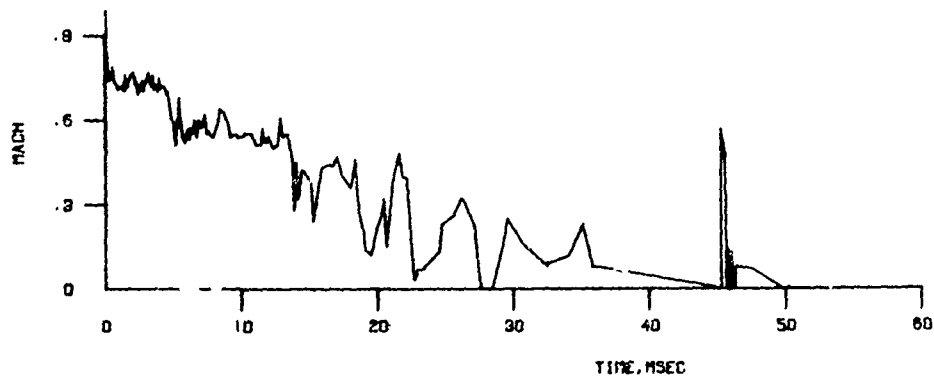
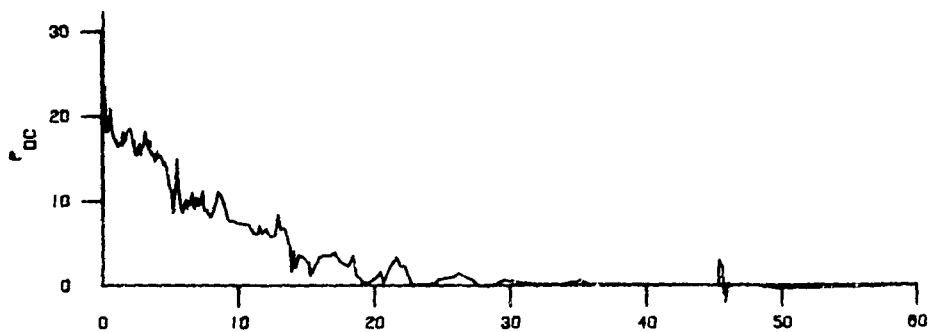
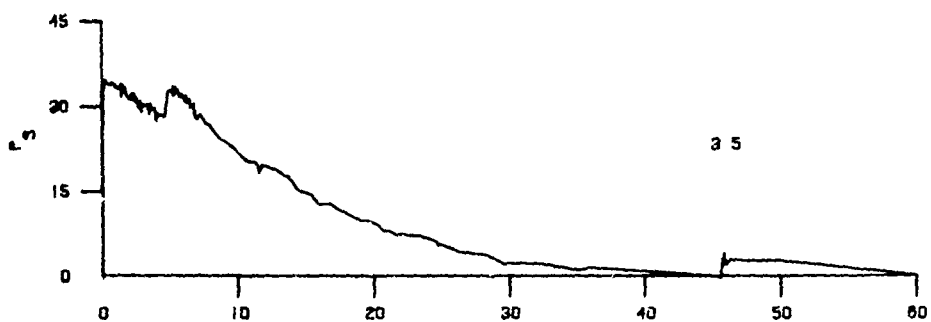
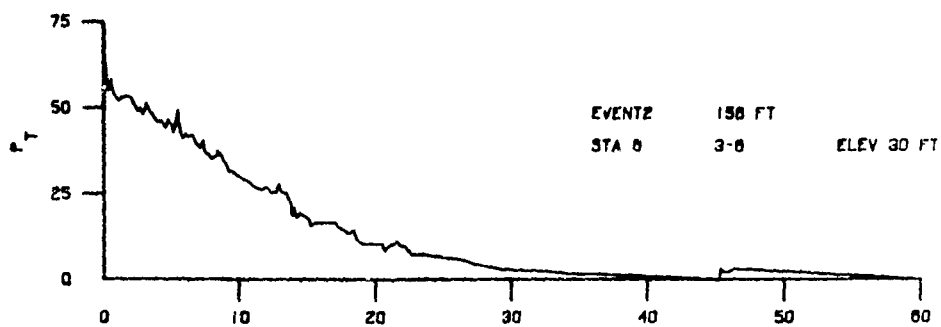
A.11 Pressure-Time Records Showing Negative Phase, Stations 12-15



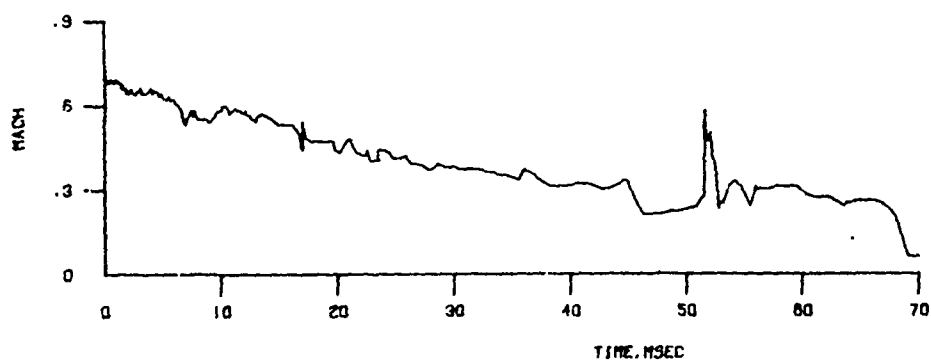
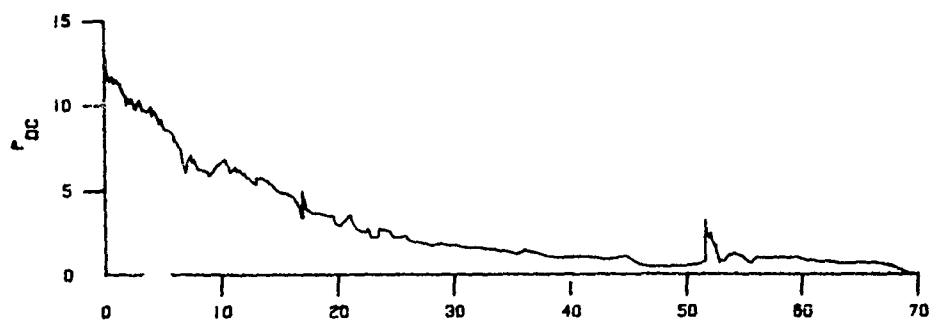
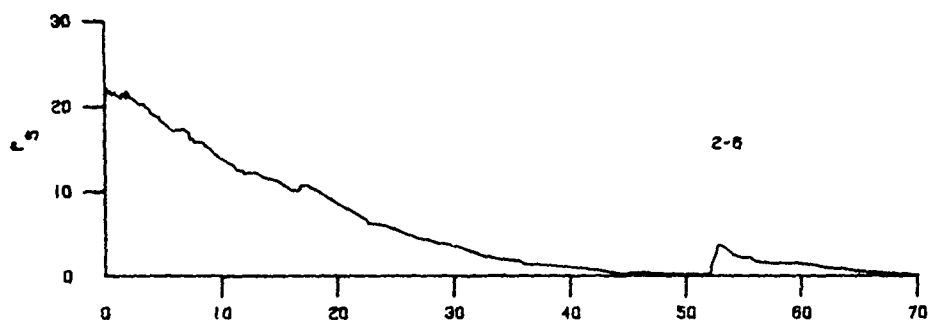
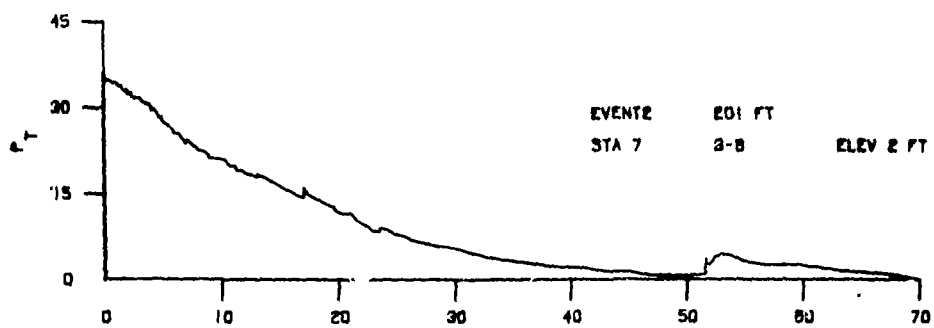
A.12 Dynamic Pressure-Time Data, 2 ft. Elevation
Station 6



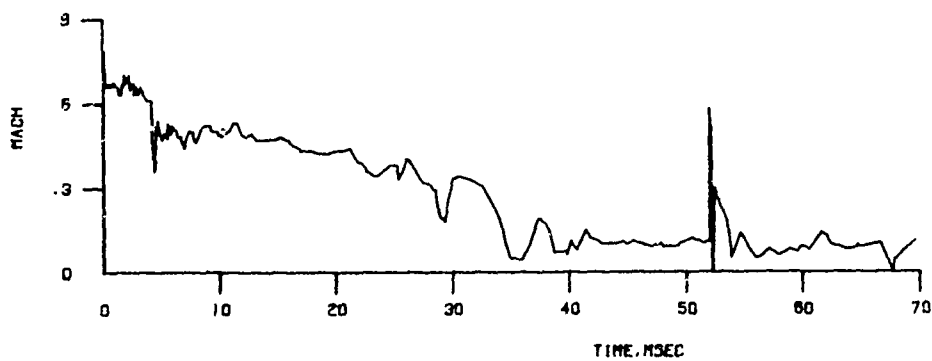
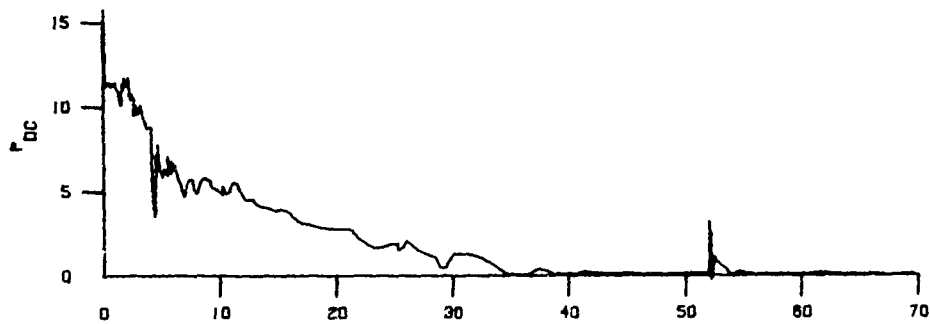
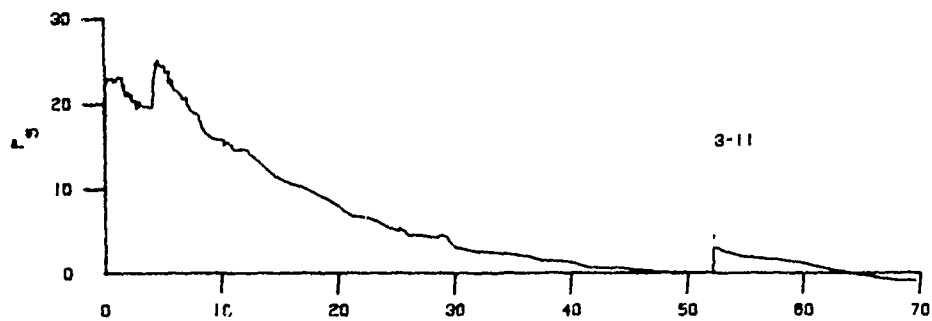
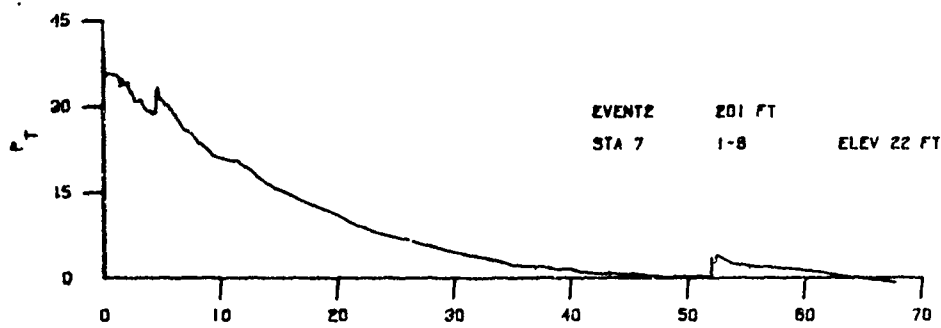
A.13 Dynamic Pressure-Time Data, 10 ft. Elevation,
Station 6



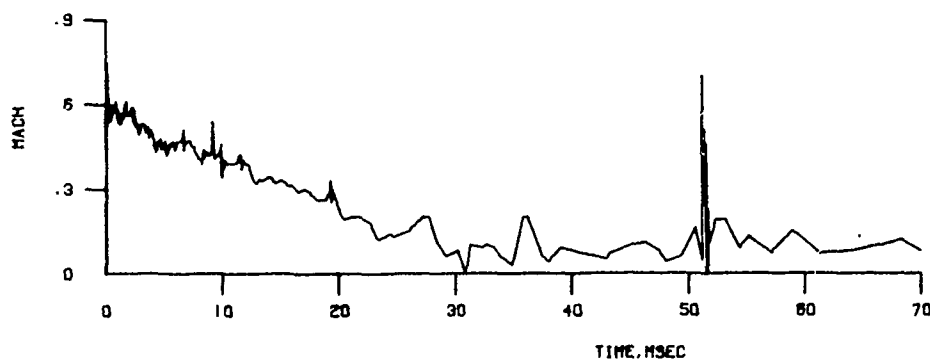
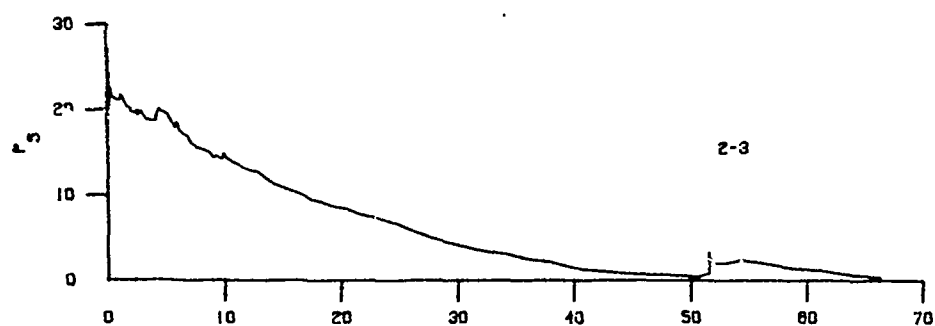
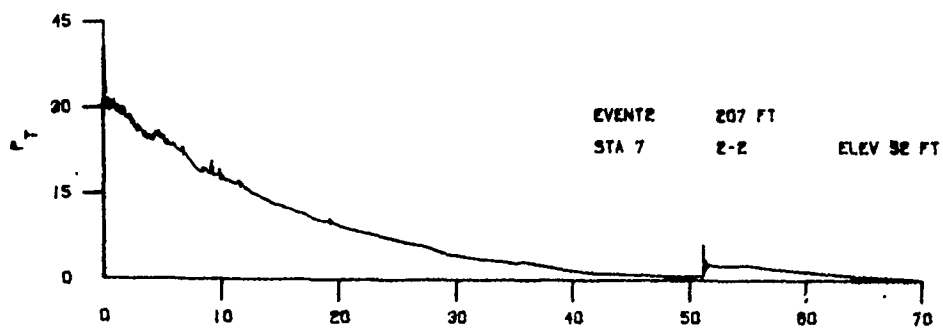
A.14 Dynamic Pressure-Time Data, 30 ft. Elevation,
Station 6



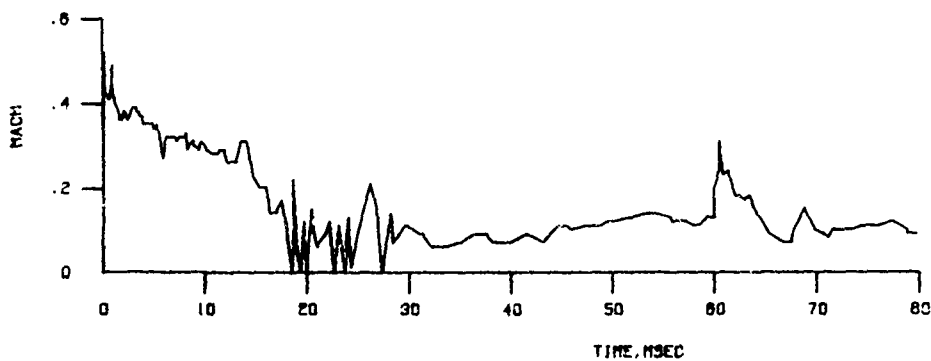
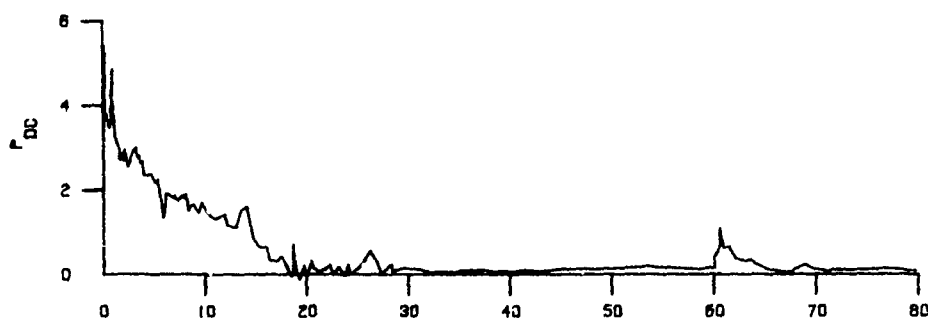
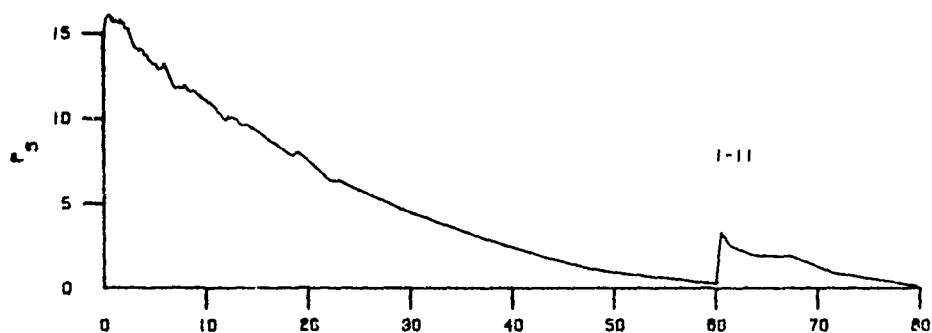
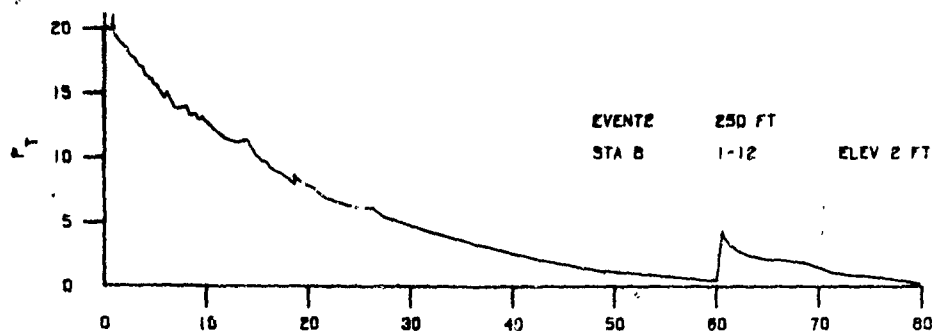
A.15 Dynamic Pressure-Time Data, 2 ft. Elevation, Station 7



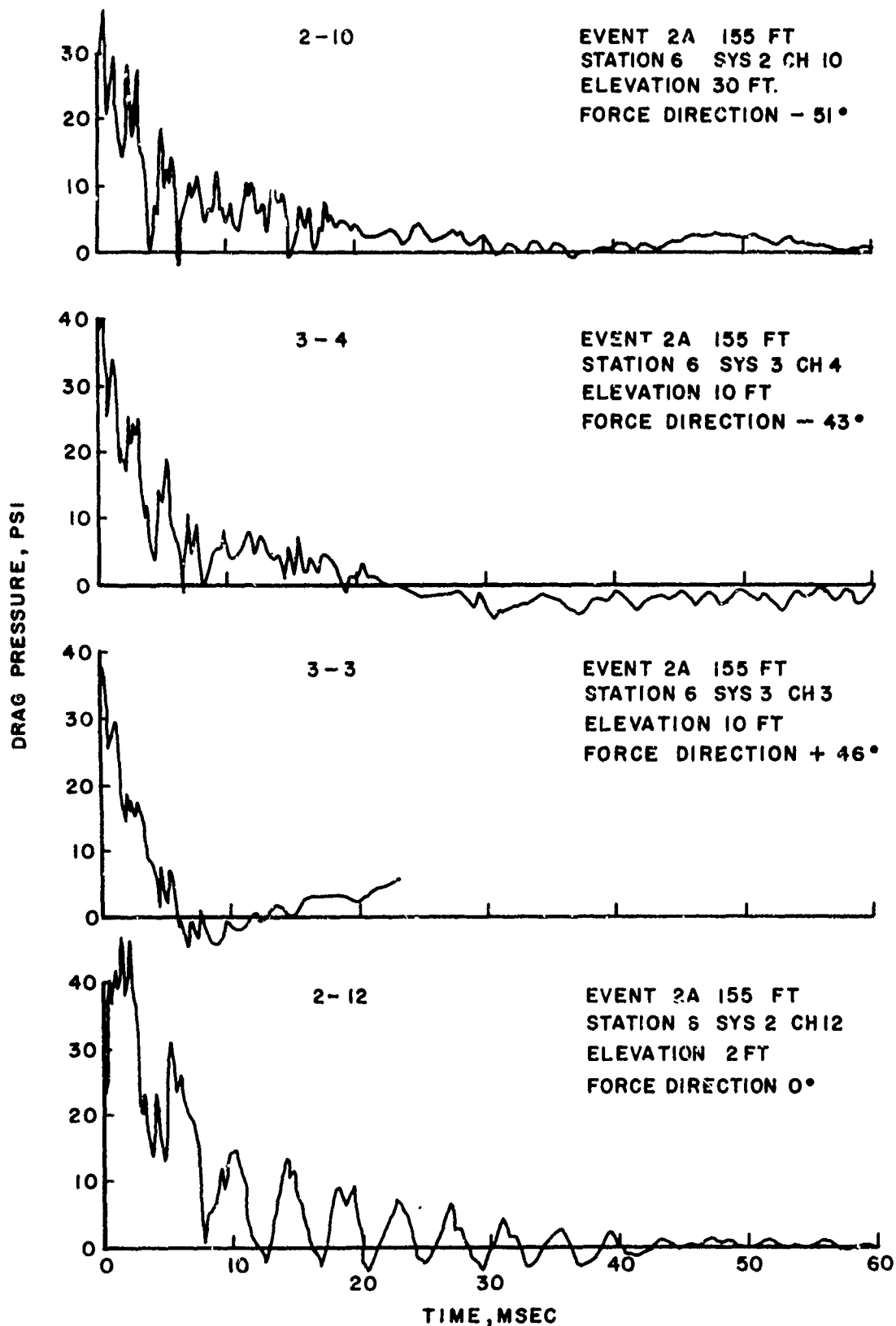
A.16 Dynamic Pressure-Time Data, 22 ft. Elevation,
Station 7



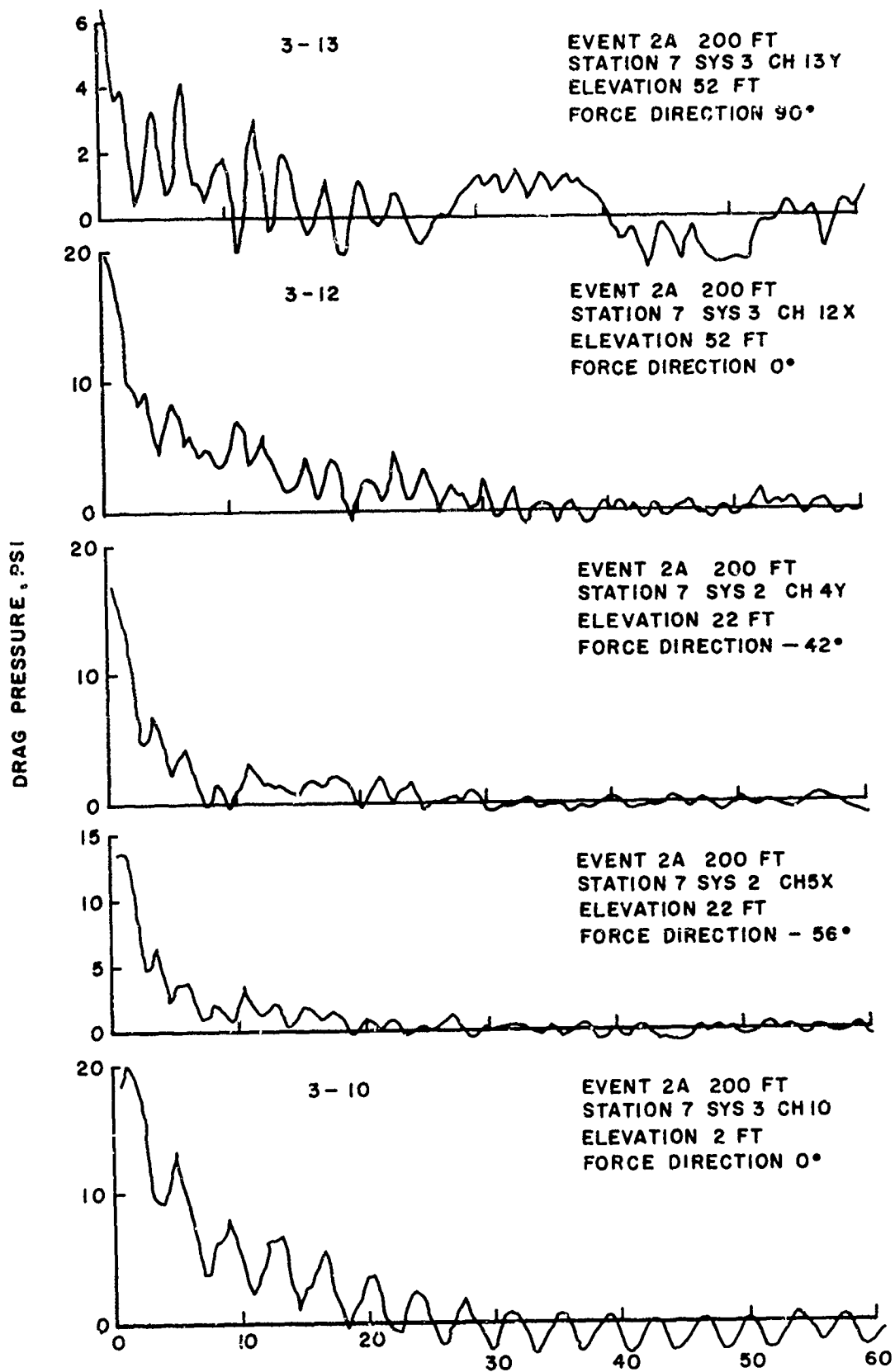
A.17 Dynamic Pressure-Time Data, 52 ft. Elevation, Station 7



A.18 Dynamic Pressure-Time Data, 2 ft. Elevation,
Station 8



A.19 Drag Pressure-Time Records, Station 6



A.20 Drag Pressure-Time Records, Station 7

APPENDIX B

Data From The Premature Detonation Of
Distant Plain Event 2 B

Distant Plain Event 2B was the name given to the re-scheduled Distant Plain Event 2. The planned shot was a detonable methane-oxygen gas mixture, 20 ton TNT equivalent, contained in a 125 ft. diameter balloon to be tethered at a height of burst of 85 feet (equal to that of Event 1). A premature detonation occurred when the balloon was 85 percent filled with methane and still on the ground surface. Investigations conducted after the incident pointed to static electricity as the most likely cause of the detonation.

Peak overpressure data were obtained by mechanical self-recording gages. The values are tabulated in Table B.1 and plotted in Figure B.1. Calculations made for yield determination indicates an average yield of 18.6 tons at the height of burst of 62.5 ft.

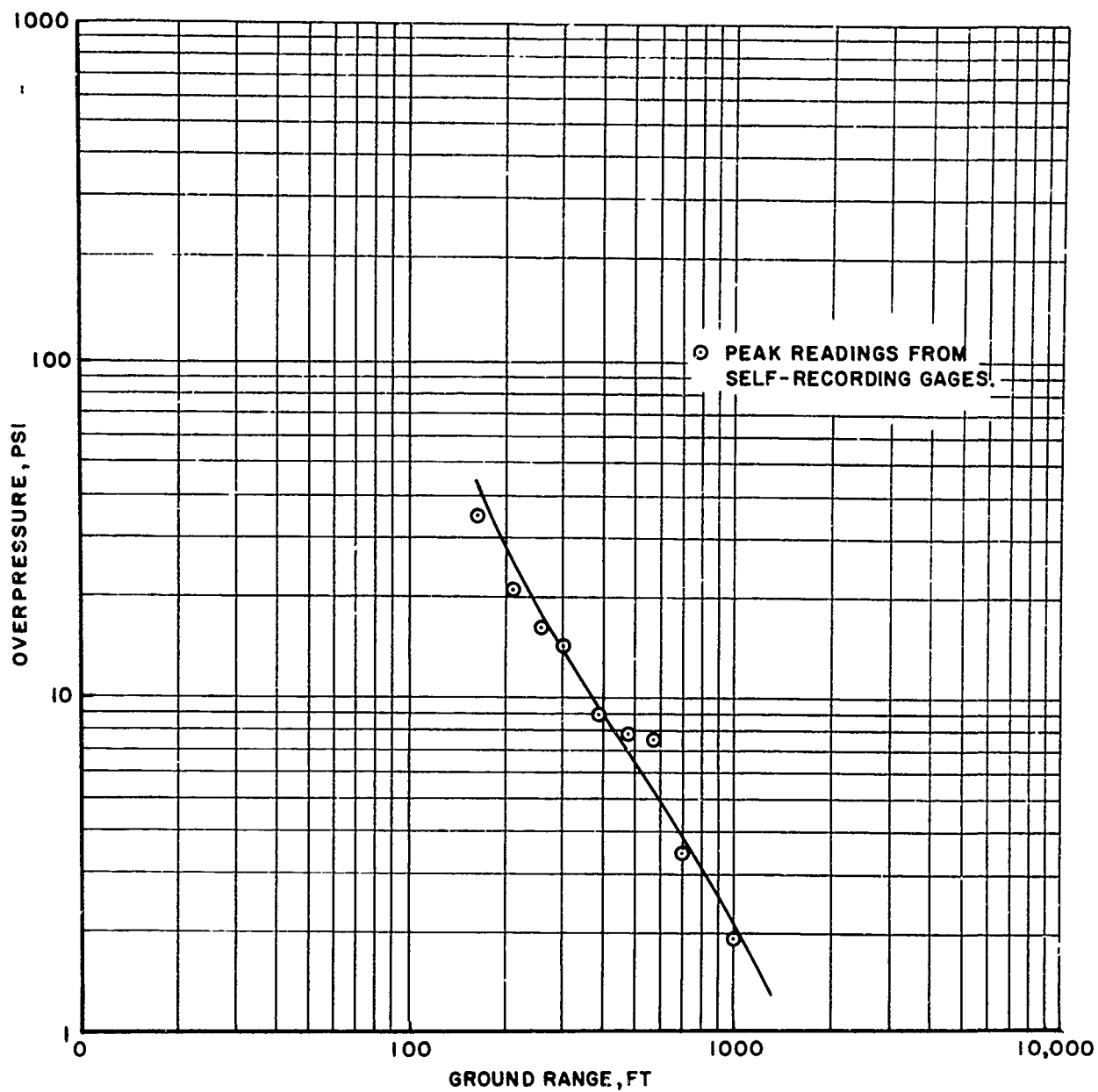


Figure B.1 Maximum Overpressure
Versus Ground Range for Event 2B

TABLE B.1 PEAK OVERPRESSURE DATA, EVENT 2B

<u>Station No.</u>	<u>Ground Range (ft)</u>	<u>Gage Number</u>	<u>Peak Overpressure (psi)</u>
6	165	12-11	34.0
7	210	50-2	20.5
9	305	25-5	14.0
10	390	10-5	8.9
11	480	10-13	7.7
12	570	10-17	7.3
13	700	5-17	3.4
14	1000	2-16	1.89